Cosmology from CMB primaries (and lensing) from space and ground-based experiments

Twitter/X: #neucosmos

Silvia Galli

Institut d'Astrophysique de Paris
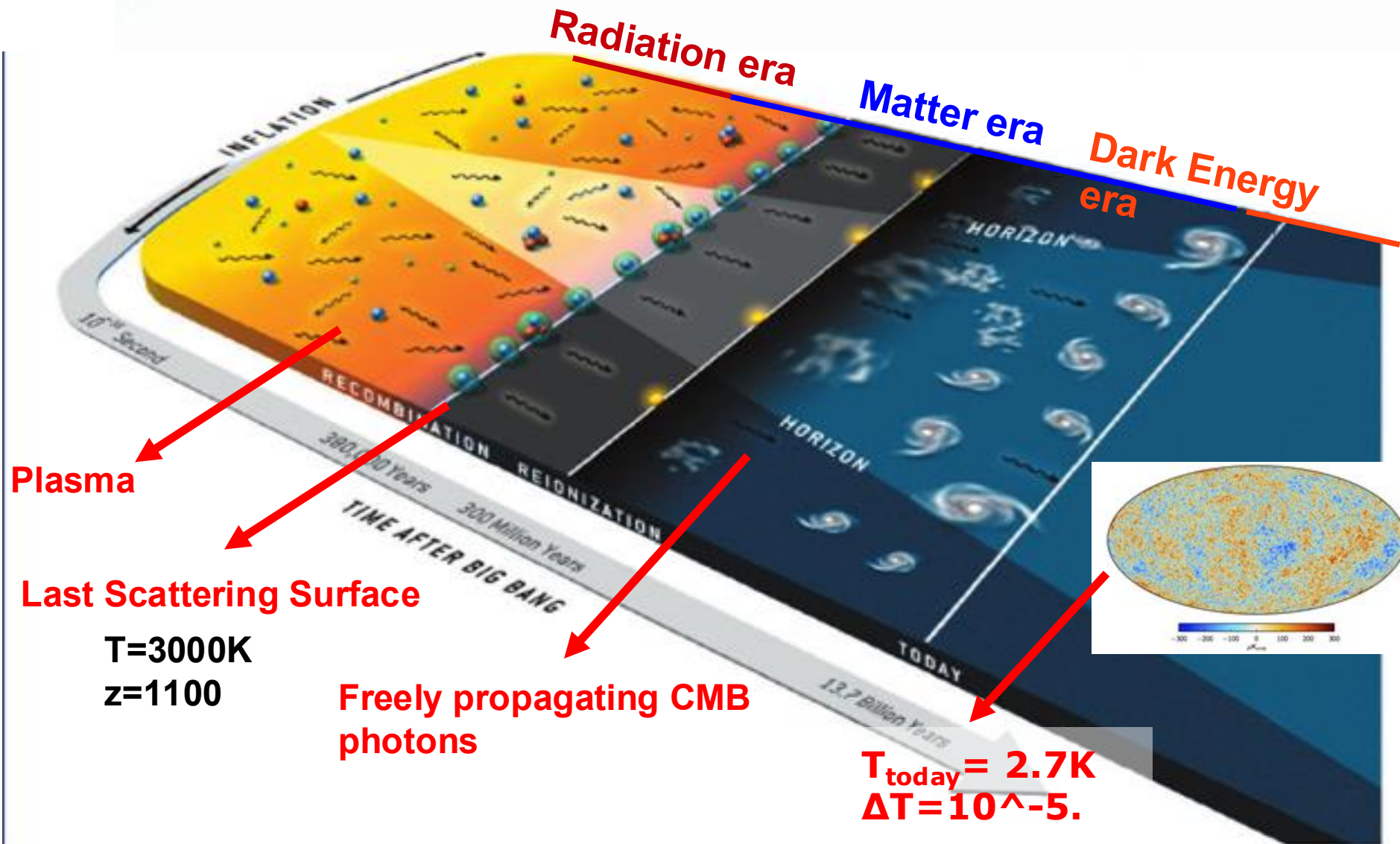
22/07/2025

Overview

1. A short introduction

2. The CMB sky and observations

    1. Monopole, dipole, anisotropies, polarization

    2. Ground, balloon and space experiments

3. From observations to cosmological parameters

    1. The CMB angular power spectrum and estimator

    2. Bayes theorem and likelihood

4. Latest results on cosmology (very Planck and SPT-3G oriented)

Overview

1. **A short introduction**

2. The CMB sky and observations

    1. Monopole, dipole, anisotropies, polarization

    2. Ground, balloon and space experiments

3. From observations to cosmological parameters

    1. The CMB angular power spectrum and estimator

    2. Bayes theorem and likelihood

4. Latest results on cosmology (very Planck and SPT-3G oriented)

CMB

Radiation era

Matter era

Dark Energy era

Plasma

Last Scattering Surface

T=3000K
z=1100

Freely propagating CMB photons

T_{today} = 2.7K
$\Delta T = 10^{-5}$.

CMB

See Julien's lectures!

Physics of recombination
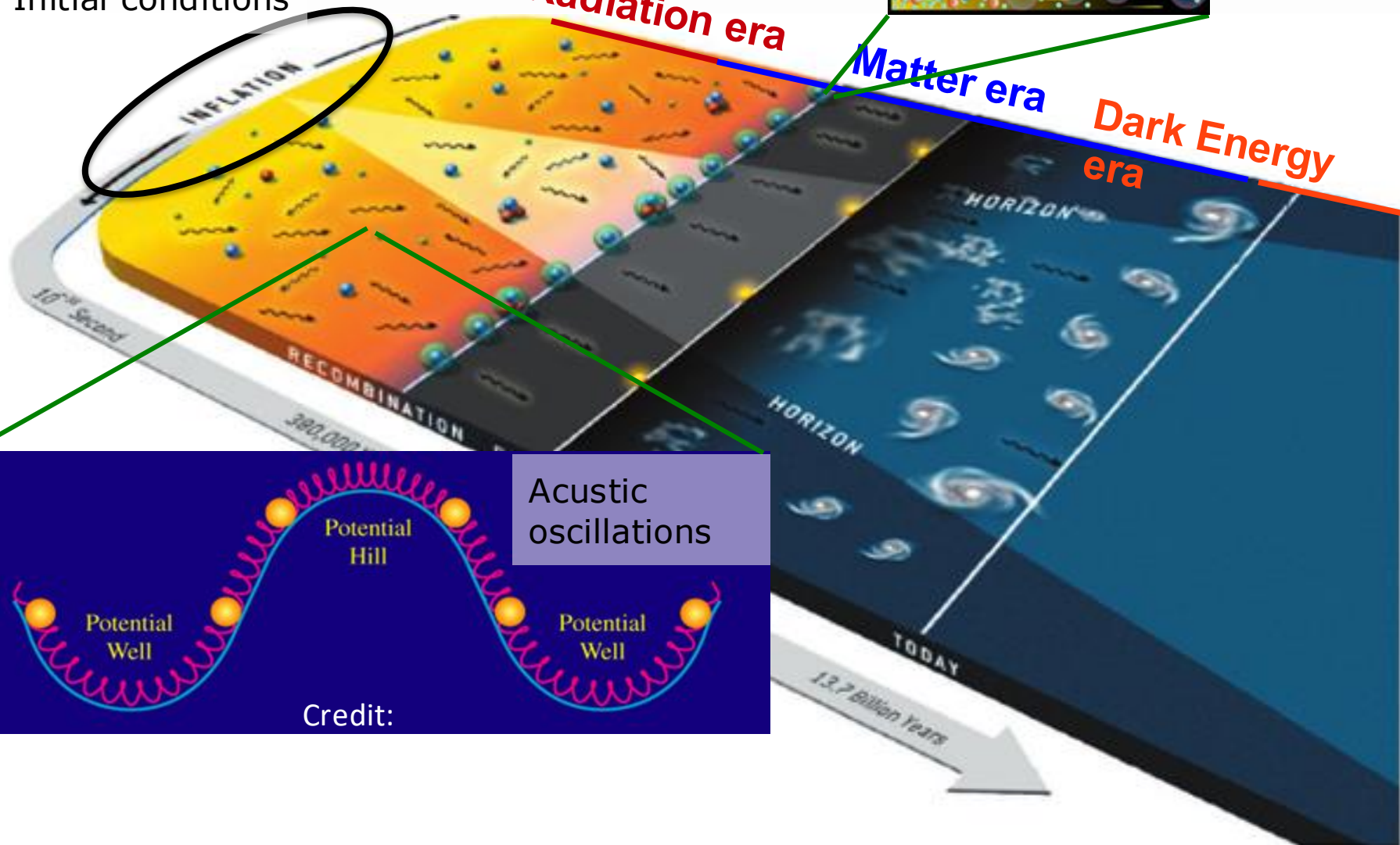
Initial conditions

Radiation era

Matter era

Dark Energy era

INFLATION

RECOMBINATION

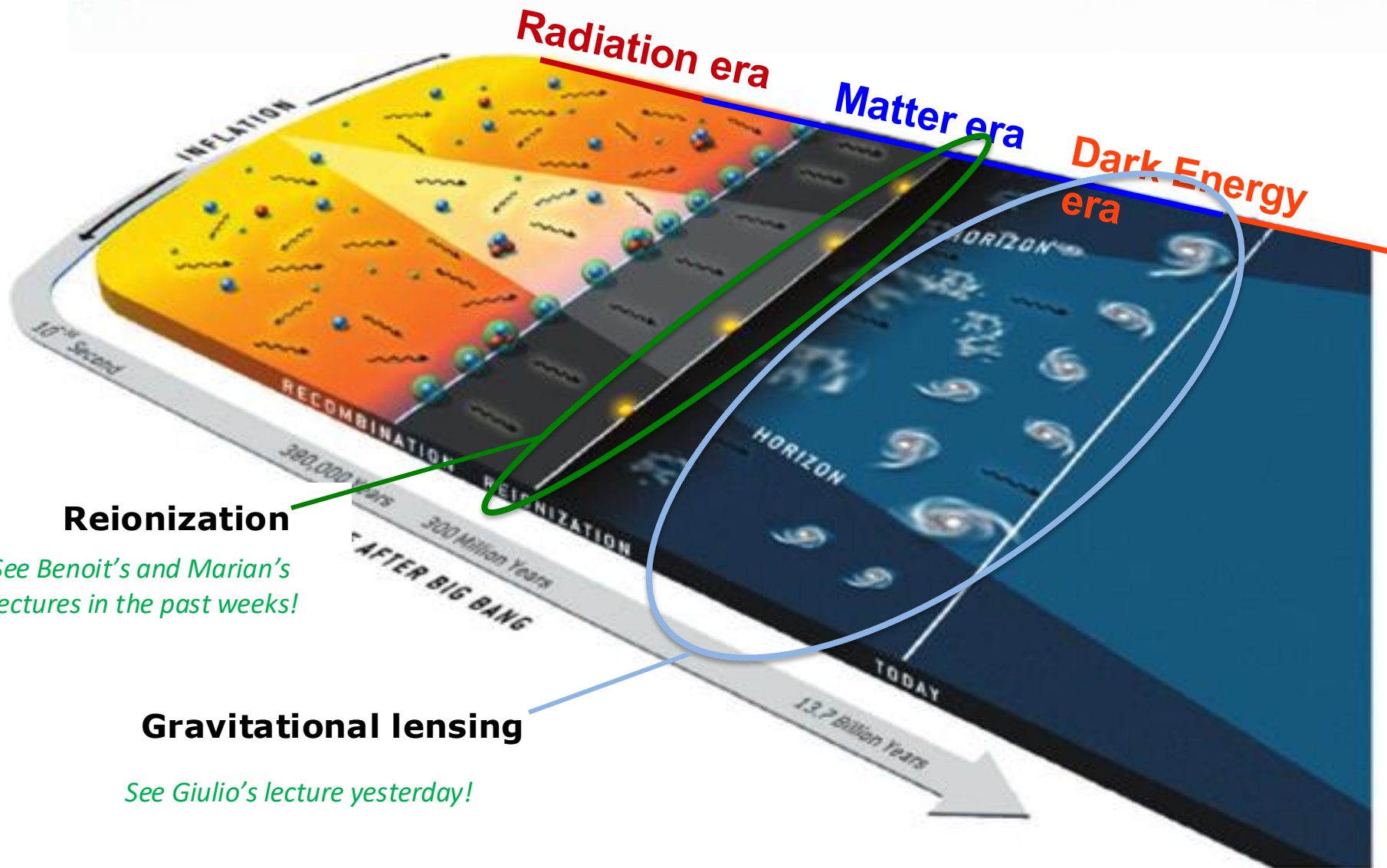380,000

10^{-36} Second

HORIZON

HORIZON

TODAY

13.7 Billion Years

Acustic oscillations

Potential Hill

Potential Well

Potential Well

Credit:

Hu & White (2004); artist B. Christie/SciAm; available at http://background.uchicago.edu

CMB

Radiation era

Matter era

Dark Energy era

Reionization
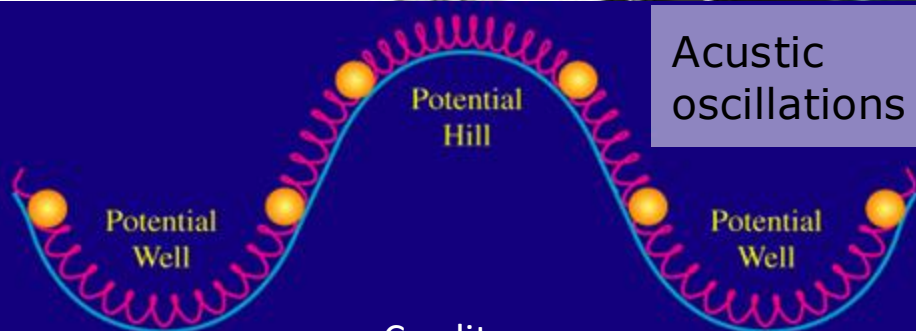
See Benoit's and Marian's lectures in the past weeks!

Gravitational lensing

See Giulio's lecture yesterday!

Hu & White (2004); artist B. Christie/SciAm; available at http://background.uchicago.edu

The Discovery of the CMB

- **A story about the importance of theoretical predictions to interpret the data, and of communication in science!**

- **1965**: **Arno Penzias and Robert Wilson** (Nobel in 1978), radio astronomers at Bell Labs in Crawford, New Jersey. Microwave horn radiometer used for **telecommunications** (through balloons).

- Uniform, **unexpected source of noise**. Cleaned birds nests (?!) before concluding its cosmological origin.

- Princeton group 60 km away (**Jim Peebles,Robert Dicke, Peter Roll, and David Wilkinson**) working on CMB prediction and detection. J. Peebles (Nobel in 2019) had **unpublished pre-print** about existence of the CMB. A friend, Bernard F. Burke, prof. at MIT, saw the pre-print and told Penzias about it.

- Princeton group confirmed Penzias and Wilson discovery of CMB and published at same time.

- Previous detections in other works, but missed discovery due to missing theoretical interpretation (Andrew McKellar 1940 interpreting obs. from W.Adams 1941; Denisse, Lequeux, Le Roux 1957, Le Roux PhD thesis 1957).

1978
2019
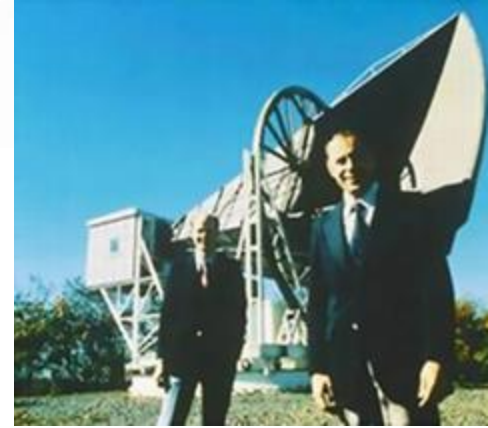
A MEASUREMENT OF EXCESS ANTENNA TEMPERATURE AT 4080 Mc/s

A. A. PENZIAS
R. W. WILSON

Astrophysical Journal, vol. 142, p.419-421

COSMIC BLACK-BODY RADIATION*

R. H. DICKE
P. J. E. PEEBLES
P. G. ROLL
D. T. WILKINSON
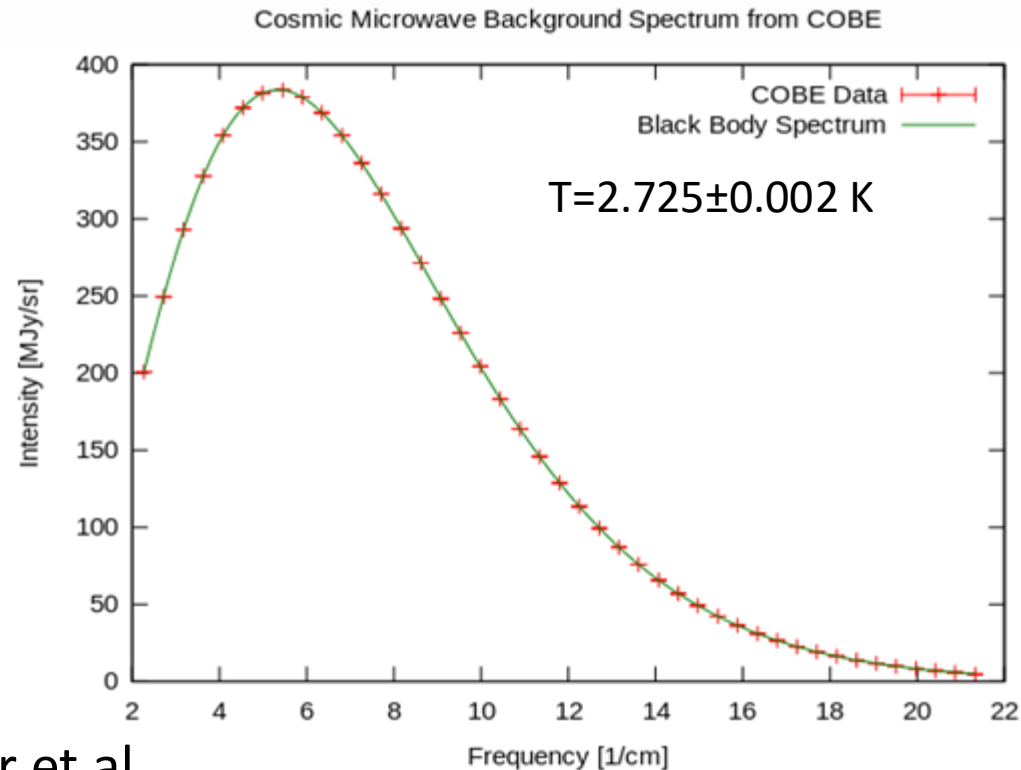
Astrophysical Journal, vol. 142, p.414-419

7

The monopole

- The CMB has a black body spectrum with average temperature of T=2.725±0.002 K (COBE)
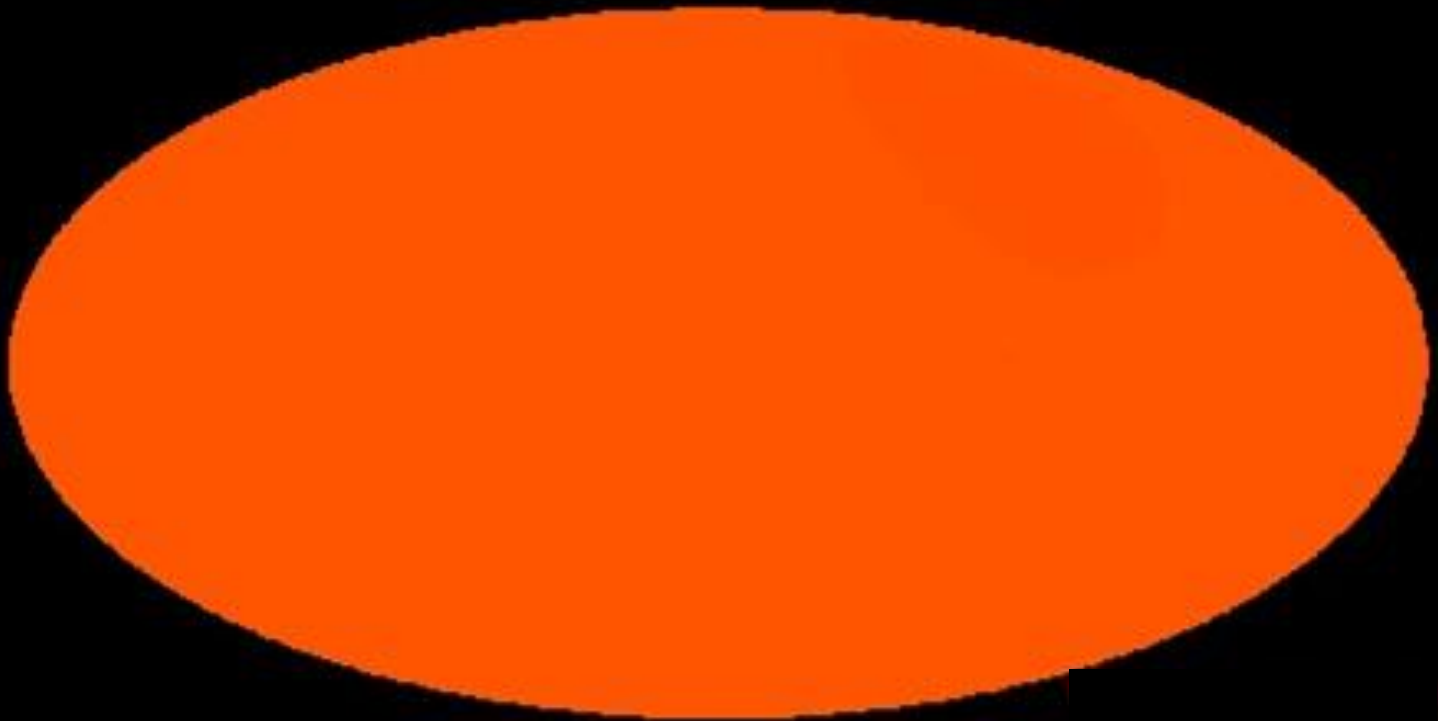
The most accurate measurement to date: COBE

- Launched in **1989**.
- Three instruments:

  - **FIRAS** (BB spectrum) [60-2880GHz],1yr
  - **DMR** (anisotropies) [31.5,53,90GHz],4yr
  - **DIRBE** (CIB) [infrared]

Cosmic Microwave Background Spectrum from COBE

T=2.725±0.002 K

COBE Data
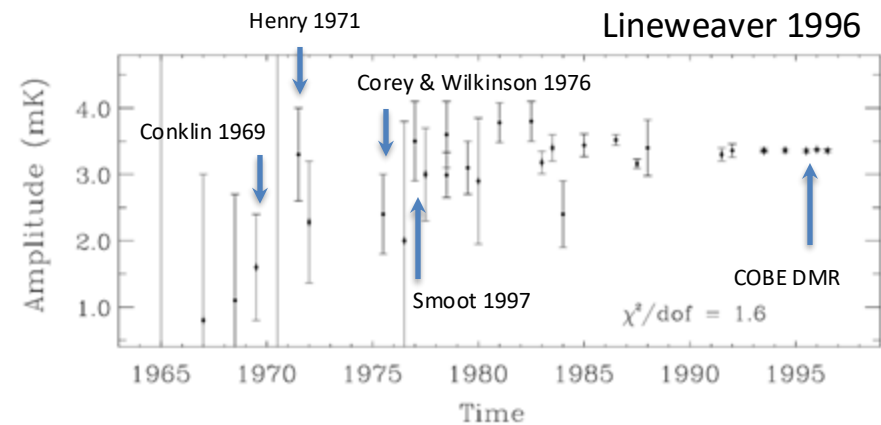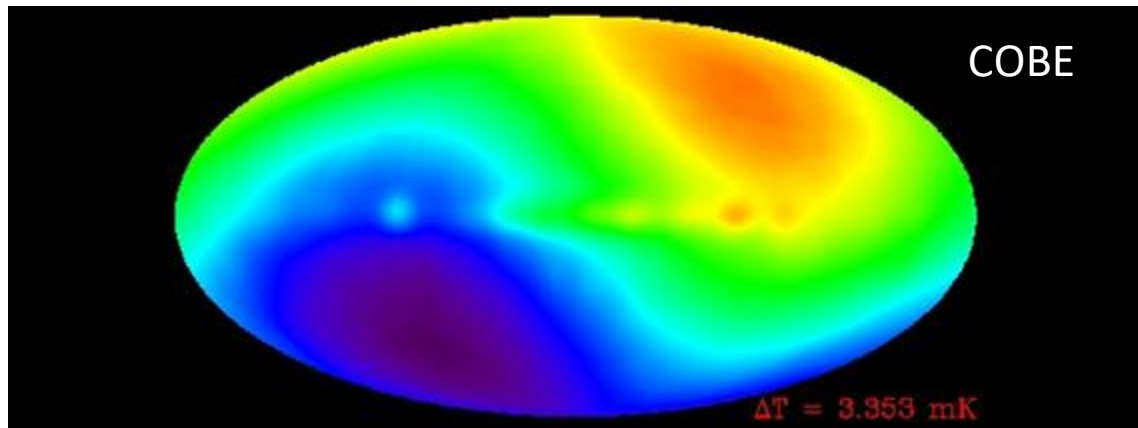Black Body Spectrum

Intensity [MJy/sr]

Frequency [1/cm]

- FIRAS measurements. Mather et al. (1994, 1996), Fixten 1996
- Peak BB(v) at ~159 GHz.
- Nobel to John Mather (PI of FIRAS) and George Smooth (PI of DMR) in 2006

2006

The most accurate measurement to date: COBE

- Launched in **1989**.
- Three instruments:

    - **FIRAS** (BB spectrum) [60-2880GHz],1yr
    - **DMR** (anisotropies) [31.5,53,90GHz],4yr
    - **DIRBE** (CIB) [infrared]

- FIRAS measurements. Mather et al. (1994, 1996), Fixten 1996
- Peak BB(v) at ~159 GHz.
- Nobel to John Mather (PI of FIRAS) and George Smooth (PI of DMR) in 2006
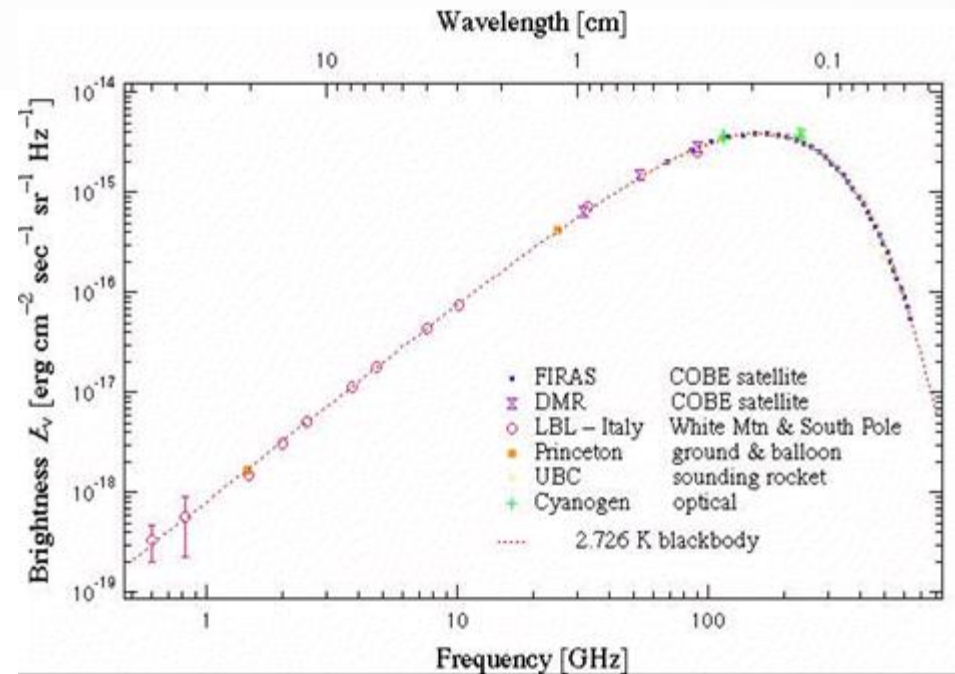

2006

The dipole

- The motion of the sun w.r.t. the CMB reference system produces a dipole of ΔT=3.36208 ± 0.00099 mK (Planck 2018) (1000 times smaller than monopole)

- Corresponds to v=369.82 ± 0.11 km/s.

- Detections shortly after discovery of CMB.
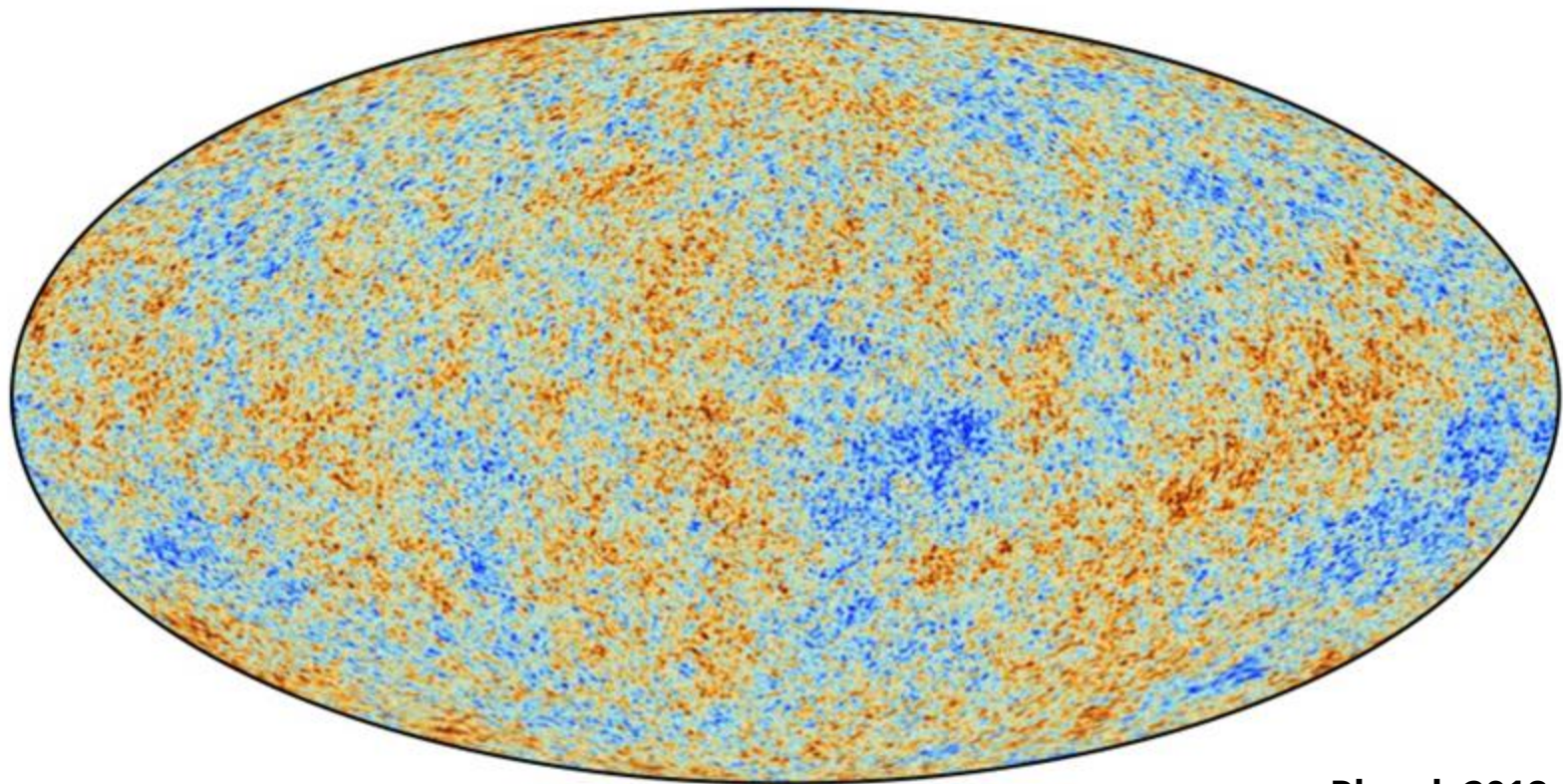
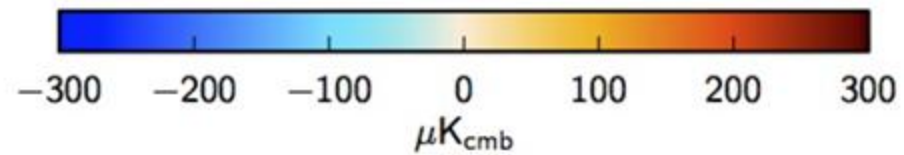- Velocity of Earth around sun 10 times smaller ~30 km/s

COBE

ΔT = 3.353 mK

Henry 1971

Lineweaver 1996

Corey & Wilkinson 1976

Conklin 1969

Amplitude (mK)

Smoot 1997

COBE DMR

χ²/dof = 1.6

1965   1970   1975   1980   1985   1990   1995

Time

Anisotropies

- At the μK level, CMB anisotropies (and foregrounds)!
- First detected by COBE DMR in 1992.
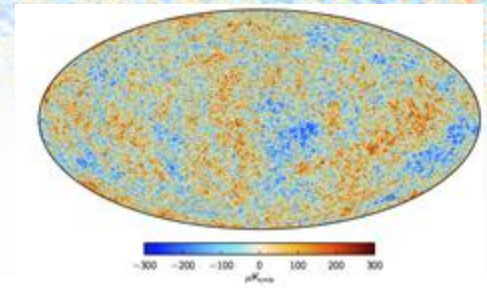
2006

COBE

$\Delta T = 18 \ \mu K$
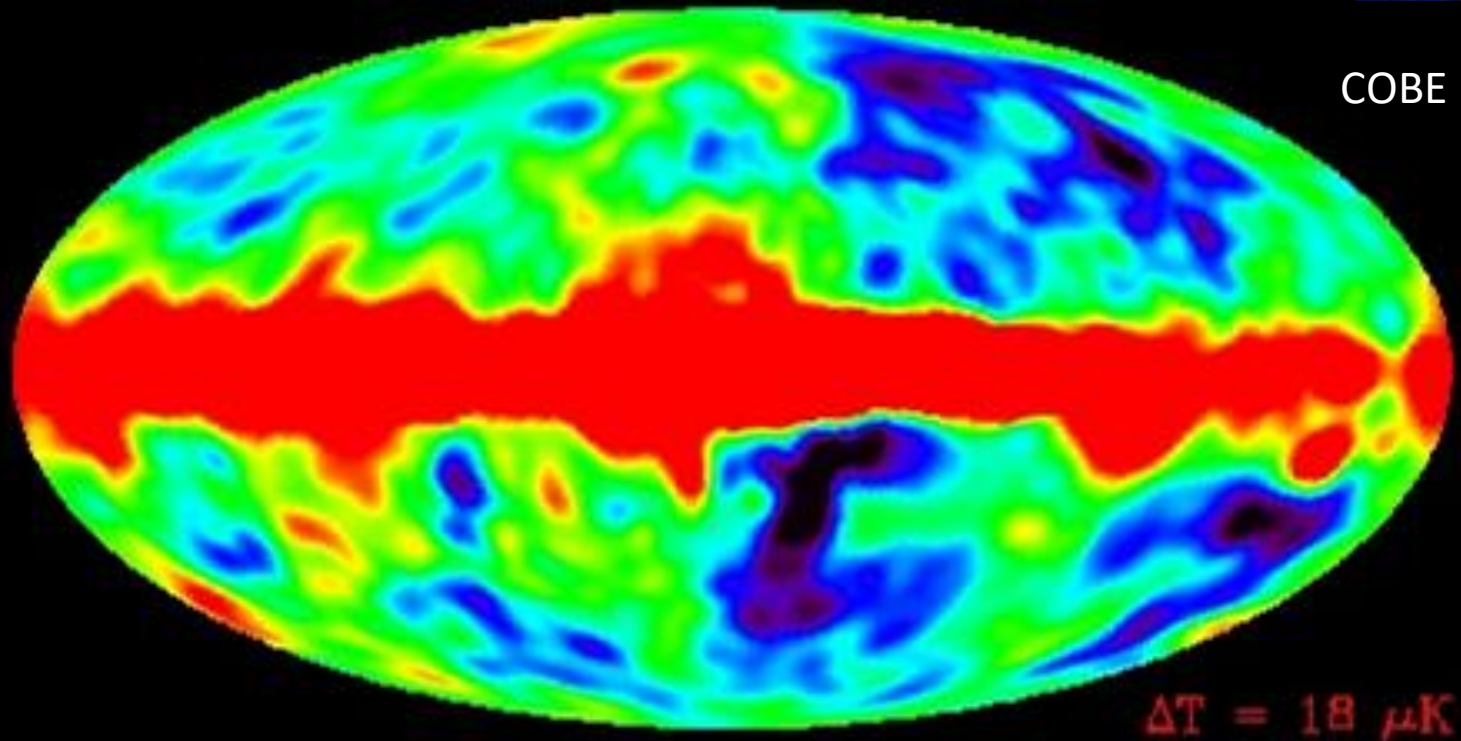
Anisotropies

Planck 2018

A note about units
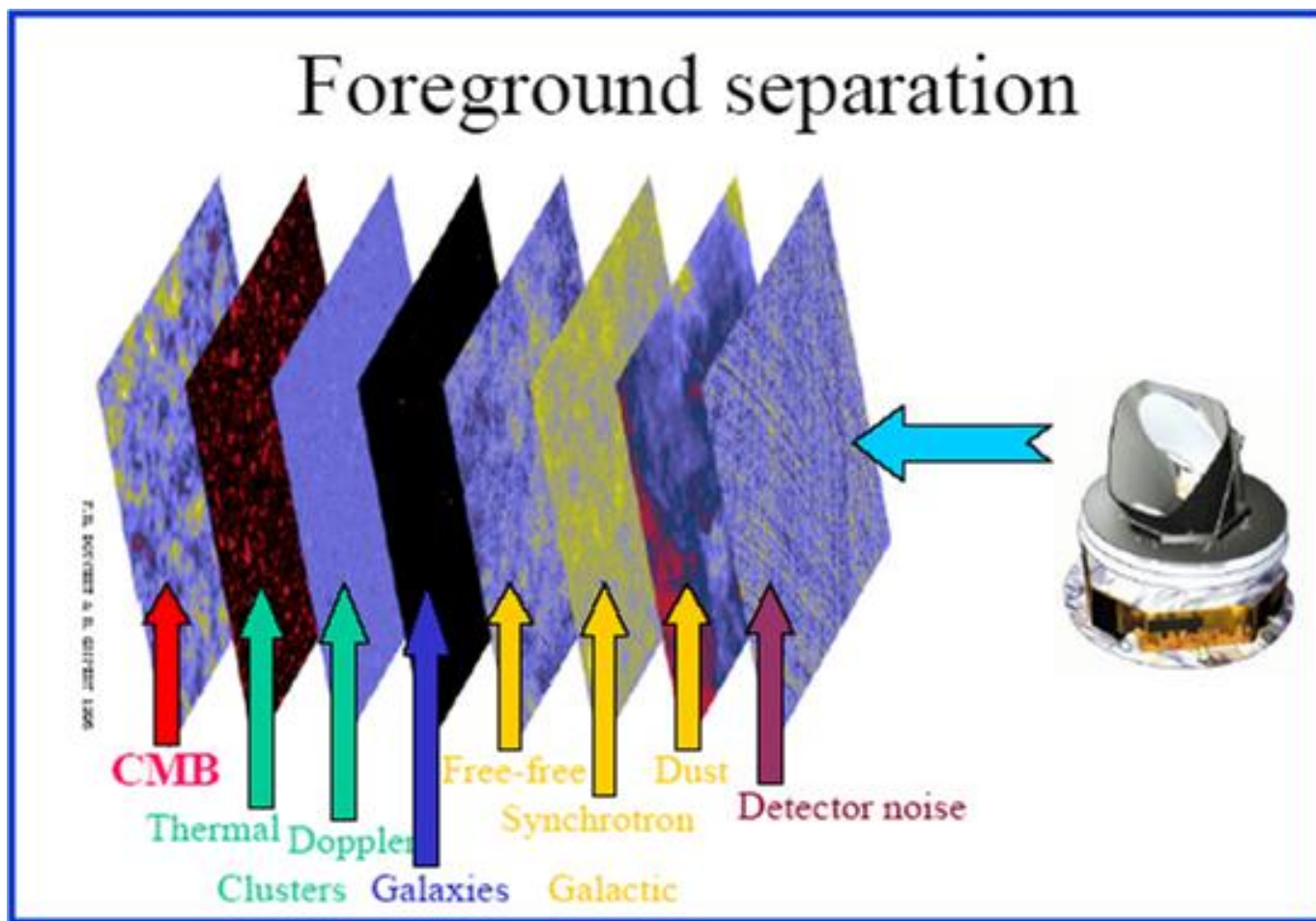

- These maps are in units of thermodinamic temperature.
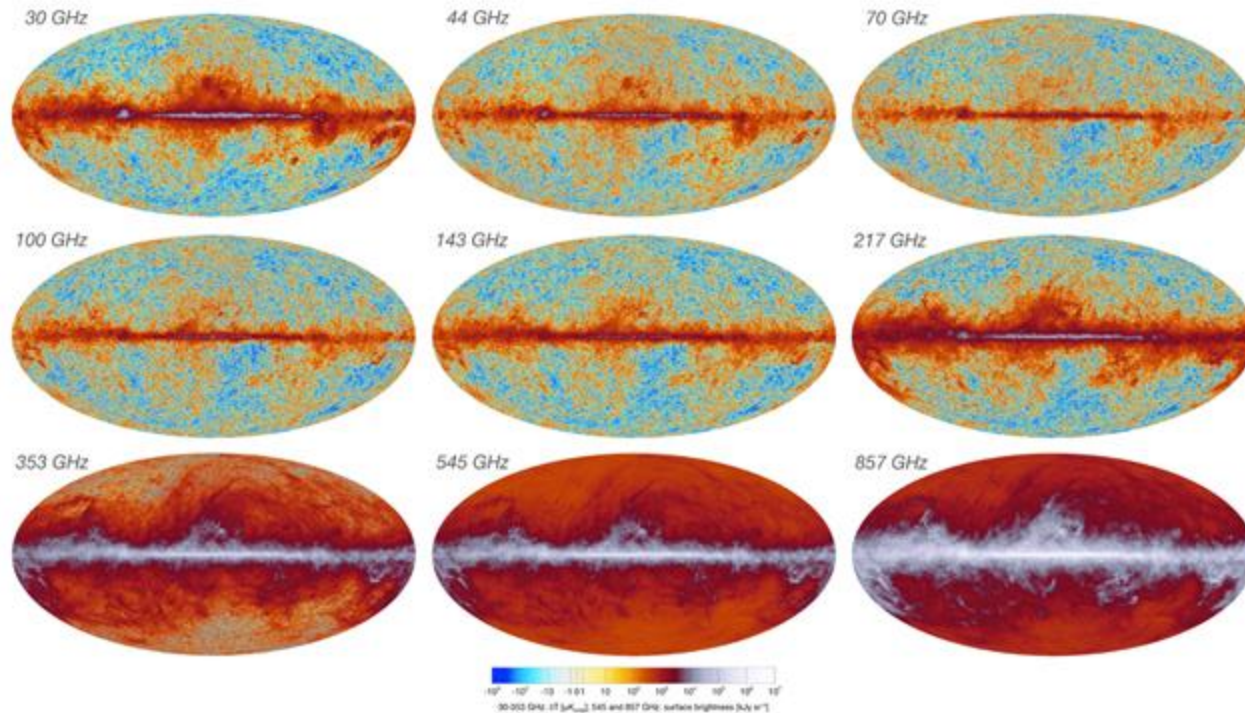- Brightness to thermodynamic temperature K_{cmb} assuming a black body spectrum:

$$BB_\nu(T) \quad = \quad \frac{dE}{d\nu\, d\Omega\, dA\, dt} = \frac{2h\nu^3}{c^2} \frac{1}{\exp(h\nu/kT) - 1}$$

- In these units, the CMB has the same temperature at all frequencies, while foregrounds with different emission spectra have different thermodynamic temperatures at different frequencies
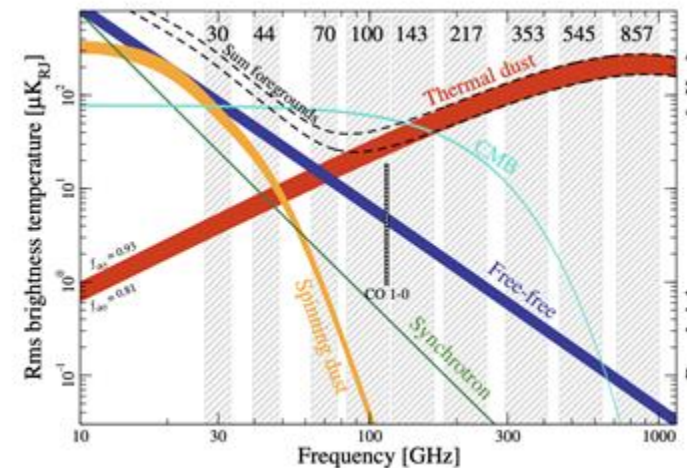
Not only CMB...

Foreground separation

CMB
Thermal Doppler
Clusters Galaxies
Free-free
Synchrotron
Galactic
Dust
Detector noise

CMB maps at different frequencies
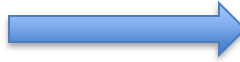

Planck collaboration I. 2019

*At 545 and 857 GHz, CMB is weak, calibrated using planets rather than the orbital dipole, units not in K_{cmb} but in surface brightness kJy sr^{-1}

Intensity and polarization in Stokes parameters

For a monochromatic plane wave:

$$E_x = a_x \cos[\omega_0 t - \theta_x(t)] \qquad E_y = a_y \cos[\omega_0 t - \theta_y(t)]$$
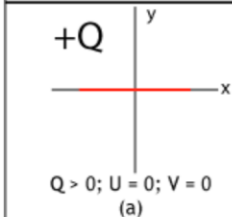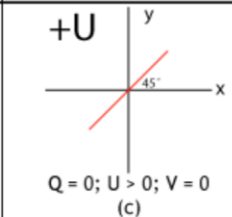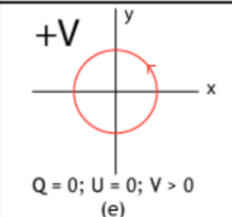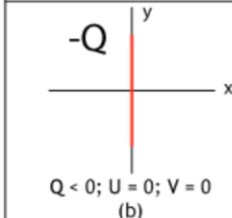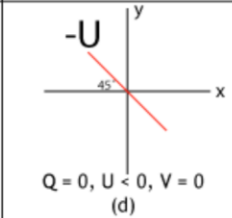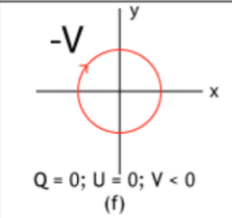
$\phi = \theta_x - \theta_y$
$\phi = 0 \Rightarrow$ linear polarization
$\phi = \pi/2,\ a_x = a_y \Rightarrow$ circular polarization

$$I \equiv \langle a_x^2 \rangle + \langle a_y^2 \rangle$$

$$Q \equiv \langle a_x^2 \rangle - \langle a_y^2 \rangle$$

$$U \equiv \langle 2 a_x a_y \cos(\theta_x - \theta_y) \rangle$$

$$V \equiv \langle 2 a_x a_y \sin(\theta_x - \theta_y) \rangle$$

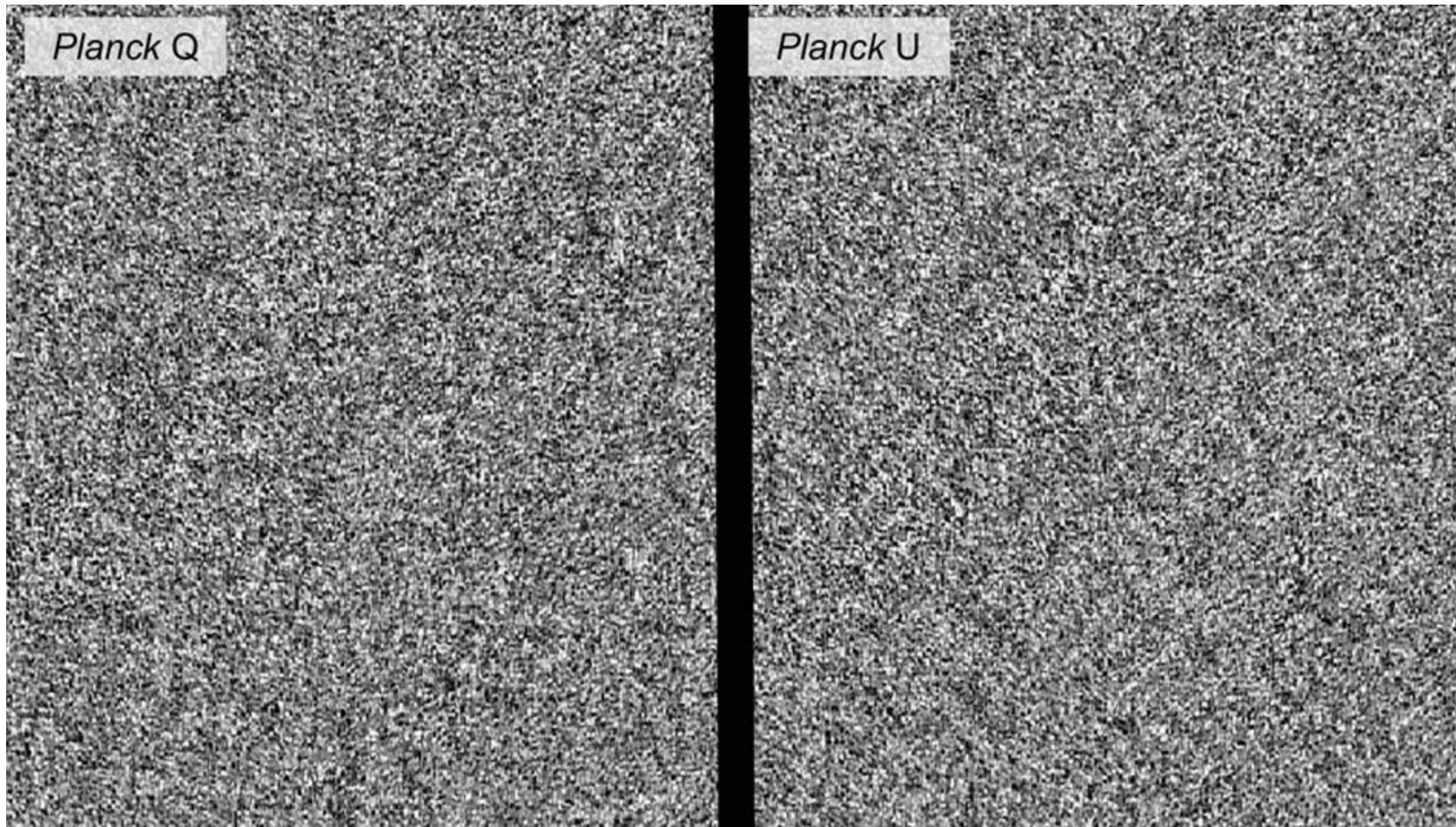| 100% Q	100% U	100% V
+Q	+U	+V
Q > 0; U = 0; V = 0 (a)	Q = 0; U > 0; V = 0 (c)	Q = 0; U = 0; V > 0 (e)
-Q	-U	-V
Q < 0; U = 0; V = 0 (b)	Q = 0, U < 0, V = 0 (d)	Q = 0; U = 0; V < 0 (f)

$$I^2 \geq Q^2 + U^2 + V^2$$

$$p \equiv \frac{\sqrt{Q^2 + U^2 + V^2}}{I}$$

- Equal holds for a monocromatic wave or, for superposition of many waves, entirely polarized radiation.
- P= degree of polarization
- In the following, we'll drop V (not produced in standard cosmology model.)

17

CMB Polarization maps

Planck Q

Planck U

Credit: W. Quan

From Q and U to E and B modes

- Polarization is a headless vector, equal to itself after a 180deg rotation=>Q and U spin 2 fields.

$$Q' \pm iU' = e^{\mp 2i\theta}[Q \pm iU]$$

- So Q and U depend on the reference system=> bad to characterize the underlying physics!

- A solution is to characterize polarization not by the characteristics in a point, but a non-local average 'pattern'around a point the sky.

$$Q > 0 \quad U = 0 \qquad Q < 0 \quad U = 0$$
$$E < 0 \qquad E > 0$$

$$Q = 0 \quad U < 0 \qquad Q = 0 \quad U > 0$$
$$B < 0 \qquad B > 0$$
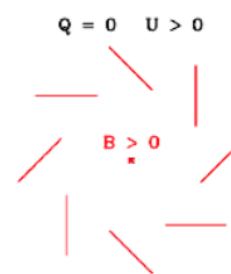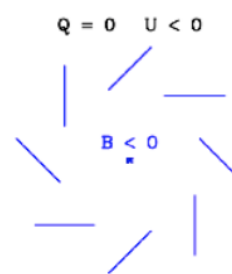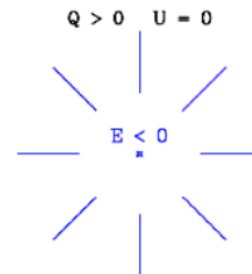
Flat sky approximation:

$$
\begin{aligned}
E(\boldsymbol{\theta}) &= \int d^2\tilde{\boldsymbol{\theta}}\,\omega(\tilde{\theta})Q_r(\boldsymbol{\theta}+\tilde{\boldsymbol{\theta}}) \\
&= \int d^2\tilde{\boldsymbol{\theta}}\,\omega(\tilde{\theta})[Q(\boldsymbol{\theta}+\tilde{\boldsymbol{\theta}})\cos(2\tilde{\psi}) - U(\boldsymbol{\theta}+\tilde{\boldsymbol{\theta}})\sin(2\tilde{\psi})] \\
B(\boldsymbol{\theta}) &= \int d^2\tilde{\boldsymbol{\theta}}\,\omega(\tilde{\theta})U_r(\boldsymbol{\theta}+\tilde{\boldsymbol{\theta}}) \\
&= \int d^2\tilde{\boldsymbol{\theta}}\,\omega(\tilde{\theta})[Q(\boldsymbol{\theta}+\tilde{\boldsymbol{\theta}})\sin(2\tilde{\psi}) + U(\boldsymbol{\theta}+\tilde{\boldsymbol{\theta}})\cos(2\tilde{\psi})]
\end{aligned}
$$

See more details in back-up slides and in Zaldarriaga astro-ph/0106174
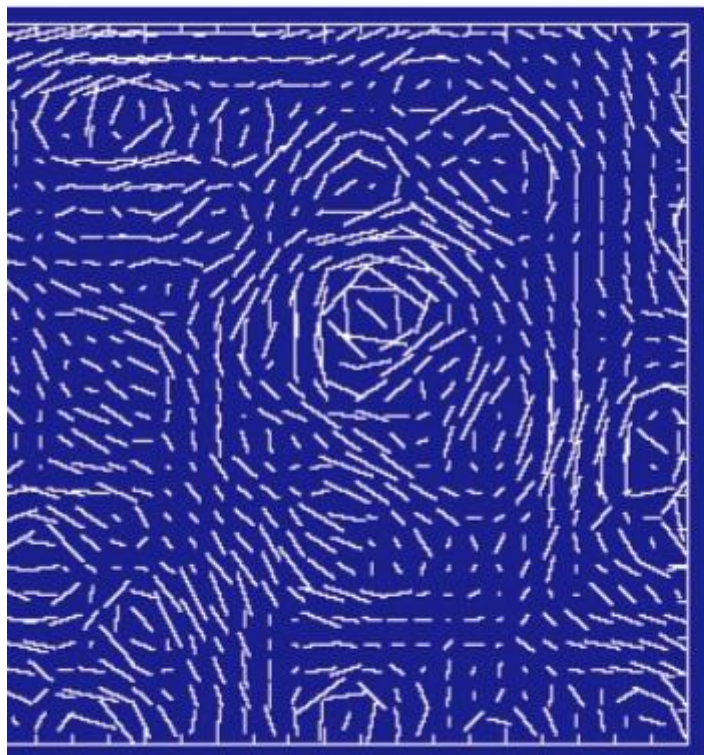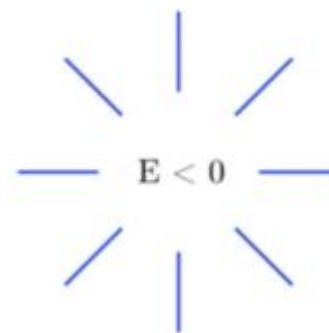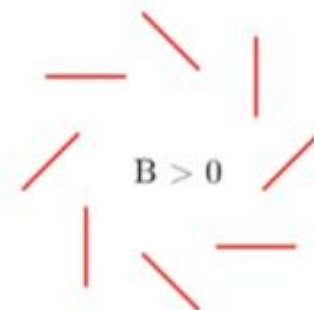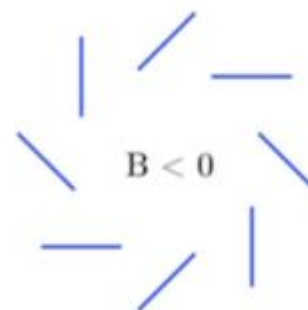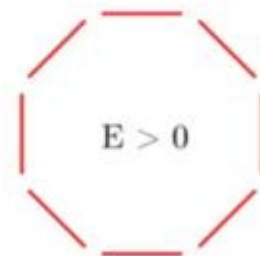
$$= \quad \begin{matrix} E < 0 \end{matrix} \quad + \quad \begin{matrix} E > 0 \end{matrix}$$

E < 0

E > 0

B < 0

B > 0

Overview

1. A short introduction

2. The CMB sky and observations
   1. Monopole, dipole, anisotropies, polarization
   2. **Ground, balloon and space experiments**
3. From observations to cosmological parameters
   1. The CMB angular power spectrum and estimator
   2. Bayes theorem and likelihood

4. Latest results on cosmology (very Planck and SPT-3G oriented)

CMB experiments (very incomplete list)

COBE | WMAP | Planck

Satellites

- **COBE** (DMR Smoot et al. **1992**; Bennett et al. 1996)
- **WMAP** (Wilkinson Microwave Anisotropy Probe: Bennett et al. **2003, 2013**)
- **Planck** (Planck I **2013, 2015, 2018**)

Boomerang

Maxima

Spider

Balloons
Boomerang and **Maxima**: first peak. **2001**
Many many others

DASI

BICEP/Keck

SPT

South Pole

Ground
DASI: second and third peak 2001, CMB polarization 2002
Many many many others!

ACT

Polarbear

SO

Atacama desert Chile

List of CMB experiments:
https://lambda.gsfc.nasa.gov/product/expt/

CMB experiments (very incomplete list)

Satellites
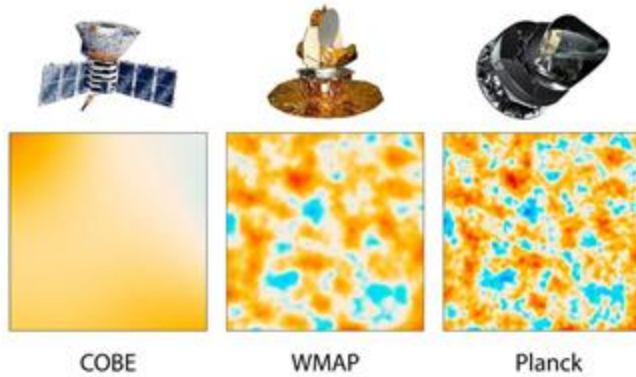
- **COBE** (DMR Smoot et al. **1992**; Bennett et al. 1996)
- **WMAP** (Wilkinson Microwave Anisotropy Probe: Bennett et al. **2003, 2013**)
- **Planck** (Planck I **2013, 2015, 2018**)

Balloons
Boomerang and **Maxima**: first peak. **2001**
Many many others

Ground
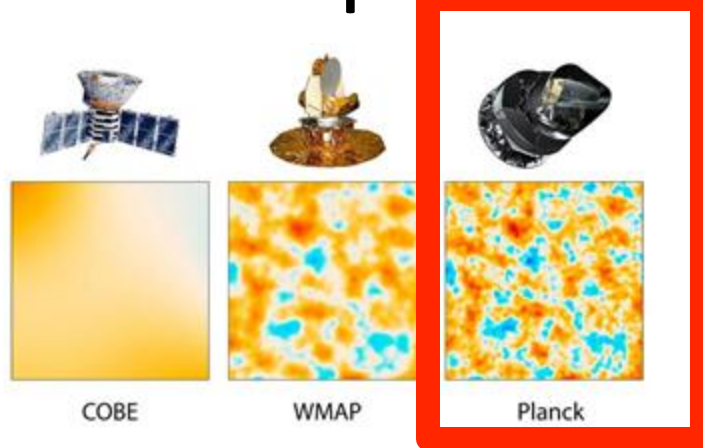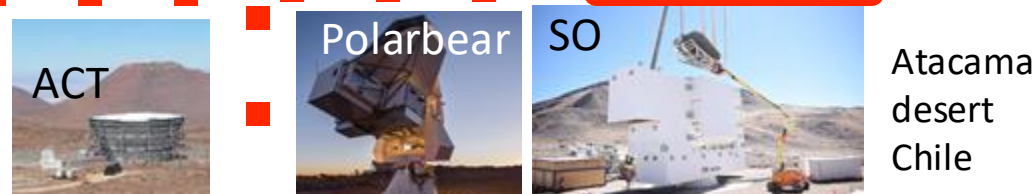**DASI**: second and third peak 2001, CMB polarization 2002
Many many many others!

List of CMB experiments:
https://lambda.gsfc.nasa.gov/product/expt/

South Pole

Atacama desert Chile

Ground, (Ballons), Satellites

Satellites

Advantages:
- Full sky observations;
- no atmosphere, large frequency span;
- in L2 Earth and sun aligned and opposite to obs direction so low contamination; stable temperature

Disadvantages:
- Slow to deploy
- small dish, limited resolution (Planck 1.5m, 7' resolution at 150Ghz);
- limited life span (determined by cooling gas/positioning fuel);
- harsh space environment, e.g. cosmic rays; instruments must survive the launch;
- inaccessible for reparations/after launch problems.

Ground

Disadvantages:
- partial sky observations;
- atmosphere limits observation windows;
- ground-pick up.

Advantages:
- Faster to deploy
- bigger dish, high resolution (e.g. SPT 10m, ~1' resolution);
- unlimited life span;
- much less cosmic rays;
- accessible for reparations/calibration.

Balloons: partial sky, less atmosphere, less ground pick up, medium to deploy, small dish, short lived, inaccessible for reparation, but payload can be recovered

Frequency coverage

Foregrounds vs CMB

Intensity

Polarization
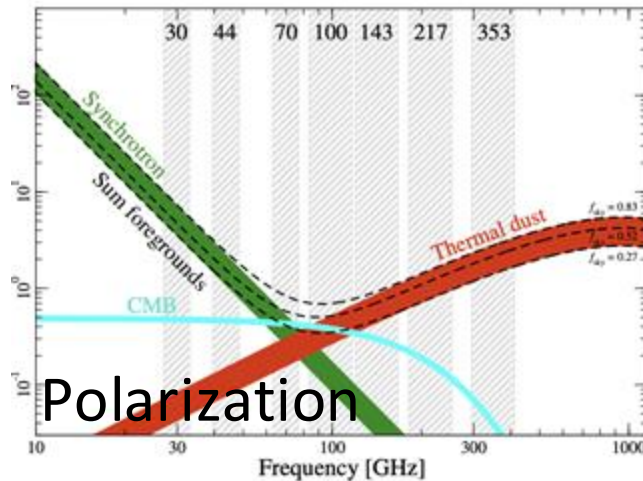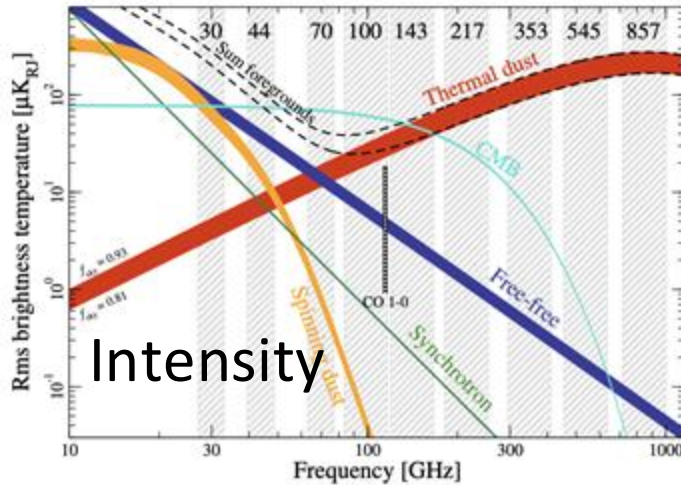
Component separation requires many frequency bands

Atmospheric transmission windows

<50GHz   100 150 220
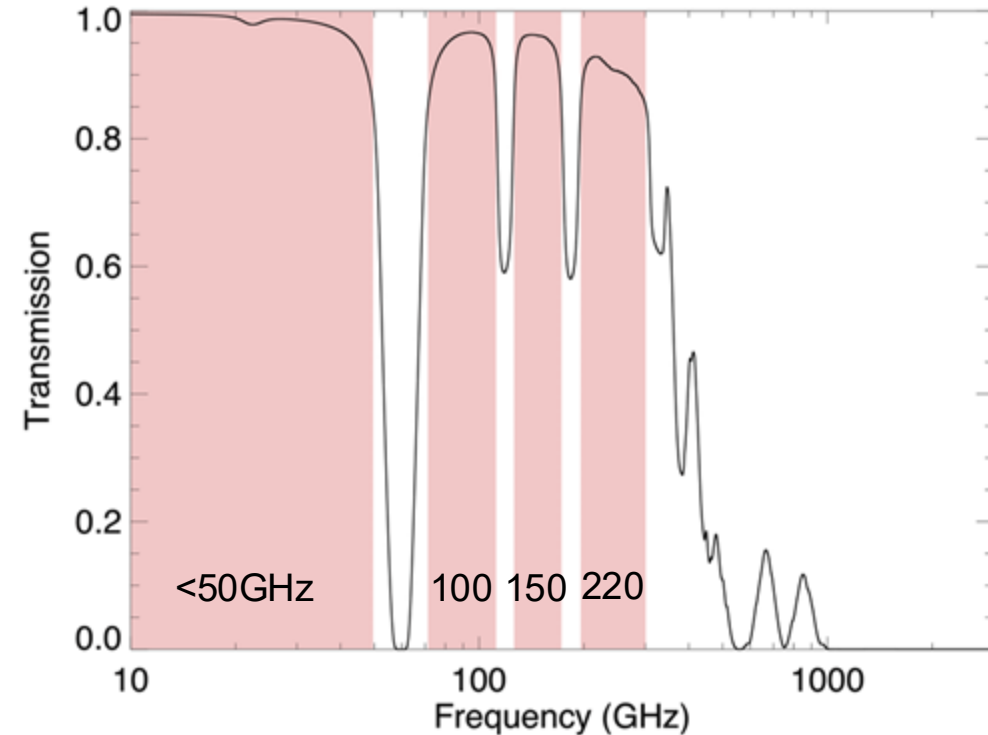
Observations from dry, elevated locations such as South Pole and Atacama desert or balloons or satellite

Ground, (Ballons), Satellites

Satellites

Advantages:
- Full sky observations;
- no atmosphere, large frequency span;
- in L2 Earth and sun aligned and opposite to obs direction so low contamination; stable temperature

Disadvantages:
- Slow to deploy
- small dish, limited resolution (Planck 1.5m, 7' resolution at 150Ghz);
- limited life span (determined by cooling gas/positioning fuel);
- harsh space environment, e.g. cosmic rays; instruments must survive the launch;
- inaccessible for reparations/after launch problems.

Ground

Disadvantages:
- partial sky observations;
- atmosphere limits observation windows;
- ground-pick up.

Advantages:
- Faster to deploy
- bigger dish, high resolution (e.g. SPT 10m, ~1' resolution);
- unlimited life span;
- much less cosmic rays;
- accessible for reparations/calibration.

Balloons: partial sky, less atmosphere, less ground pick up, medium to deploy, small dish, short lived, inaccessible for reparation, but payload can be recovered

Overview

1. A short introduction

2. The CMB sky and observations

   1. Monopole, dipole, anisotropies, polarization

   2. Ground, balloon and space experiments

3. From observations to cosmological parameters

   1. **The CMB angular power spectrum and estimator**

   2. Bayes theorem and likelihood

4. Latest results on cosmology (very Planck and SPT-3G oriented)

The angular power spectrum

- The anisotropies are distributed as a **gaussian** random field, so all information is contained in its mean and variance.

- Variance is two point correlation function in real space. Physics correlates temperature in different directions of the sky at ~1deg. Universe is isotropic, the correlation depends only on angular separation, not on the orientation.

- Physical processes put a band limit (limit to the small scale power of the CMB) so useful to decompose it into a complete set of harmonic coefficients.

- Two point correlation in harmonic space is **angular power spectrum**. Isotropy makes each multipole independent from each other.
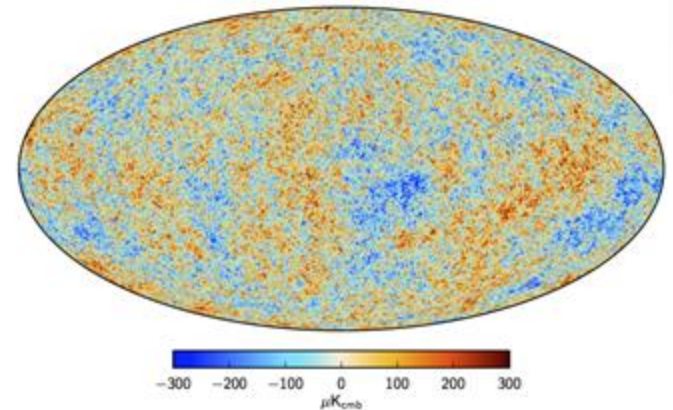
$$\Theta(\vec{x}, \hat{p}, \eta) \equiv \frac{T(\vec{x}, \hat{p}, \eta) - \bar{T}}{\bar{T}}$$

$$\Theta(\vec{x}, \hat{p}, \eta) = \sum_{l=1}^{\infty} \sum_{m=-l}^{l} a_{lm}(\vec{x}, \eta) Y_{lm}(\hat{p})$$

$$\langle a_{lm} a_{l'm'}^* \rangle = \delta_{ll'} \delta_{mm'} C_l$$

See Julien's lecture this morning!

Angular power spectrum

$D_l = C_l * l * (l+1)/2\pi$

$\mathcal{D}_\ell^{TT} \, [\mu K^2]$

Multipole l
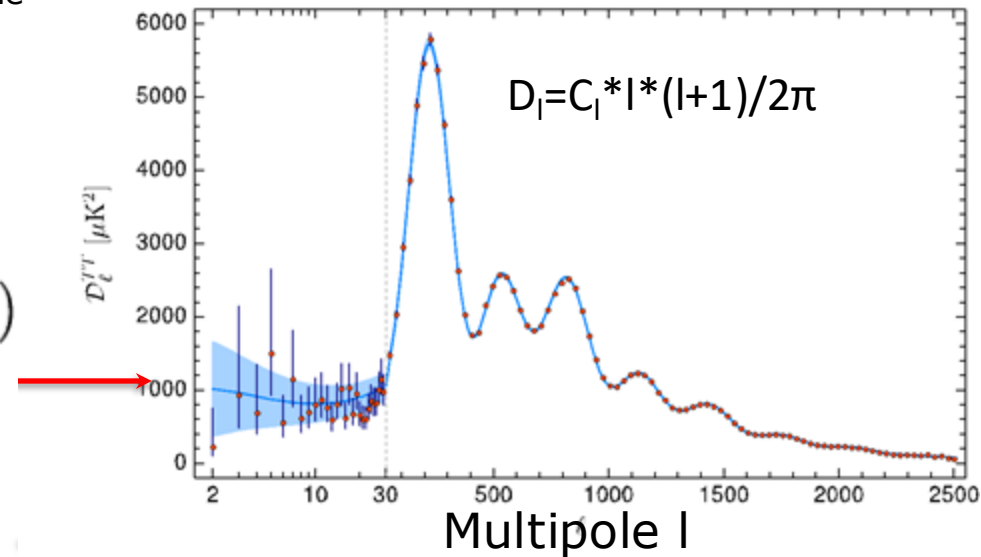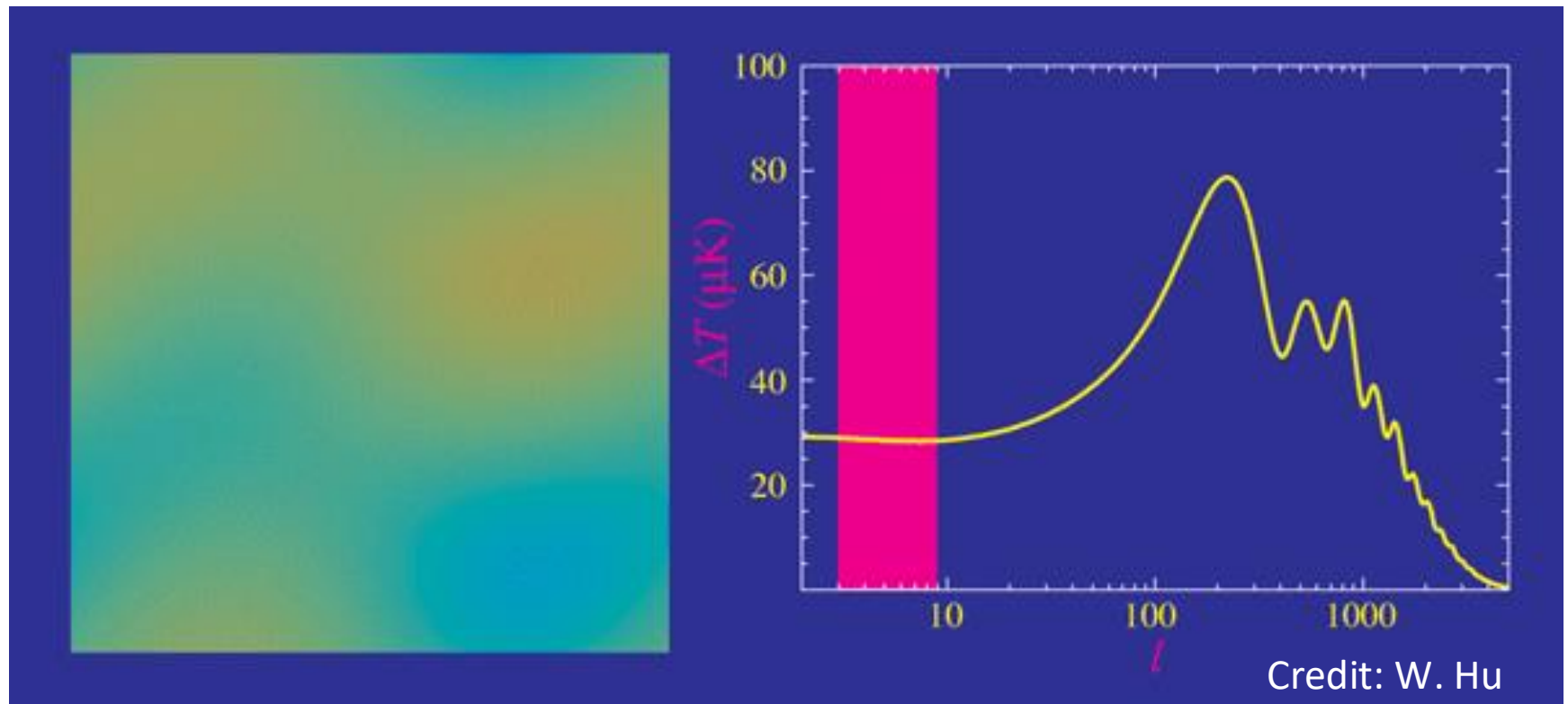
Large scales   Small scales

Cl's, Dl's and the 2-point correlation function

- We can relate the angular power spectrum to the 2-point correlation function in real space using the Legendre polynomials and the addition theorem:

$$\sum_m Y_{\ell m}^*(\mathbf{n}_i) Y_{\ell m}(\mathbf{n}_j) = \frac{2\ell+1}{4\pi} P_\ell(\hat{\mathbf{n}}_i \cdot \hat{\mathbf{n}}_j)$$

$$\langle \Theta_i \Theta_j \rangle = \sum_\ell \frac{2\ell+1}{4\pi} C_\ell P_\ell(\hat{\mathbf{n}}_i \cdot \hat{\mathbf{n}}_j)$$

- Because of isotropy, the two-point correlation function depends only on the angular separation in the sky θ, not on the orientation of the separation.

- The Dl's are just the contribution to the total temperature variance per logarithmic interval in l

$$\langle \Theta(\hat{\mathbf{n}}) \Theta(\hat{\mathbf{n}}) \rangle_{\ell \pm \Delta\ell/2} \approx \Delta\ell \frac{2\ell+1}{4\pi} C_\ell \quad \xrightarrow{\quad \Delta\ell \sim \ell \Delta \ln \ell \quad} \quad \frac{\ell^2}{2\pi} C_\ell$$

See Julien's lecture this morning!

Credit: W. Hu

Each of these maps are drawn from gaussian distributions with 0 mean and variance given by the Cl in the corresponding pink band. There is an infinite number of possible realizations.

An estimator for the Cl's

$$\langle a_{lm} a^*_{l'm'} \rangle = \delta_{ll'} \delta_{mm'} C_l$$

- We only observe one universe=> average over many realizations of the universe not possible.

- Because of isotropy, all the m-modes $a_{\ell m}$ with the same ℓ are drawn from a gaussian with the same theoretical C_ℓ. An estimator of C_ℓ is then:

$$\hat{C}_\ell = \frac{1}{2\ell + 1} \sum_m a_{lm} a^*_{l'm'}$$

At each l, 2l+1 m modes.

Sample Variance

- The expected value is <Cl>=Cl

$$\hat{C}_\ell = \frac{1}{2\ell + 1} \sum_m a_{lm} a^*_{l'm'}$$

- Since we only have 2l+1 samples for each l, there is an intrinsic uncertainty!

$$\frac{\sigma^2_{C_\ell}}{C^2_\ell} = \frac{\langle (\hat{C}_\ell - C_\ell)(\hat{C}_\ell - C_\ell) \rangle}{C^2_\ell} = \frac{\langle \hat{C}_\ell \hat{C}_\ell \rangle - C^2_\ell}{C^2_\ell}$$

$$= \frac{1}{(2\ell + 1)^2 C^2_\ell} \langle \sum_{mm'} a^*_{\ell m} a_{\ell m} a^*_{\ell m'} a_{\ell m'} \rangle - 1$$

$$= \frac{1}{(2\ell + 1)^2} \sum_{mm'} (\delta_{mm'} + \delta_{m-m'}) = \frac{2}{2\ell + 1}$$

$$\boxed{\sigma^2_{C_\ell} = \frac{2}{2\ell + 1} C^2_\ell}$$

For a gaussian field, Wick's theorem says that any N-point (N even) statistics can be written as a function of the 2-point correlation function. Useful relations in the back-up slides.
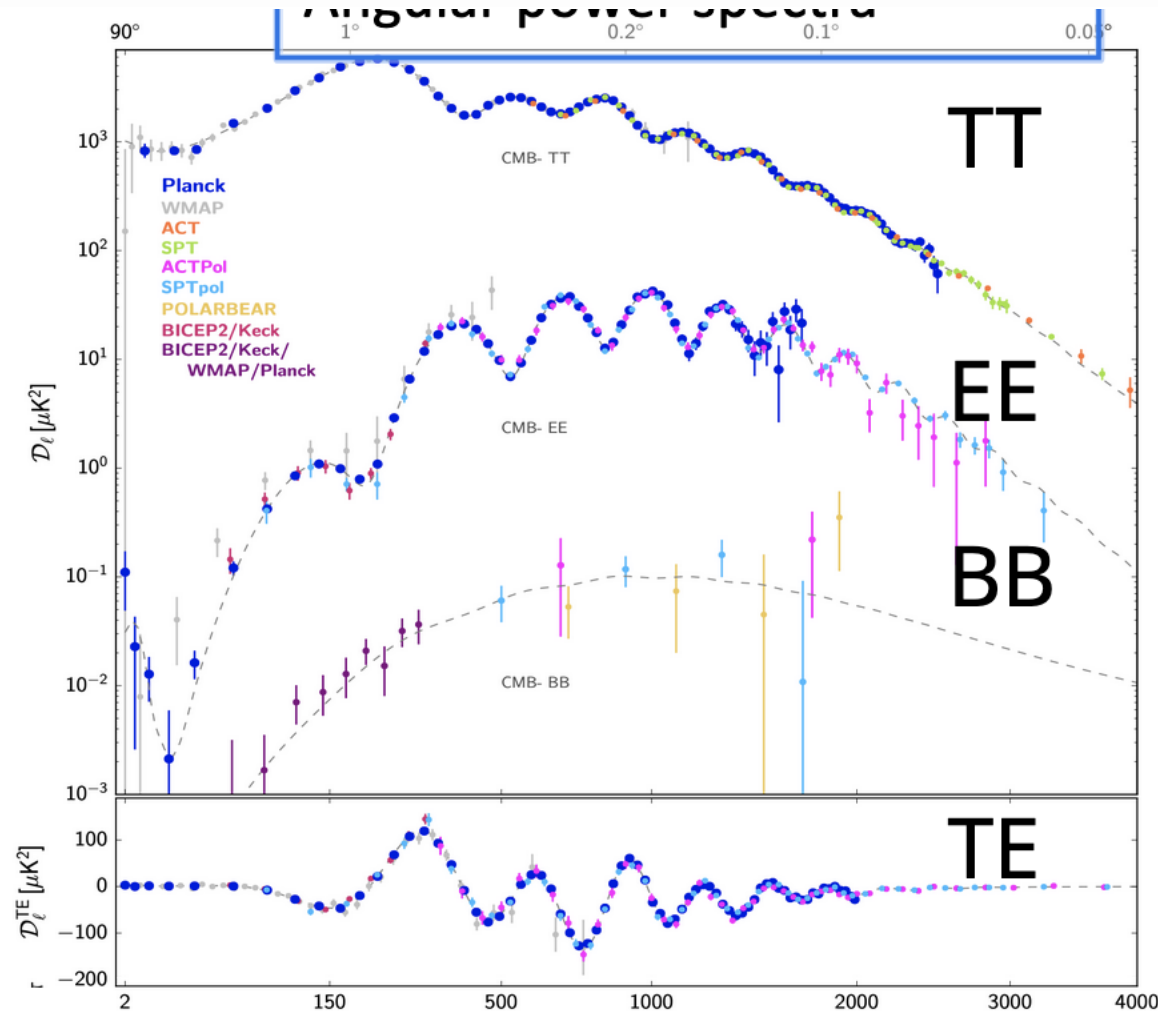
See Julien's lecture this morning!

$$C_{Tl} = \frac{1}{2l+1} \sum_m \langle a^*_{T,lm} a_{T,lm} \rangle$$

$$C_{El} = \frac{1}{2l+1} \sum_m \langle a^*_{E,lm} a_{E,lm} \rangle$$

$$C_{Bl} = \frac{1}{2l+1} \sum_m \langle a^*_{B,lm} a_{B,lm} \rangle$$

$$C_{Cl} = \frac{1}{2l+1} \sum_m \langle a^*_{T,lm} a_{E,lm} \rangle$$

Overview

1. A short introduction

2. The CMB sky and observations

   1. Monopole, dipole, anisotropies, polarization

   2. Ground, balloon and space experiments

3. From observations to cosmological parameters

   1. The CMB angular power spectrum and estimator

   2. **Bayes theorem and likelihood**

4. Latest results on cosmology (very Planck and SPT-3G oriented)

From maps to parameters

We want to measure parameters (cosmological+others) from maps. We want to evaluate the posterior distribution of the parameters θ given the data d, P(θ|d).

Bayes theorem

- To relate the posterior of the parameters given the data to the probability of the data given the parameters (the likelihood), use Bayes:

$$P(d,\theta) = P(d\,|\,\theta)P(\theta) = P(\theta\,|\,d)P(d)$$

$$\Rightarrow P(\theta\,|\,d) = \frac{P(d\,|\,\theta)P(\theta)}{P(d)}$$

Posterior

Likelihood

Prior

So, what is the likelihood for CMB data?

Map-based Likelihood

- CMB maps (m) have gaussian fluctuations with zero mean and pixel-space covariance matrix M.

$$\mathcal{L}(C_\ell) = \mathcal{P}(\boldsymbol{m}|C_\ell) = \frac{1}{|2\pi M|^{1/2}} \exp\left(-\frac{1}{2}\boldsymbol{m}^{T} M^{-1}\boldsymbol{m}\right)$$

m= data vector containing the pixels of the map.

M=S(θ)+N=pixel covariance matrix, where S is the two-point correlation function that depends on cosmological parameters

- In practice, this is only used at large scales/low resolutions. Inversion and determinant of covmat is unfeasible for maps with O(10^6) pixels.

The full-sky likelihood of the C_l

- Instead of using the maps, we can compress the information in the estimator of $\hat{C}_l$ from the maps, and use that as our « data».
- For an ideal noiseless full-sky experiment, temperature alone.

$$\hat{C}_\ell = \frac{1}{2\ell + 1} \sum_{m=-\ell}^{\ell} |a_{\ell m}|^2.$$

- The sum of the square of $v=2l+1$ normal N(0,1) variables $(a_{lm}/\text{sqrt}(C_l))$ (with C_l the theoretical C_l) has a χ^2 distribution, i.e.:

$$\hat{Y} = \sum_{m=-\ell}^{\ell} \left| \frac{a_{lm}}{\sqrt{C_\ell}} \right|^2 = (2\ell+1)\hat{C}_\ell / C_\ell \rightarrow \quad \chi^2 \text{ distribution with } v=2\ell+1 \text{ d.o.f.}$$

$$\hat{C}_\ell = \hat{Y} C_\ell / (2\ell+1) \rightarrow \quad \Gamma \text{ distribution with } v=2\ell+1 \text{ d.o.f.}$$

$$<\hat{C}_\ell> = C_\ell$$

$$Var(\hat{C}_\ell) = \frac{2(C_\ell)^2}{v} = \frac{2(C_\ell)^2}{2\ell+1} \quad \text{Cosmic Variance}$$

- See Percival and Brown 2006.
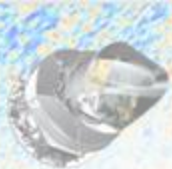
The full-sky likelihood of the C$_l$

- If we have polarization as well, this formalism extends to give a Wishart distribution for:

$$\hat{\mathbf{X}}_C = \begin{pmatrix} \hat{C}_l^{\mathrm{TT}} \\ \hat{C}_l^{\mathrm{TE}} \\ \hat{C}_l^{\mathrm{EE}} \end{pmatrix}$$

- For ν -> ∞, Gaussian distribution (for central limit theorem), with covariance:

$$\mathbf{Y} = \frac{1}{\nu} \begin{pmatrix} 2(C_l^{\mathrm{TT}})^2 & 2C_l^{\mathrm{TT}}C_l^{\mathrm{TE}} & 2(C_l^{\mathrm{TE}})^2 \\ 2C_l^{\mathrm{TT}}C_l^{\mathrm{TE}} & C_l^{\mathrm{TT}}C_l^{\mathrm{EE}} + (C_l^{\mathrm{TE}})^2 & 2C_l^{\mathrm{TE}}C_l^{\mathrm{EE}} \\ 2(C_l^{\mathrm{TE}})^2 & 2C_l^{\mathrm{TE}}C_l^{\mathrm{EE}} & 2(C_l^{\mathrm{EE}})^2 \end{pmatrix}$$

Life is more complicated...

- Masking the sky, noise, beams invalidates the analytic calculation of the likelihood

- Pseudo-Cl in presence of sky cut:

$$
\begin{aligned}
\tilde{a}_{\ell m} &= \int d\mathbf{n} \Delta T(\mathbf{n}) W(\mathbf{n}) Y_{\ell m}^*(\mathbf{n}), \\
&= \sum_{\ell' m'} a_{\ell' m'} \int d\mathbf{n} Y_{\ell' m'}(\mathbf{n}) W(\mathbf{n}) Y_{\ell m}^*(\mathbf{n}) \\
&= \sum_{\ell' m'} a_{\ell' m'} K_{\ell m l' m'}[W],
\end{aligned}
$$

Hivon 2002

- $\tilde{a}_{lm}$ are still gaussian, but not independent since they all depend on the sum of $a_{l'm'}$. $\tilde{a}_{l1m1}$ and $\tilde{a}_{l2m2}$ are correlated

Life is more complicated…

- Masking the sky, noise, beams invalidates the analytic calculation of the likelihood

$$\tilde{C}_\ell = \frac{1}{2\ell + 1} \sum_{m=-\ell}^{\ell} |\tilde{a}_{\ell m}|^2$$

$$\tilde{a}_{\ell m} = \sum_{\ell' m'} a_{\ell' m'} K_{\ell m l' m'}[W]$$

The pseudo Cl are now the sum of the square of gaussians with different variances. Not distributed like a Wishart!

The Gaussian approximation

- For large degrees of freedom $v=2l+1$, the distribution of the $\hat{C}_l$ tends to a gaussian distribution (central limit theorem).

$$-\ln \mathcal{L}(\hat{\boldsymbol{C}}|\boldsymbol{C}(\theta)) = \frac{1}{2}\left[\hat{\boldsymbol{C}} - \boldsymbol{C}(\theta)\right]^T \mathbf{C}^{-1}\left[\hat{\boldsymbol{C}} - \boldsymbol{C}(\theta)\right] + \text{const}$$

C_l covariance matrix
(can be estimated with a fixed fiducial set of parameters)

data

Model (that depends on the parameters we want to determine)

It works only at high-l (large dof). Used in Planck, ACT, SPT.

What goes in the likelihood:

$$- \ln \mathcal{L}(\hat{C}|C(\theta)) = \frac{1}{2}\left[\hat{C} - C(\theta)\right]^T \mathbf{C}^{-1}\left[\hat{C} - C(\theta)\right] + \text{const}$$

Power spectrum estimation from the maps at different frequencies

$$\hat{C}^{TT} = \left(\hat{C}^{TT}_{100\times100}, \hat{C}^{TT}_{143\times143}, \hat{C}^{TT}_{143\times217}, \hat{C}^{TT}_{217\times217}\right)$$
$$\hat{C}^{EE} = \left(\hat{C}^{EE}_{100\times100}, \hat{C}^{EE}_{100\times143}, \hat{C}^{EE}_{100\times217}, \hat{C}^{EE}_{143\times143}, \hat{C}^{EE}_{143\times217}, \hat{C}^{EE}_{217\times217}\right)$$
$$\hat{C}^{TE} = \left(\hat{C}^{TE}_{100\times100}, \hat{C}^{TE}_{100\times143}, \hat{C}^{TE}_{100\times217}, \hat{C}^{TE}_{143\times143}, \hat{C}^{TE}_{143\times217}, \hat{C}^{TE}_{217\times217}\right).$$

Model includes:
* the theoretical CMB power spectrum depending on a cosmological model
* the contribution from foregrounds
* Instrumental and systematic effects such as calibration, beams, etc…

Covariance matrix, estimated on simulations and/or analytically

$$\mathbf{C} = \begin{pmatrix} C^{TTTT} & C^{TTEE} & C^{TTTE} \\ C^{EETT} & C^{EEEE} & C^{EETE} \\ C^{TETT} & C^{TEEE} & C^{TETE} \end{pmatrix}$$

$$C^{TTTT} = \begin{pmatrix} (100\times100)\times(100\times100) & (100\times100)\times(143\times143) & (100\times100)\times(217\times217) & (100\times100)\times(143\times217) \\ (143\times143)\times(100\times100) & (143\times143)\times(143\times143) & (143\times143)\times(217\times217) & (143\times143)\times(143\times217) \\ (217\times217)\times(100\times100) & (217\times217)\times(143\times143) & (217\times217)\times(217\times217) & (217\times217)\times(143\times217) \\ (143\times217)\times(100\times100) & (143\times217)\times(143\times143) & (143\times217)\times(217\times217) & (143\times217)\times(143\times217) \end{pmatrix}$$

Exploring the likelihood to infer cosmological parameters

$$- \ln \mathcal{L}(\hat{C}|C(\theta)) = \frac{1}{2}\left[\hat{C} - C(\theta)\right]^{T} C^{-1}\left[\hat{C} - C(\theta)\right] + \text{const}$$

Since the dependence of the Cl on parameters is non-linear and non-trivial, we need Monte Carlo Markov Chains to explore the likelihood to map the posterior distribution of parameters.
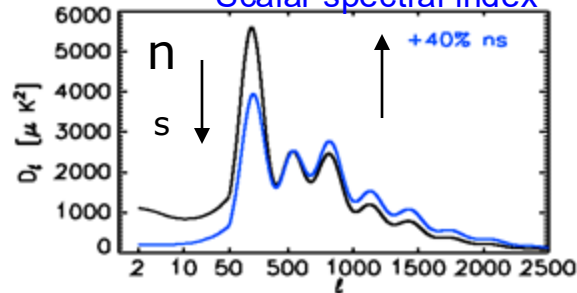
The ΛCDM model

Standard model of cosmology: General relativity to describe gravity, standard model of particles for particle interactions, cosmological constant for dark energy and cold dark matter.

Scalar Amplitude primordial spectru
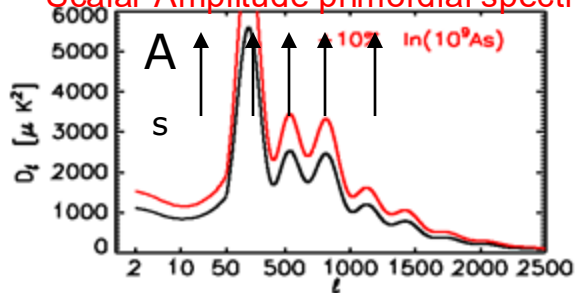
A_s 10% ln($10^9 A_s$)

Scalar spectral index

n_s +40% n_s

Angular scale of sound horizon

θ   +8% θ

Optical depth to reionization

τ   +40% τ

Physical density of baryons

$\Omega_b h^2$ +40% $\Omega_b h^2$
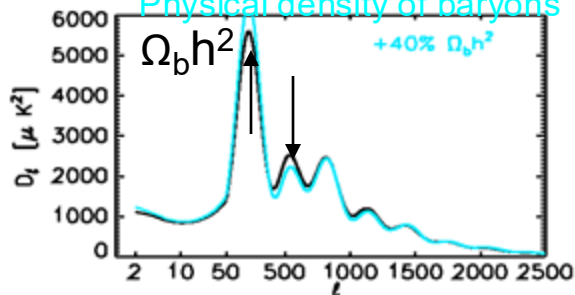
Physical density of dark matter
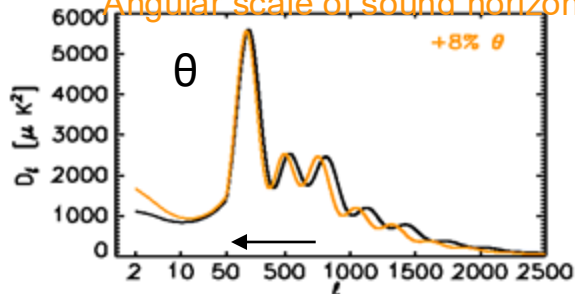
$\Omega_c h^2$ +40% $\Omega_c h^2$

6 parameters:

- Initial conditions A_s, n_s
- Acoustic scale of sound horizon θ
- Reionization τ
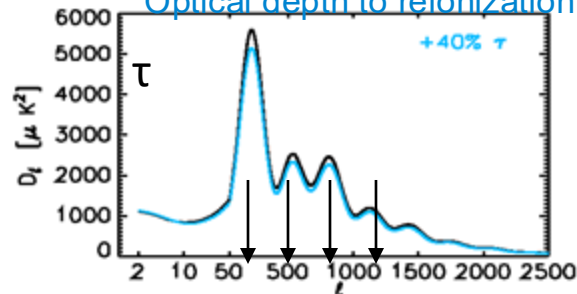- Dark Matter density $\Omega_c h^2$
- Baryon density $\Omega_b h^2$

Assumptions:
- Adiabatic initial conditions
- Neff=3.046
- 1 massive neutrino 0.06eV.
- Tanh reionization (Δz=0.5)
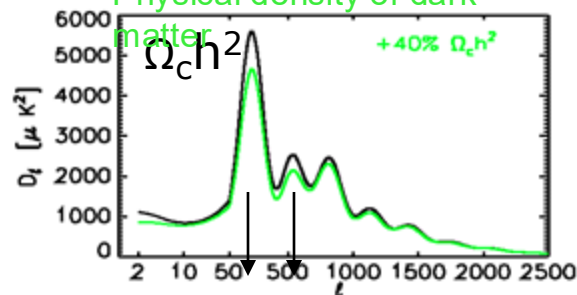
The CMB is a laboratory to constrain cosmology and fundamental physics

Overview

1. A short introduction

2. The CMB sky and observations

   1. Monopole, dipole, anisotropies, polarization

   2. Ground, balloon and space experiments

3. From observations to cosmological parameters

   1. The CMB angular power spectrum and estimator

   2. Bayes theorem and likelihood

4. **Latest results on cosmology (very Planck and SPT-3G oriented)**

The Planck satellite

3rd generation full sky satellites (COBE, WMAP)
Launched in 2009, operated till 2013.
2 Instruments, 9 frequencies to **disentangle CMB from foregrounds**.

LFI:
- 22 radiometers at **30, 44, 70 Ghz.**

HFI:
- 50 bolometers (32 polarized) at **100, 143, 217, 353, 545, 857 Ghz.**
- **30-353 Ghz polarized.**

- **1st release 2013: Nominal mission,**15.5 months, Temperature only (large scale polarization from WMAP).

- **2nd release 2015: Full mission**, 29 months for HFI, 48 months for LFI, Temperature + Polarization, large scale pol. from LFI.
  Intermediate results 2016: low-l polarization from HFI

- **3nd release 2018 (PR3): Full mission, improved polarization, low/high-l from HFI.** Better control of systematics specially in pol., still systematics limited.

Post PR3: new maps PR4 (LFI+HFI map-making, improved low-ell in polarization); new likelihoods and parameters from PR4; new maps Sroll2 (better low-ell polarization); several new estimation of opt. depth to reionization.
No substantially new result compared to PR3.

47

Planck 2018 power spectra

Planck collaboration 2018 VI.

ΛCDM is an excellent fit to the data. No evidence of preference for classical extensions of ΛCDM from Planck (and non-classical ones: dm annihilation, variation of fund. constants, primordial magnetic fields, variations in recombination, isocurvature, sterile neutrinos, dark energy, modified gravity).....

Baseline ΛCDM results 2018 (Temperature+polarization+CMB lensing)

	Mean	σ	[%]
$\Omega_b h^2$ Baryon density	0.02237	0.00015	0.7
$\Omega_c h^2$ DM density	0.1200	0.0012	1
100θ Acoustic scale	1.04092	0.00031	0.03
τ Reion. Optical depth	0.0544	0.0073	13
$\ln(A_s 10^{10})$ Power Spectrum amplitude	3.044	0.014	0.7
n_s Scalar spectral index	0.9649	0.0042	0.4
H_0 Hubble	67.36	0.54	0.8
Ω_m Matter density	0.3153	0.0073	2.3
σ_8 Matter perturbation amplitude	0.8111	0.0060	0.7

- Most of parameters determined at (sub-) percent level!

- Best determined parameter is the angular scale of sound horizon θ to 0.03%.

- τ low and tight, reionization at z~7.

- n_s is 8σ away from scale invariance (even in extended models, always >3σ)

- Best (indirect) **0.8%** determination of the Hubble constant to date.

Planck 2018 results. VI. Cosmological parameters (SG co-correponding author)   49

The Hubble tension

The Hubble tensions is the difference in the expansion rate of the universe today as measured from Supernovae IA calibrated with Cepheids and from the CMB and other early universe probes. Since the early universe measurements depend on a cosmological model, it could indicate the need of a change in the model, and thus **the discovery of new physics.**

Murakami+ 2023
Breuval+ 2024

5.7σ tension

Supernovae IA
+cepheid
SH0ES
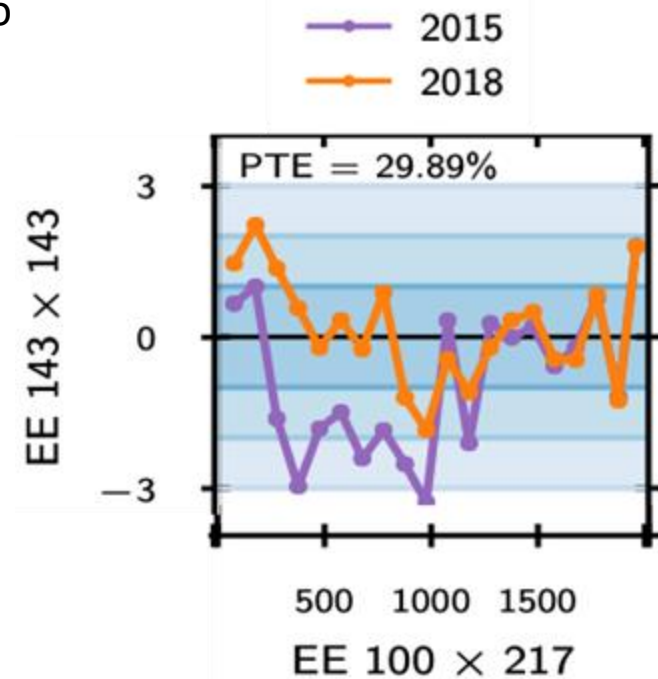H_0= **73.29±0.90** km/s/Mpc.

CMB (also BAO)
Planck 2018

H_0 =**67.36±0.54** km/s/Mpc.

The importance of robustness of results

- A **large impact** on the field (tens of thousands of citations)
- **Responsibility to provide the community robust results.**
- Many Tests:
  - **Redundancy** of the data is key in order to be able to do consistency tests at power spectrum or cosmological parameters level from **subsets of the data**, i.e.
    - from different frequency channels, which also corresponds to different detectors.
    - from different map cuts (half mission, versus detector sets)
    - from TT, TE or EE (model dependent).

  - Tested the consistency between a large number of **different analysis choices** on cosmological **parameters** (model dependent).
  - Compared different **analysis pipelines**, which was essential to improve the robustness of the final product.
  - **End-to-end simulations** also allowed us to validate the pipeline.

Difference between CMB-only, frequency power spectra in units of error bars in 2015 and 2018

In the second Planck 2015 release, test failed for polarization data. culprit was uncorrected systematics.

Planck 2018 results V.

Beyond Planck

- Planck results had a tremendous impact on cosmology. They confirmed the LCDM model. They were checked with many consistency tests.

- Planck opened new mysteries, such as the Hubble tension, that we will explore with upcoming and future experiments.

- There is still a very large amount of information in CMB to be uncovered. Upcoming experiments have two main goals:

    - at large scales in polarization, to detect primordial gravitational waves and measure reionization.

    - At small angular scales in polarization, to test cosmological models and the properties of the energy content of the universe.

NB: only full sky observations from satellites have access to very large scales (l~2).
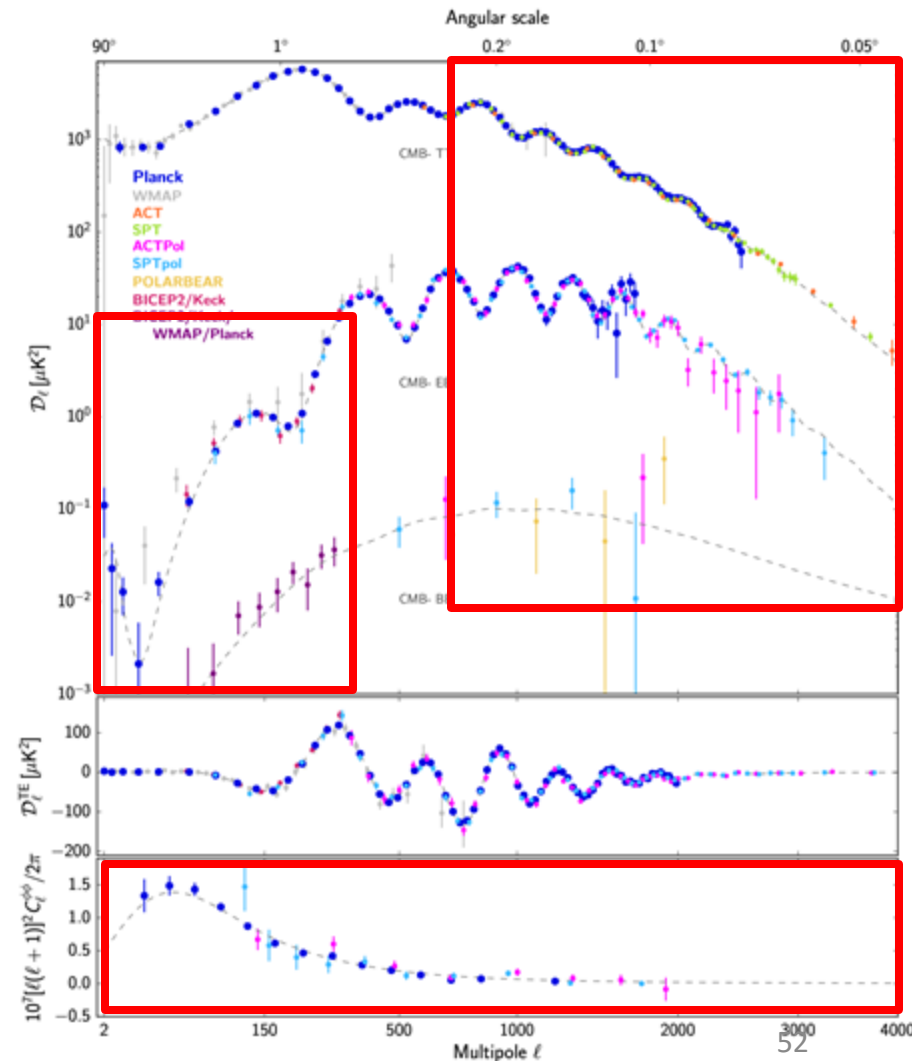
The quest for primordial gravitational waves

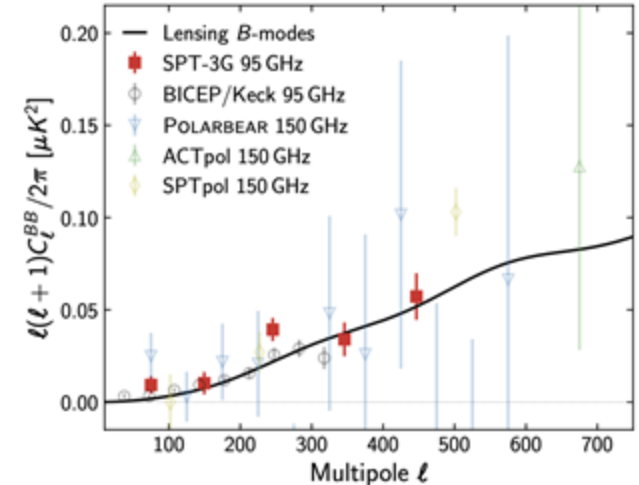## Current best constraints from experiments at the South Pole
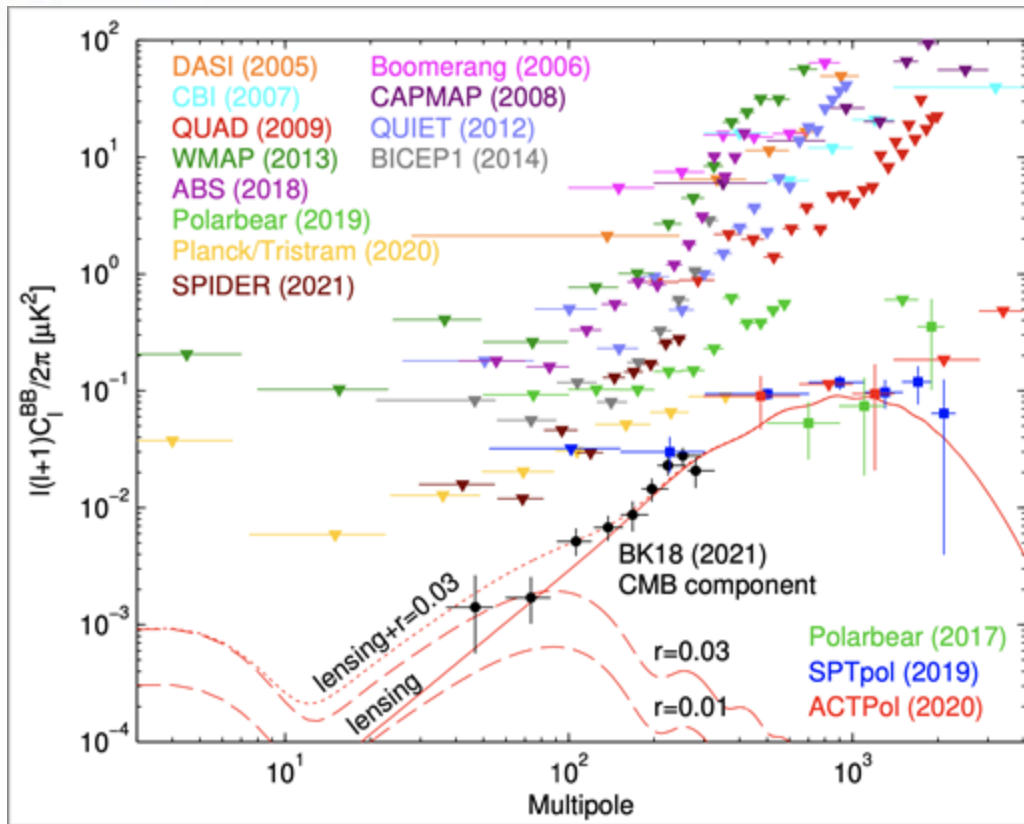
FIG. 7. Ground-based B-mode measurement landscape. Data are from SPTpol [32], ACT [28], POLARBEAR [1], and BICEP/Keck [4].

Best constraints on BB from BICEP/Keck (BK collaboration 2021)

BICEP/Keck

Second best constraints from SPT-3G (Zebrowski+ 2025)

Best CMB high resolution experiments

ACT:

- a 6m telescope observing from Atacama at 98, 150, 220Ghz.

- Recently had last data-release, ACT DR6.

- Observed 16000 square degrees, only 10000 used for cosmology.

- Recently substituted by Simons Observatory, which had first light this year.

ACT

SPT-3G:

- a 10m telescope observing from the Amudsen-Scott station at the South Pole.

- Recently had release of results, SPT-3G D1, based on 1500 square degrees.

- Already observed a total of 10000 square degrees, analysis in progress.

SPT

The South Pole Telescope

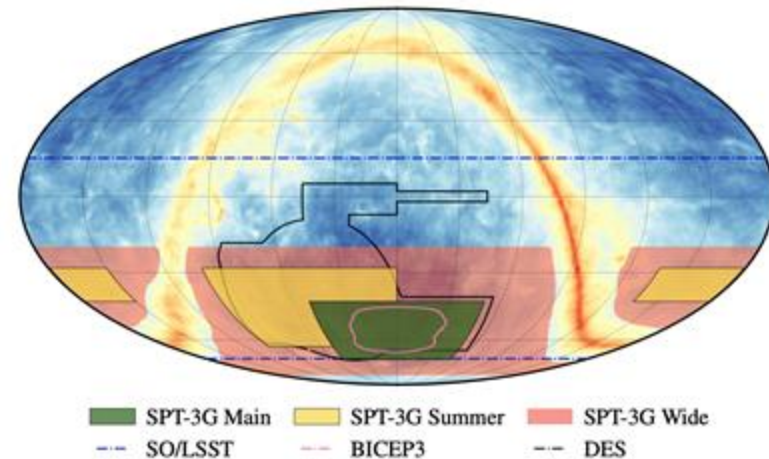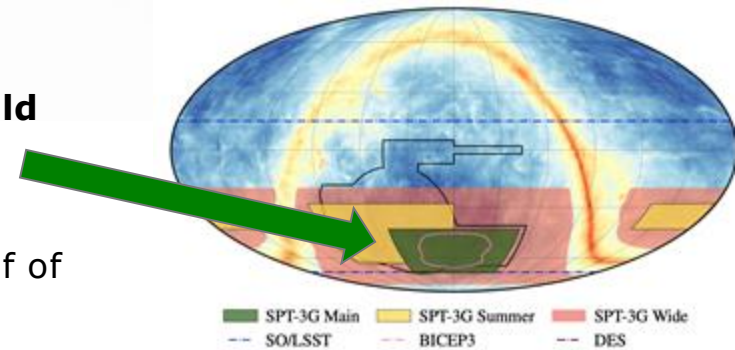- SPT is a 10m telescope at the South Pole. It is observing with its third generation camera, SPT-3G, with ~16,000 detectors at 95, 150, and 220 GHz at high resolution (~1 arcmin).

- It has observed **25%** of the sky:
  - **Main** Winter Field **1500 deg²** (5yrs done, 2yr TBD)
    Coadded noise **~17X** better than Planck**.**

  - **Summer** fields **2650 deg²** (4yrs done),
    coadded noise **4X** better than Planck**.**

  - **Wide** field **6000 deg²** (1yr)
    coadded noise **3X** better than Planck.

- Many scientific goals:
  - **Cosmological constraints from CMB primary anisotropies and CMB lensing**
  - Delensing of the BICEP/Keck field to improve constraints on tensor to scalar ratio r.
  - High-ell TT foregrounds (including kSZ), Cross-correlations with other surveys, High-z galaxies, Clusters of galaxies, Transients etc…

SPT-3G Main | SPT-3G Summer | SPT-3G Wide
SO/LSST | BICEP3 | DES

*Planck 2018 had 74, 36, 53 µK-arcmin, coadded 27.6 µK-arcmin) over ~80% sky,
ACT-DR6 has 15 µK-arcmin over 40% of sky

Prabhu…,**SG** et al. 2024

Published power spectrum SPT-3G results from Main field

Results based on the observations of the small but **deep Main field** observed during the Austral winter.

- **4 months of observations "SPT-3G 2018":** Used only half of the focal plane [published in 2021-2023]:
  - Analysis of **TEEE** (Dutcher,...SG+ 2021, Balkenhol,...SG+ 2021)
  - Analysis of **TTTEEE** (Balkenhol,...SG+ 2023)

- **2 years of observations "SPT-3G 2 year Main field":** Based on ~16 months of observations with the full focal plane.

  - Cosmology from CMB lensing and delensed EE power from polarization with **MUSE** (Ge., Millea,...SG+ 2024)

  - Constraints on Inflationary Gravitational Waves from large scale **BB** (Zebrowski,...SG+ 2025)

  - SPT-3G D1: CMB temperature and polarization power spectra and cosmology from 2019 and 2020 observations of the SPT-3G Main field (Camphuis,...SG+ 2025)

SPT-3G D1: CMB temperature and polarization power spectra and cosmology from 2019 and 2020 observations of the SPT-3G Main field

E. Camphuis [1], W. Quan,[2, 3, 4] L. Balkenhol [1], A. R. Khalife [1], F. Ge,[5, 6, 7] F. Guidi [1], N. Huang [8],
G. P. Lynch [7], Y. Omori,[9, 4] C. Trendafilova,[10] A. J. Anderson [11, 4, 9], B. Ansarinejad,[12] M. Archipley [9, 4],
P. S. Barry [34], K. Benabed,[1] A. N. Bender [2, 4, 9], B. A. Benson [11, 4, 9], F. Bianchini [5, 6, 13], L. E. Bleem [2, 4, 9],
F. R. Bouchet [1], L. Bryant,[14] M. G. Campitiello,[2] J. E. Carlstrom [4, 14, 3, 2, 9], C. L. Chang,[2, 4, 9] P. Chaubal,[12]
P. M. Chichura [3, 4], A. Chokshi,[9] T.-L. Chou [9, 4, 15], A. Coerver,[8] T. M. Crawford [9, 4], C. Daley [16, 17],
T. de Haan,[18] K. R. Dibert,[9, 4] M. A. Dobbs,[19, 20] M. Doohan,[12] A. Doussot,[1] D. Dutcher [21], W. Everett,[22]
C. Feng,[23] K. R. Ferguson [24, 25], K. Fichman,[3, 4] A. Foster [21], S. Galli,[1] A. E. Gambrel,[4] R. W. Gardner,[14]
N. Goeckner-Wald,[6, 5] R. Gualtieri [2, 26], S. Guns,[8] N. W. Halverson,[27, 28] E. Hivon [1], G. P. Holder [23],
W. L. Holzapfel,[8] J. C. Hood,[4] A. Hryciuk,[3, 4] F. Kéruzoré,[2] L. Knox,[7] M. Korman,[29] K. Kornoelje,[9, 4, 2]
C.-L. Kuo,[5, 6, 13] K. Levy,[12] A. E. Lowitz [4], C. Lu,[23] A. Maniyar,[5, 6, 13] E. S. Martsen,[9, 4] F. Menanteau,[17, 10]
M. Millea [8], J. Montgomery,[19] Y. Nakato,[6] T. Natoli,[4] G. I. Noble [30, 31], A. Ouellette,[23] Z. Pan [2, 4, 3],
P. Paschos,[14] K. A. Phadke [17, 10, 32], A. W. Pollak,[9] K. Prabhu,[7] S. Raghunathan [10], M. Rahimi,[12] A. Rahlin [9, 4],
C. L. Reichardt [12], M. Rouble,[19] J. E. Ruhl,[29] E. Schiappucci,[12] A. Simpson,[9, 4] J. A. Sobrin [11, 4],
A. A. Stark,[33] J. Stephen,[14] C. Tandoi,[17] B. Thorne,[7] C. Umilta [23], J. D. Vieira [17, 23, 10], A. Vitrier [1],
Y. Wan,[17, 10] N. Whitehorn [25], W. L. K. Wu [5, 13], M. R. Young,[11, 4] and J. A. Zebrowski[4, 9, 11]

(SPT-3G Collaboration)

[1] Sorbonne Université, CNRS, UMR 7095, Institut d'Astrophysique de Paris, 98 bis bd Arago, 75014 Paris, France
[2] High-Energy Physics Division, Argonne National Laboratory,
9700 South Cass Avenue, Lemont, IL, 60439, USA
[3] Department of Physics, University of Chicago, 5640 South Ellis Avenue, Chicago, IL, 60637, USA
[4] Kavli Institute for Cosmological Physics, University of Chicago,
5640 South Ellis Avenue, Chicago, IL, 60637, USA

25 June 2025

Etienne Camphuis (IAP)
Postdoc at IAP

Wei Quan (U. Chicago)
Postdoc at Argonne

Lennart Balkenhol
Postdoc at IAP

Ali Rida Khalife
Postdoc at IAP

A New Dataset: SPT-3G D1

SPT-3G Main (this work)   SPT-3G Summer   SPT-3G Wide
Planck galactic mask   ACT DR6

- SPT-3G D1: observations taken in the 2019 & 2020 austral winter seasons (March to November) on the SPT-3G Main field

  - Much larger than the 2018 dataset (~2x detectors, ~4x observing time)

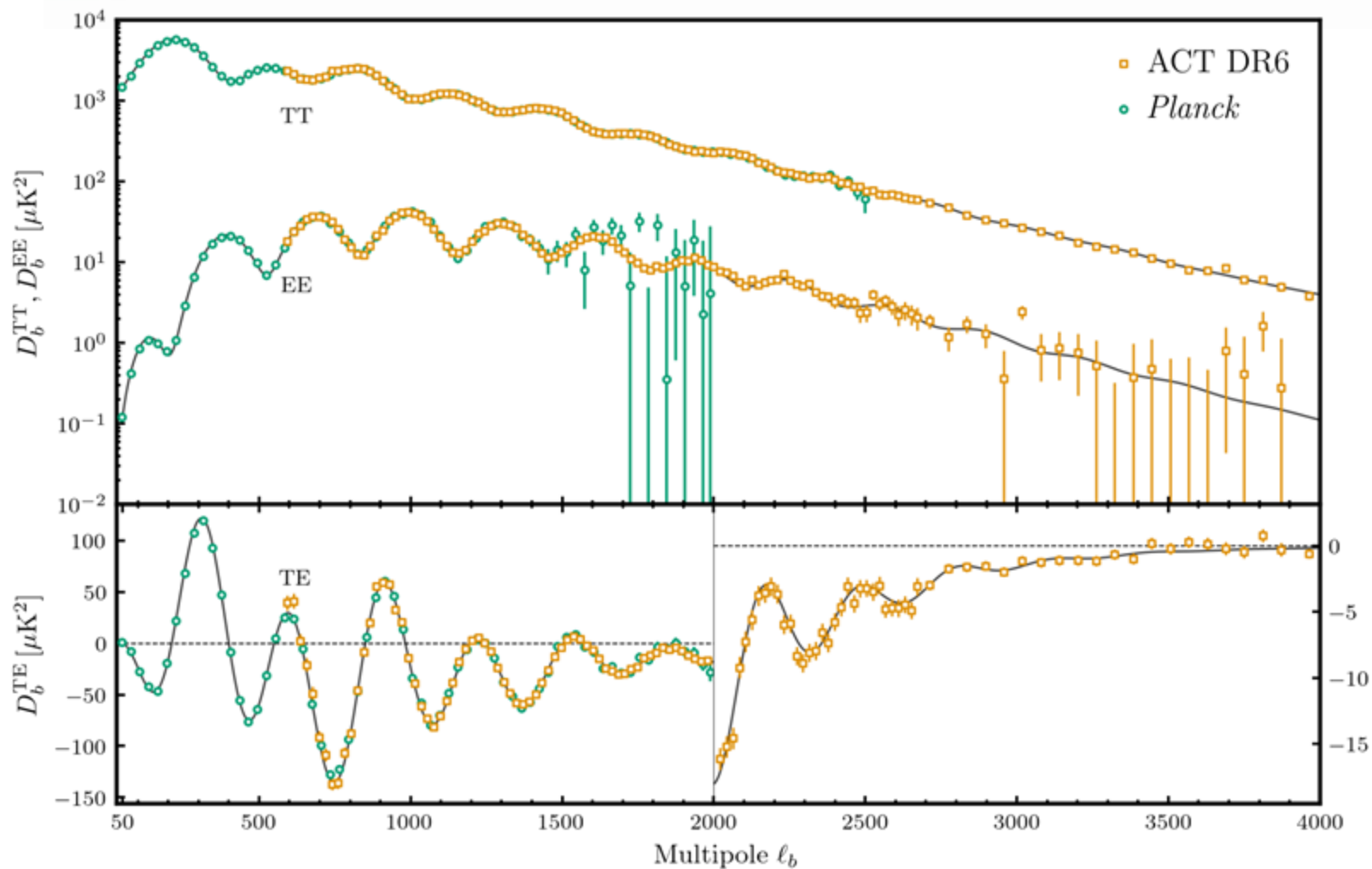 - Small, deep survey complementing *Planck* and ACT

Deepest CMB maps at arcminute resolution for TT/TE/EE measurements

Planck PR3 numbers based on *Planck* 2018 results IV
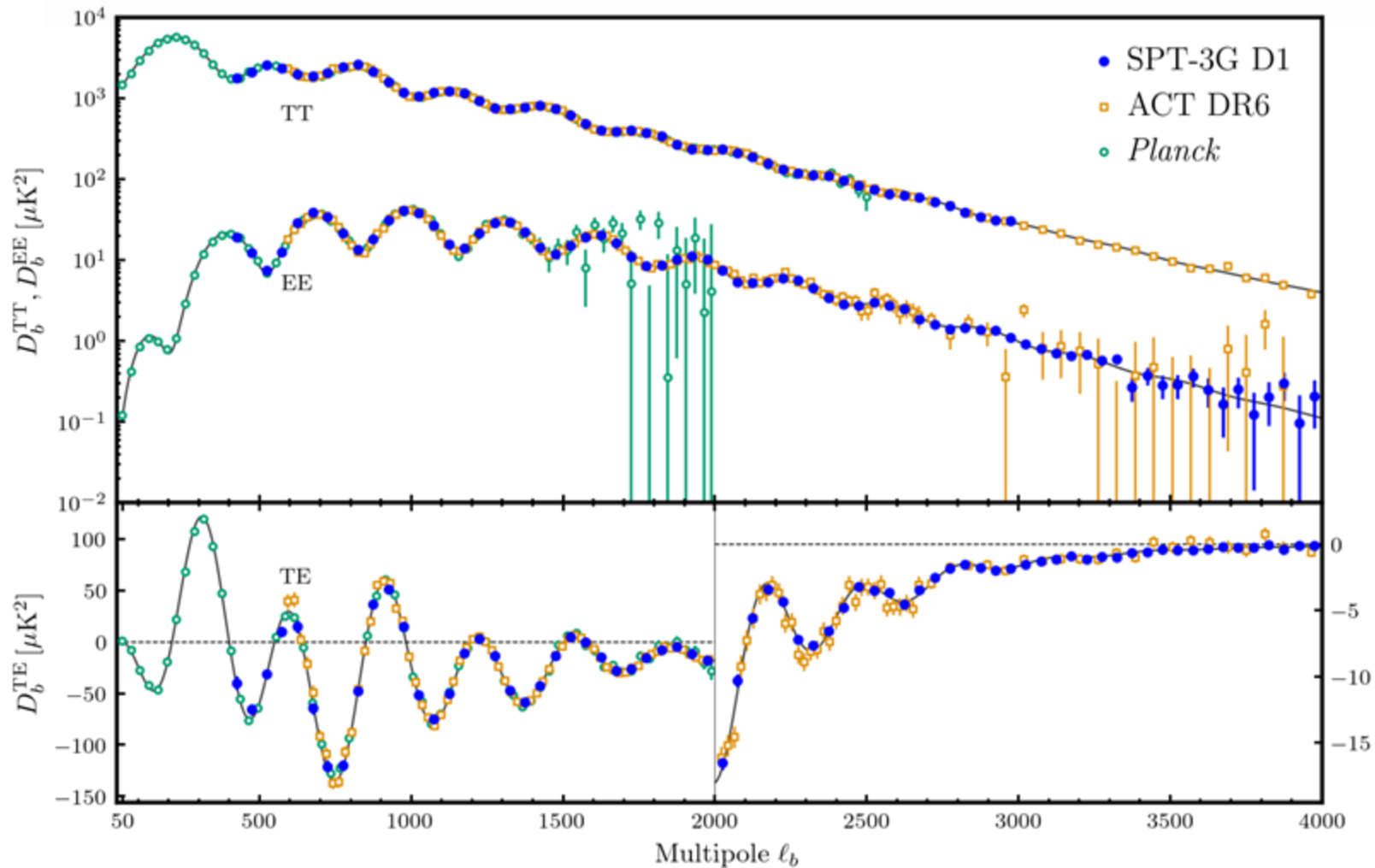ACT DR6 numbers from Næss *et al.*, 2025
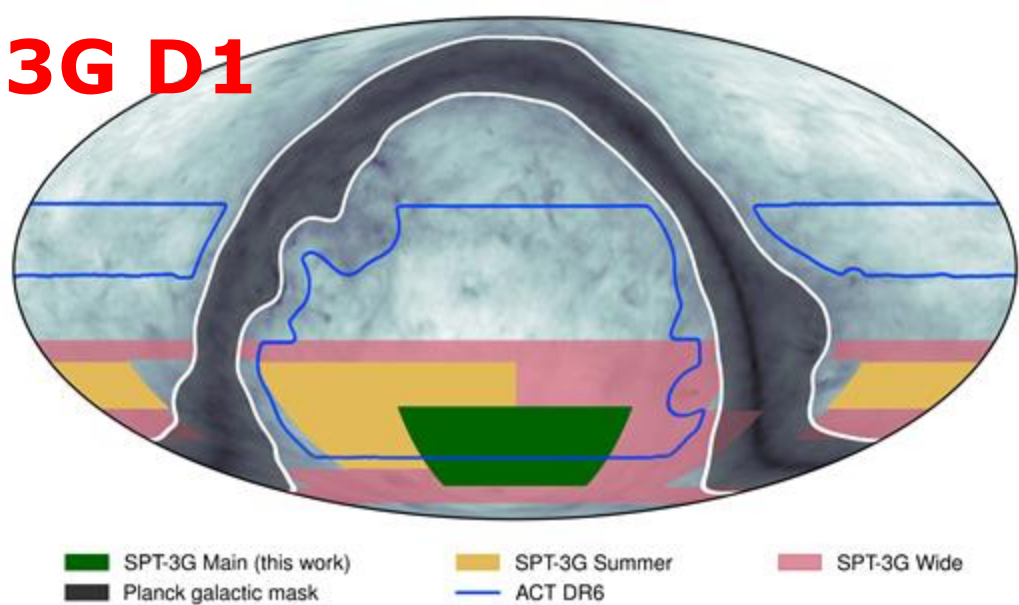
	Observed sky fraction [%]	Coadded noise level [μK-arcmin]
Planck PR3	100	35
ACT DR6	45 (25 for cosmology)	10
SPT-3G D1	**4**	**3.3**

CMB angular power spectra
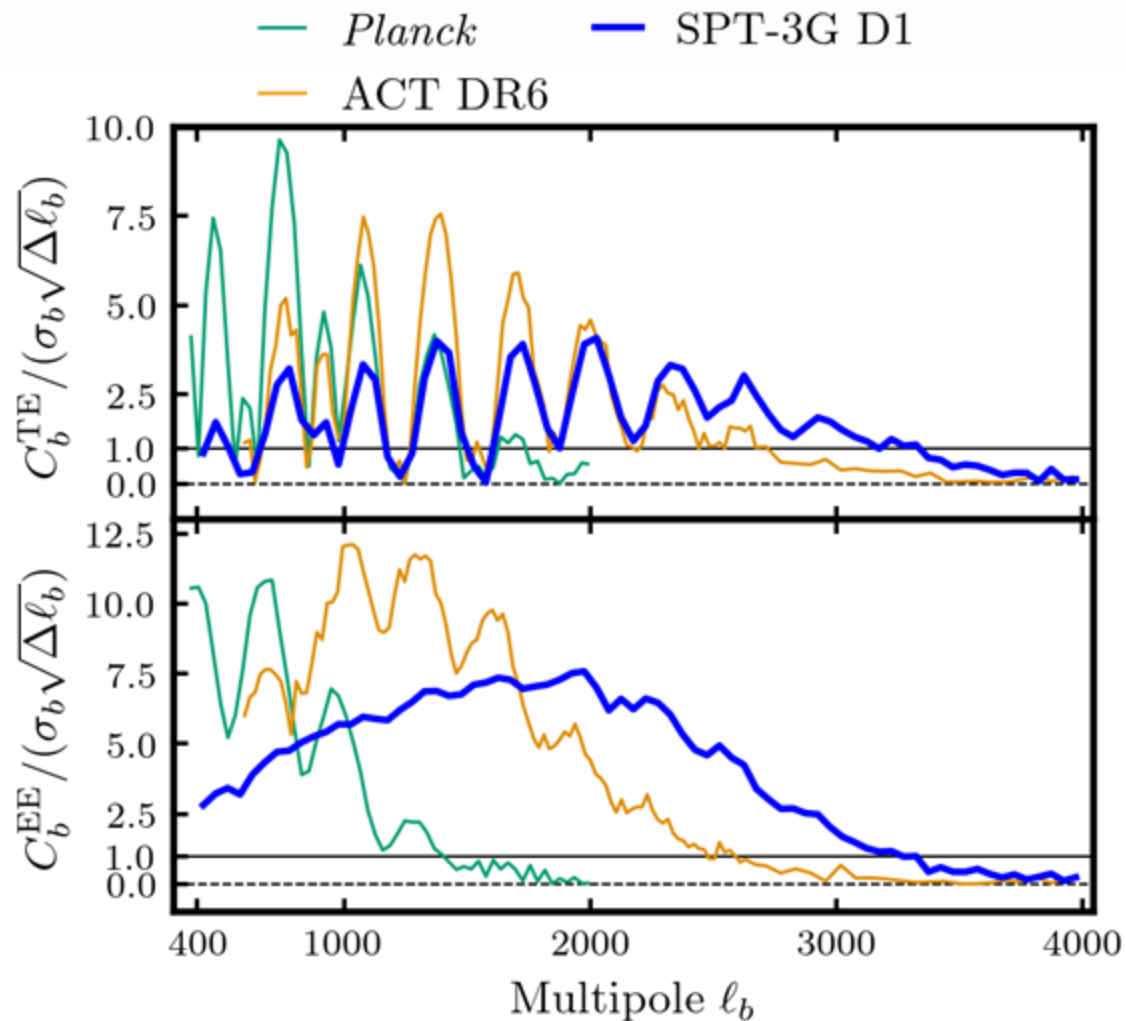
CMB angular power spectra

Complementary CMB experiments

	Observed sky fraction [%]	Coadded noise level [μK-arcmin]
Planck PR3	100	35
ACT DR6	45	10
SPT-3G D1	**4**	**3.3**

SPT-3G D1 is the tightest band power measurement:
- **In TE at ℓ in [2200,4000]**
- **In EE at ℓ in [1800,4000]**

Likelihood

Foreground and nuisance model improved over SPT-3G 2018

More details in the paper !

CAMB   OLÉ

CLASS

$$-\ln \mathcal{L}(\hat{C}|C^{\mathrm{model}}(\theta)) \propto$$
$$\frac{1}{2}\left[\hat{C}_b - C_b^{\mathrm{model}}(\theta)\right]\Sigma_{bb'}^{-1}\left[\hat{C}_{b'} - C_{b'}^{\mathrm{model}}(\theta)\right]$$

candl ▽

Differentiable and robust python JAX-likelihood code   Balkenhol,...SG et al. 2024

Semi-analytical covariance matrix from Camphuis, ... SG et al, 2023

Analysis validation

- Validation of the pipeline is done **blind**, without looking at obtained cosmological parameters or comparing to previous experiments. We allow changes after unblinding, but report all of the changes in a transparent way.

- Validation tests include:

  - Null tests at the map level, where we split the data in two according to some criterion (Sun, moon, azimuth, year, scan direction, detector wafers) and then take the difference between the two maps.

  - Differences at the power spectrum level between different spectra at different frequencies, to check that the CMB signal is the same.

  - Differences at the cosmological parameter level from different frequency channels, assuming LCDM.

  - Check that the pipeline is unbiased on simulations.

Data Sets

- **SPT-3G D1:**
  - D1 = Observations of the Main field in 2019-2020.
  - This work, i.e. SPT-3G Main field T&E* data + ΦΦ band-powers from [Ge _et al_ [SPT-3G], 2024](#).

- _Planck:_ Planck 2018 (PR3) [high-ℓ T&E + low-ℓ TT] ([Planck Collaboration _et al._, 2018](#)) + PR4 ΦΦ band-powers ([Carron _et al_, 2022](#)).

- **SPT+ACT:** SPT-3G D1 + ACT DR6 T&E ([Louis _et al_ [ACT], 2025](#)) + ACT DR6 ΦΦ band-powers ([Madhavacheril _et al_ [ACT], 2023](#); [Qu _et al_ [ACT], 2023](#)).

- **CMB-SPA:** SPT-3G D1 + P-ACT([Louis et al [ACT], 2025](#)).

- $\tau_{\mathbf{reio}}$ **prior:** for all the data sets above, we use a prior from _Planck_ PR4 ([Akrami _et al_ [Planck], 2020](#)) on τ_{reio} = 0.051 ± 0.006

* T&E = TT/TE/EE band-powers.

ΛCDM: Most Precise Constraints from CMB to Date
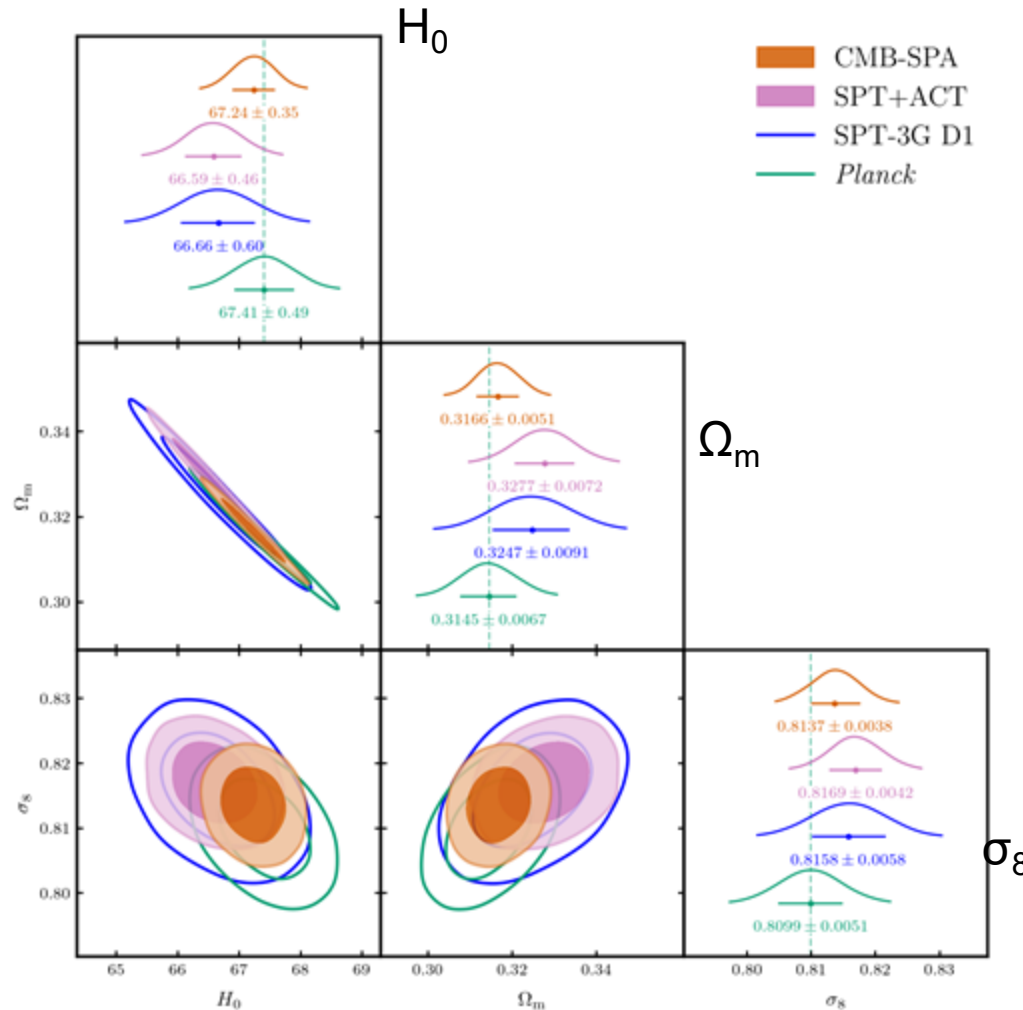
H₀ = 67.24 ± 0.35 km/s/Mpc (CMB-SPA)
H₀ = 67.41 ± 0.49 km/s/Mpc (Planck)

- With just 4% of the sky, SPT-3G's constraints on H_0 and σ_8 are comparable to Planck (within 25%) or ACT.
  Our data agree very well with ΛCDM predictions.

- CMB SPT+ACT finally reach Planck's precision (on some parameters)!

- CMB-SPA yields the most precise determination of ΛCDM parameters from a single probe.
  All three experiments agree with each other within 1.1σ. CMB science is very robust!

ΛCDM: Hubble Tension with SH0ES

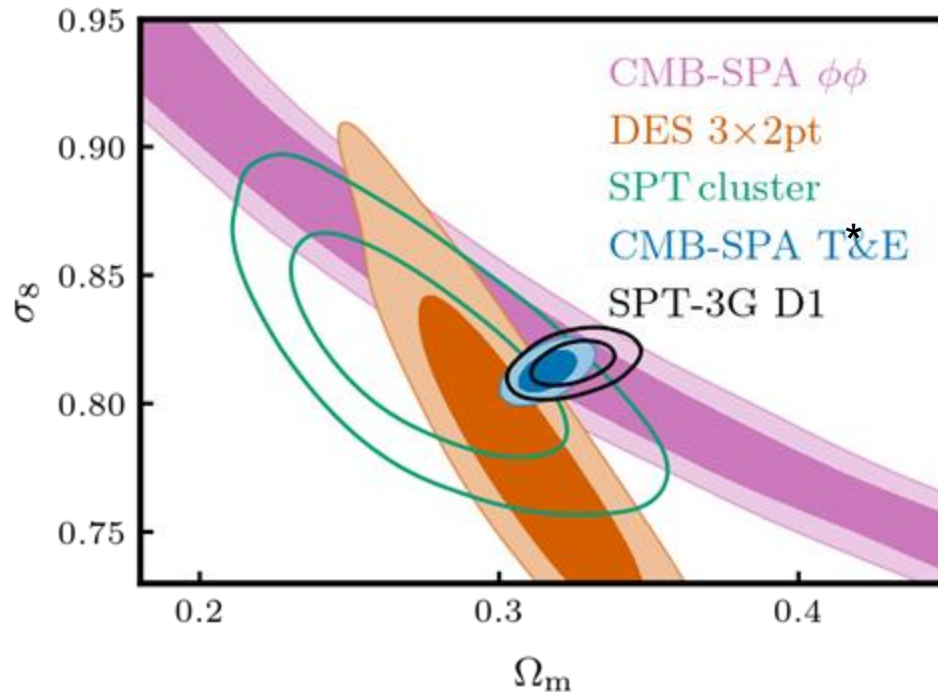**Three independent and complementary experiments confirm the Hubble tension.**

Breuval *et al.* [SH0ES],2024
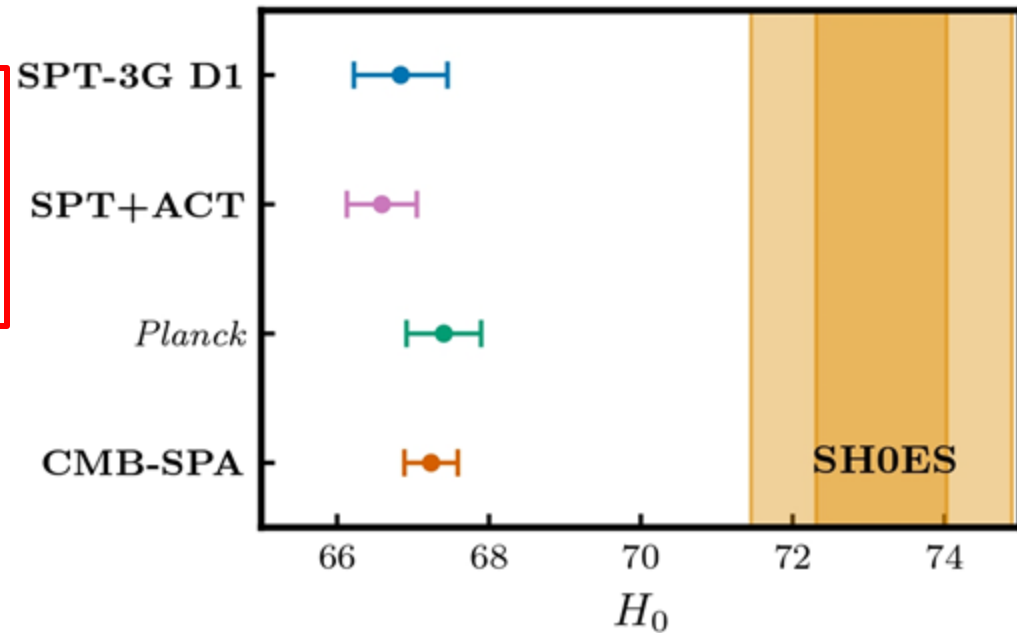
H_0 = 73.17 ± 0.86 km/s/Mpc

- Hubble Tension at **6.2σ** from **SPT-3G** alone.
  H_0 = 66.66 ± 0.60 km/s/Mpc

- **SPT+ACT** and **CMB-SPA** are at **6.8σ** and **6.4σ** tension, respectively.

ΛCDM: Clustering of Matter

0.95
0.90
0.85
0.80
0.75

σ_8

CMB-SPA $\phi\phi$
DES 3×2pt
SPT cluster
CMB-SPA T&E *
SPT-3G D1

0.2   0.3   0.4

Ω_m

SPT-3G D1 alone, with only 4% of the sky, constrain σ_8 almost as well as *Planck*.

- A variety of probes, spanning a wide range of epochs, are now consistent with each other (including the latest KiDS-legacy cosmic shear results, KiDS collaboration, 2025).

- σ_8 = 0.8137 ± 0.0038

  Ω_m = 0.3166 ± 0.0051

  CMB-SPA

*SPT cluster = Constraints from SPT identified abundance of clusters (Bocquet *et al.* [SPT,DES], 2024).

ΛCDM Extensions

- The addition of SPT+ACT to *Planck* reduces the upper limit on Σm_ν by ~30%:

$$\Sigma m_\nu < 0.25 \text{ eV (95\% C.L.) } (Planck)$$
$$\Sigma m_\nu < 0.18 \text{ eV (95\% C.L.) (CMB-SPA)}$$

This shows again the constraining power of SPT+ACT.

- We also explored extensions with N_{eff}, Y_P and modified recombination.

$$N_{eff} = 2.86 \pm 0.19 \ (Planck)$$
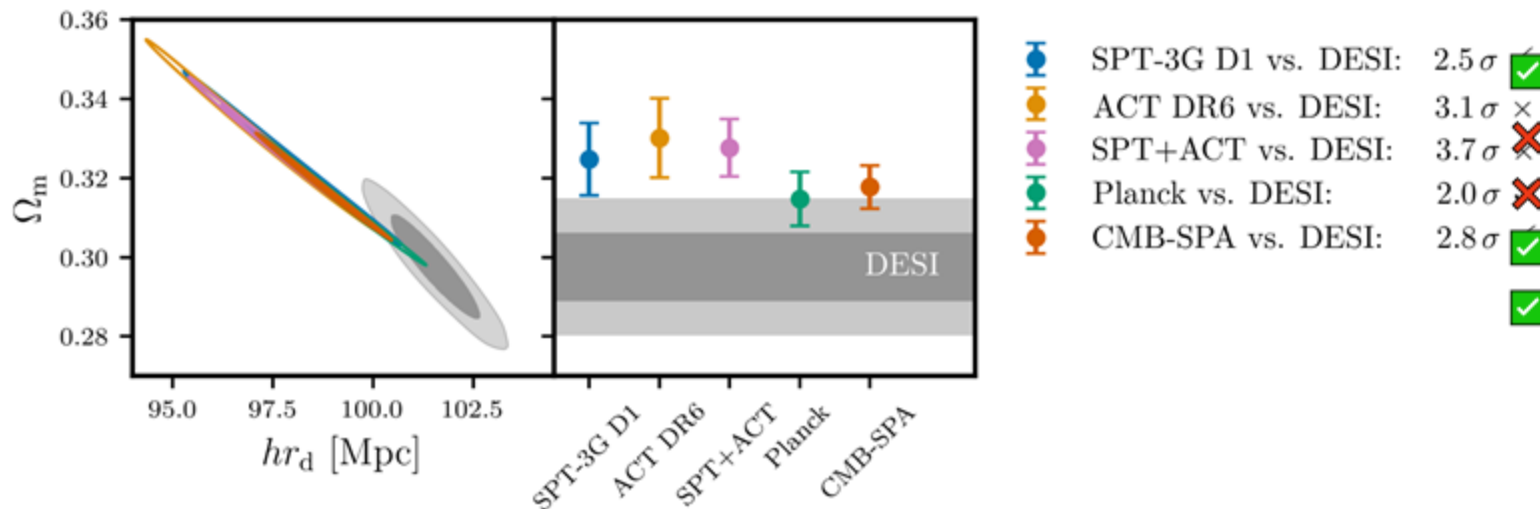$$N_{eff} = 2.81 \pm 0.12 \ (\text{CMB-SPA})$$

We do not find any statistically significant deviations from ΛCDM.

A new CMB-BAO tension?
Evaluating the Consistency of CMB vs DESI in ΛCDM

- ACT and SPT+ACT above consistency threshold
- Planck data regularise combined results, **CMB-SPA consistent with DESI**
- Given borderline differences, **joint analyses to be performed with caution**

Constraints from CMB and BAO data beyond ΛCDM

Differences between CMB and DESI can be accommodated by 2-3σ deviations from ΛCDM.

| Model Class	Preference over ΛCDM
Rescaling of lensing in CMB	3.1σ
Light relics	<1.5σ
Modified recombination	2.0σ
Spatial curvature	2.5σ
Spatial curvature and electron mass	2.1σ
Neutrino mass	2.8σ
Dynamical dark energy	3.2σ

CMB-SPA

-0.88 ± 0.48

CMB-SPA+DESI

0.26 ± 0.11

$100 \, \Omega_\mathrm{k}$
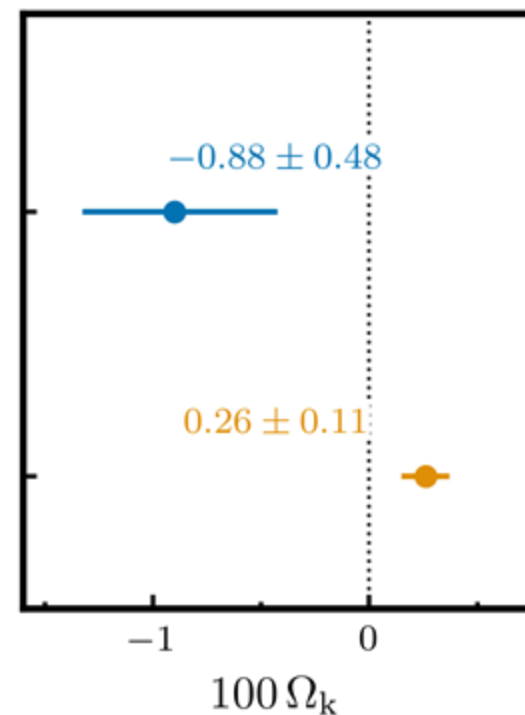
Constraints from CMB and BAO data beyond ΛCDM

- With current data, **no definitive evidence for a breakdown of ΛCDM**

  - Evidence is moderate, 3σ-level

  - So far no detection by individual probe

  - Statistical fluctuation or systematic origin not ruled out
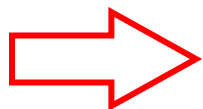
⟹ **More data needed** for a stronger judgement (CMB, BAO, others)

Upcoming SPT-3G results

Very soon: Lensing update
- Same observations as in today's results
- φφ from temperature+polarization, quadratic estimator

Soon: Summer
- Ext-4K = Summer + Main (first 2 years)
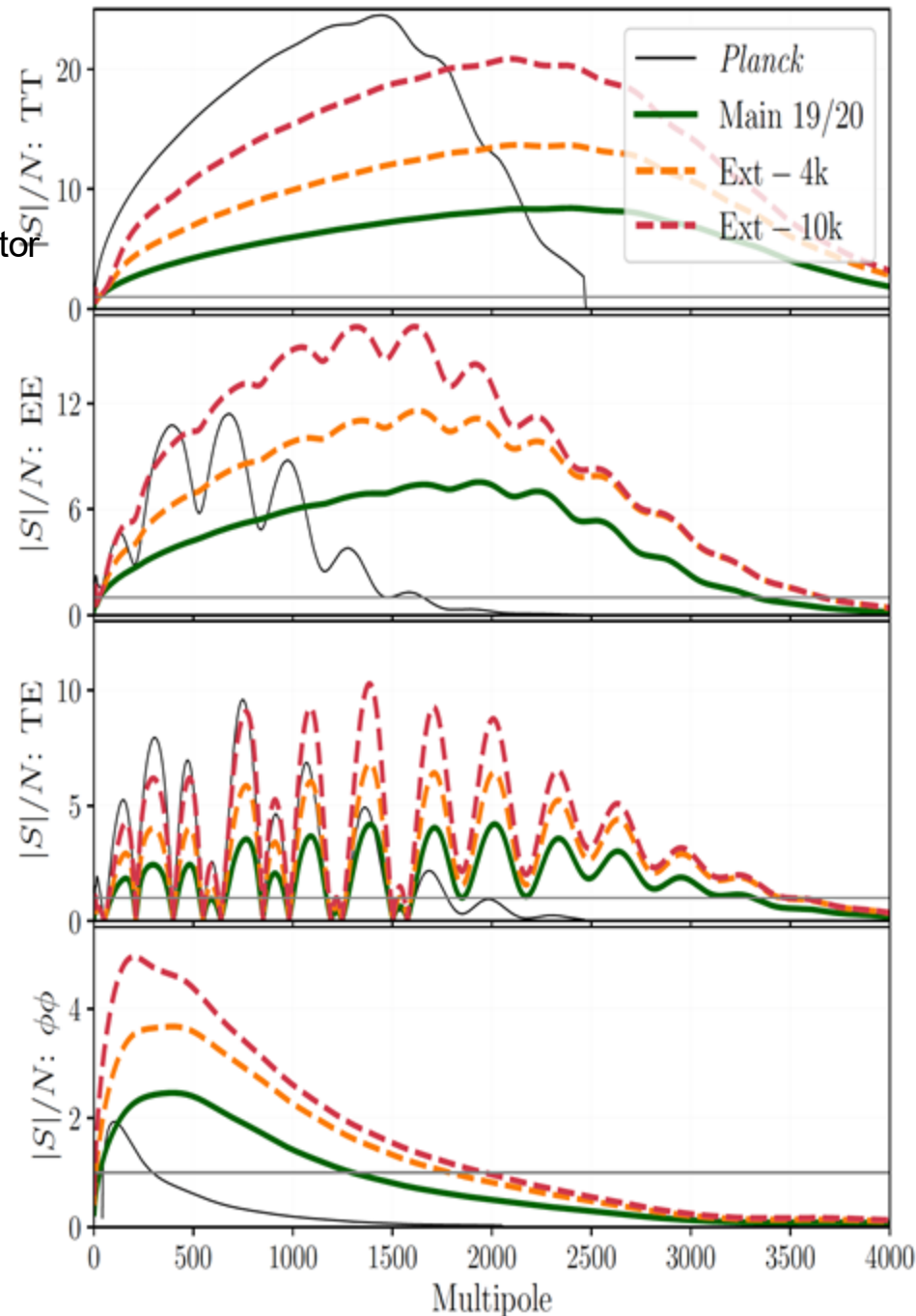 - → 3 times more sky than in today's results
- TT, TE, EE
- φφ

In progress: Wide
- Ext-10K = Wide + Summer + Main
  - → 7 times more sky than in today's results
- TT, TE, EE
- φφ

Cosmology forecasts: *Prabhu et al. [SPT-3G], 2024*

Future:
- Main and Summer full depth
- SPT-3G+ camera starting in 2029

Prospects

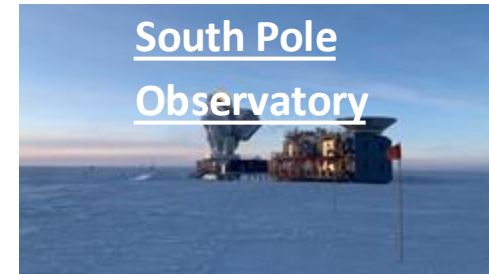**Soon:**

- SPT-3G

- Simons Observatory (SO)

~2028

- SPT-3G+ and its combination with

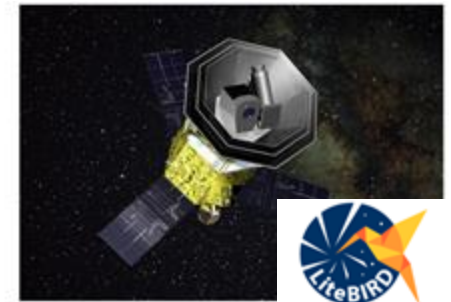 BICEP/Keck, South Pole Observatory (SPO)

- Advanced SO

~2035+

- Litebird

Very recent news of the termination of the S4

project from USA funding agencies. **Change of**

strategy towards funding upgrades on existing

experiments and their combinations, still very

strong support to CMB science.

Current/upcoming

South Pole Observatory

Future

More details about CMB STATISTICS

- CMB anisotropies are expected to be distributed as a gaussian random field.
- We cannot theoretically predict the value of the temperature in the pixels, but only predict their statistical properties.
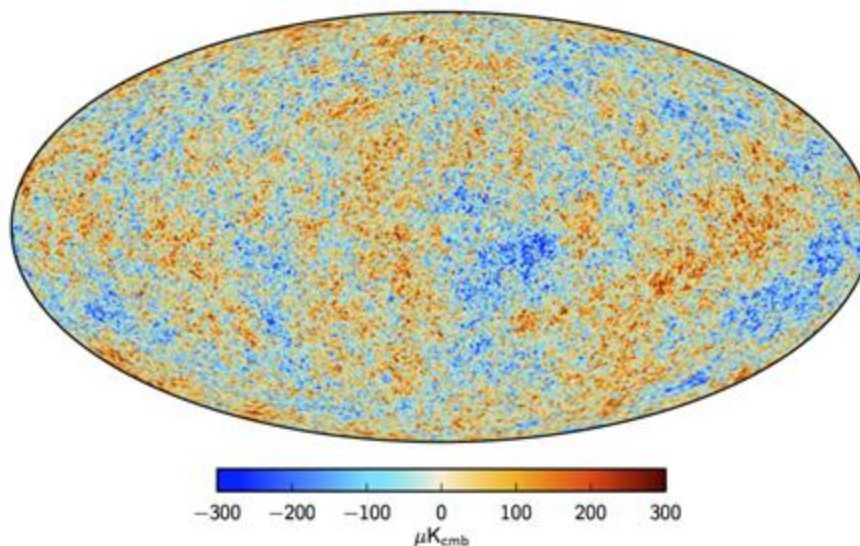
- A gaussian distribution is fully characterized by a mean and variance. All higher odd moments are 0, even moments can be written in terms of the variance (Wick's theorem)
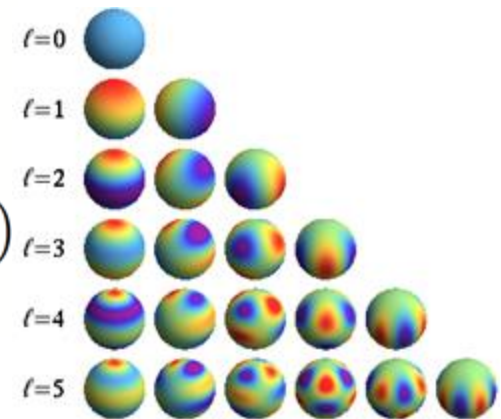
Spherical harmonics

- We can decompose the temperature maps in spherical harmonics.

- SH are a horto-normal basis of functions on the sphere. They are the eigenfunctions of the angular part of the Laplace operator in spherical coordinates.

$$\nabla^2 Y_\ell^m = -[l(l+1)]Y_\ell^m$$

$$\int d\hat{\mathbf{n}} Y_\ell^{m*}(\hat{\mathbf{n}}) Y_{\ell'}^{m'}(\hat{\mathbf{n}}) = \delta_{\ell\ell'}\delta_{mm'}$$

$$\sum_{\ell m} Y_\ell^{m*}(\hat{\mathbf{n}}) Y_\ell^m(\hat{\mathbf{n}}') = \delta(\phi - \phi')\delta(\cos\theta - \cos\theta')$$

- Complex. Conjugation $Y_\ell^{m*} = (-1)^m Y_\ell^{-m}$

- Characterized the degree (multipole) ℓ and the order m.

- $\ell \sim \pi/\theta$, with the θ angular separation in the sky.

- For each ℓ, $-\ell <= m <= \ell$ There are 2l+1 m-modes for each l. For a real field, as the CMB intensity, there are (2l+1)/2 independent modes because $a_{lm} = a_{lm}^* = (-1)^m a_{l-m}$

- The projection on the m-modes depends on the reference system.

Decomposition in spherical harmonics

- Decompose the fractional temperature variation in spherical harmonics

$$\frac{\Delta T}{T}(\hat{n}, \vec{x}, \eta) = \Theta(\hat{n}, \vec{x}, \eta) = \sum_{\ell m} \Theta_{\ell m}(\vec{x}, \eta) Y_\ell^m(\hat{n})$$

Line of sight

Position in the sky (us ,x=0)

Conformal time (us, $\eta=\eta_0$) $\eta \equiv \int dt/a$

Also often called $a_{\ell m}$ in the literature

- Applying the orthogonality of spherical harmonics:

$$\Theta_{\ell m}(\vec{x}, \eta) = \int_\Omega d\hat{n}\, \Theta(\hat{n}, \vec{x}, \eta) Y_{\ell m}^*(\hat{n})$$

- In the simplest models of inflation, $\Theta(\hat{n})$ is a gaussian random field. Then, $\Theta_{\ell m}$ are statistically independent and randomly distributed, each described by a gaussian distribution.

Cl's in theory

- To characterize the statistical properties of a gaussian random field, we can calculate the mean and the variance of the field. For the CMB, the mean of the anisotropies is zero (by definition). The variance can be calculated either as the 2-point correlation function in real space, or equivalently, as the **angular power spectrum in harmonic space**.

$$< \Theta_{\ell m} >= 0 \qquad < \Theta_{\ell m} \Theta_{\ell' m'} >= \delta_{\ell \ell'} \delta_{mm'} C_\ell$$

- <> are ensemble averages over many realizations of the sky.
- Because of isotropy, $\Theta_{\ell m}$ with same ℓ and different m are extracted from gaussian distribution with the same variance C_ℓ

Cl's and 2-point correlation function

- We can relate the angular power spectrum to the 2-point correlation function in real space using the Legendre polynomials and the addition theorem:

$$\sum_m Y_{\ell m}^*(\mathbf{n}_i) Y_{\ell m}(\mathbf{n}_j) = \frac{2\ell+1}{4\pi} P_\ell(\hat{\mathbf{n}}_i \cdot \hat{\mathbf{n}}_j)$$

$$\langle \Theta_i \Theta_j \rangle = \sum_\ell \frac{2\ell+1}{4\pi} C_\ell P_\ell(\hat{\mathbf{n}}_i \cdot \hat{\mathbf{n}}_j)$$

- Because of isotropy, the two-point correlation function depends only on the angular separation in the sky θ, not on the orientation of the separation.

Dodelson
et al. 2004
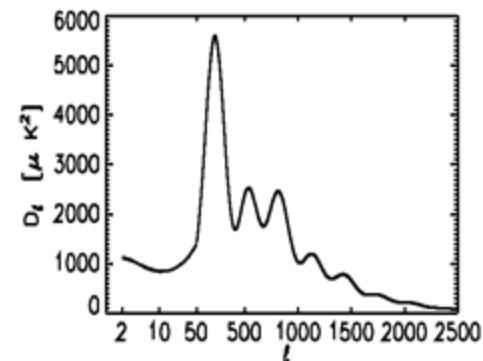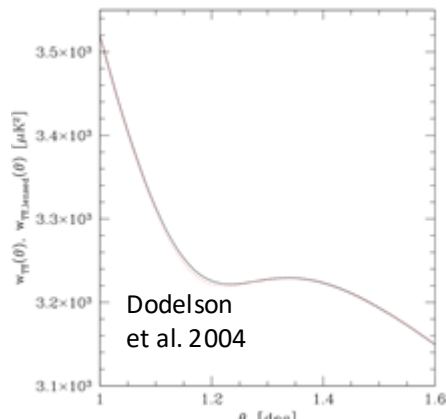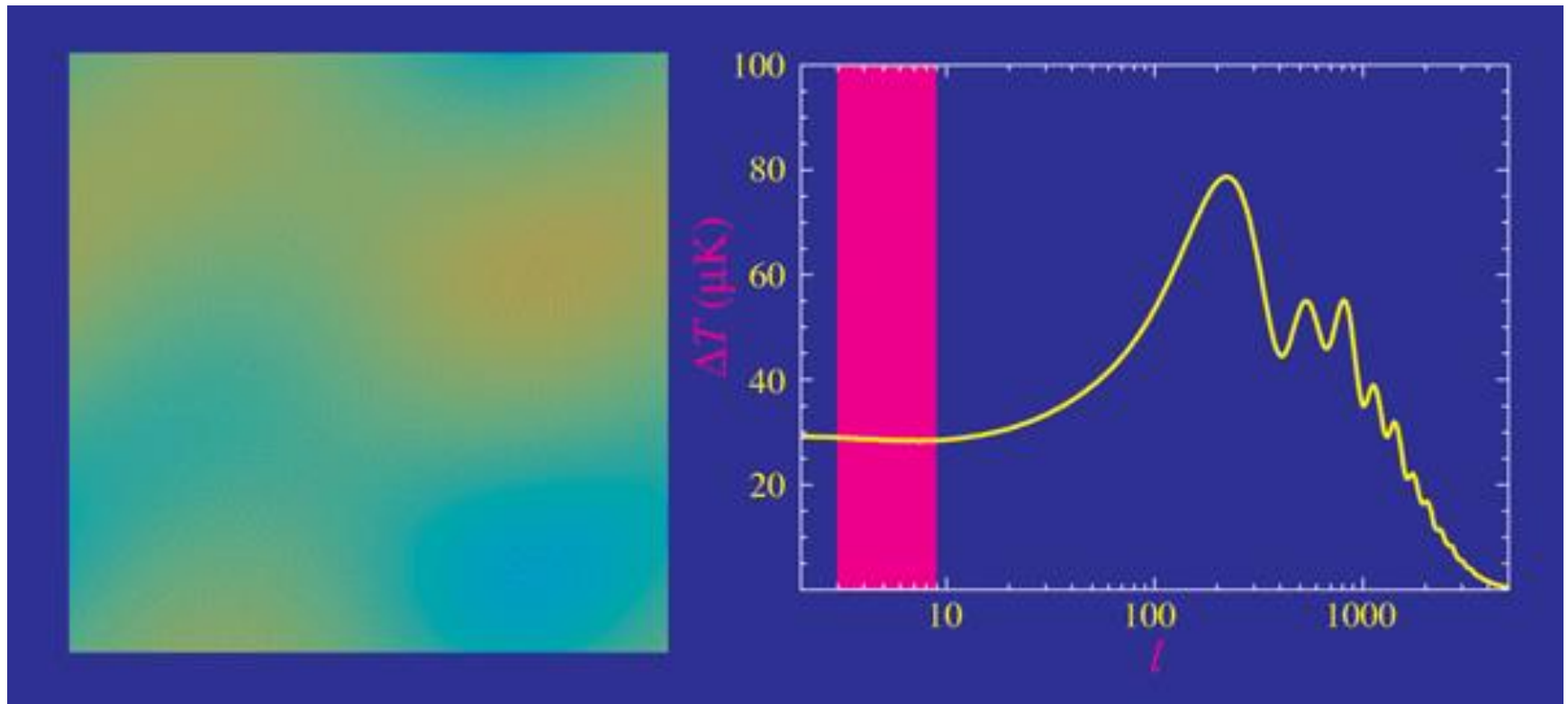
Each of these maps are extracted from gaussian distributions with 0 mean and variance given by the Cl in the corresponding pink band. There is an infinite number of possible realizations.

An estimator for the Cl's

$$< \Theta_{\ell m} >= 0 \qquad < \Theta_{\ell m} \Theta_{\ell' m'} >= \delta_{\ell \ell'} \delta_{mm'} C_\ell$$

- We only observe one universe=> average not possible.

- Because of isotropy, all the m-modes $\Theta_{\ell m}$ with the same ℓ have the same theoretical C_ℓ. An estimator of C_ℓ is then:

$$\hat{C}_\ell = \frac{1}{2\ell + 1} \sum_m \Theta_{\ell m} \Theta_{\ell m}^*$$

Cosmic Variance

- The expected value is $\langle \hat{C}l \rangle = Cl$
- Since we only have $2l+1$ samples for each l, there is an intrinsic uncertainty!

$$\hat{C}_\ell = \frac{1}{2\ell + 1} \sum_m \Theta_{\ell m} \Theta^*_{\ell m}$$

$$\frac{\sigma^2_{C_\ell}}{C^2_\ell} = \frac{\langle (\hat{C}_\ell - C_\ell)(\hat{C}_\ell - C_\ell) \rangle}{C^2_\ell} = \frac{\langle \hat{C}_\ell \hat{C}_\ell \rangle - C^2_\ell}{C^2_\ell}$$

$$= \frac{1}{(2\ell + 1)^2 C^2_\ell} \langle \sum_{mm'} \Theta^*_{\ell m} \Theta_{\ell m} \Theta^*_{\ell m'} \Theta_{\ell m'} \rangle - 1$$

$$= \frac{1}{(2\ell + 1)^2} \sum_{mm'} (\delta_{mm'} + \delta_{m-m'}) = \frac{2}{2\ell + 1}$$

For a gaussian field, Wick's theorem says that any N-point (N even) statistics can be written as a function of the 2-point correlation function
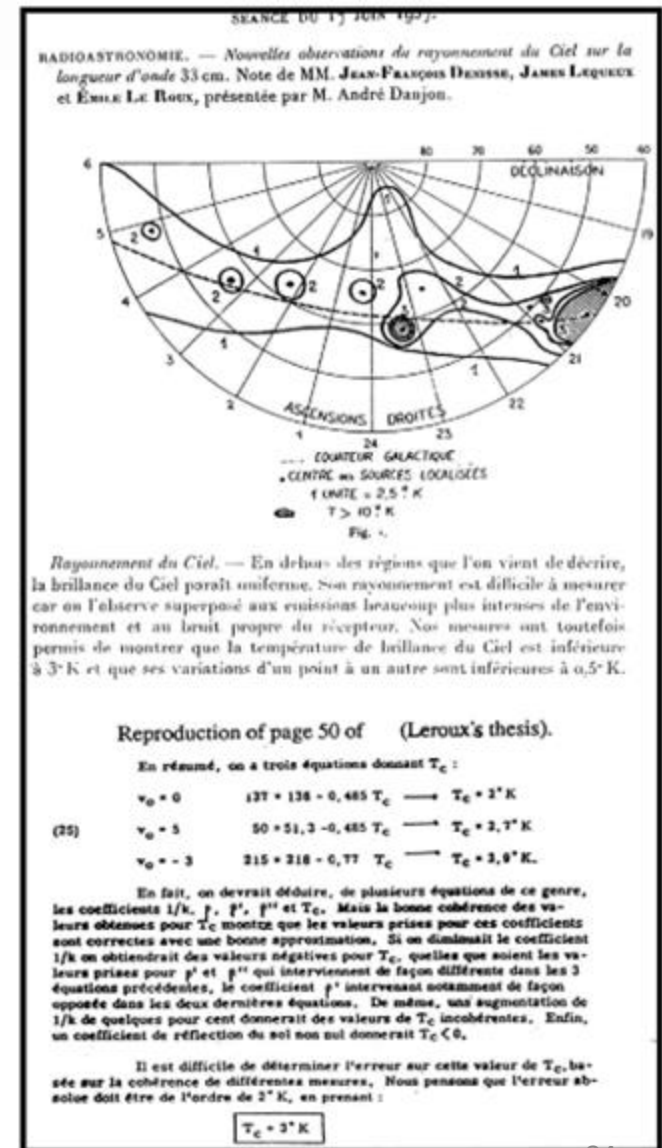
$$\boxed{\sigma^2_{C_\ell} = \frac{2}{2\ell + 1} C^2_\ell}$$

More details about earlier detections of the CMB

Earlier detections?

- 1940 Andrew McKellar observed excited rotational states of CN molecules in interstellar absorption lines. In thermal equilibrium at T~2.3K (see also W. Adams 1941)

- 1955 Émile Le Roux: survey at λ = 33 cm (Nançay Radio Observatory). Near-isotropic background at 3±2K (Denisse, Lequeux, Le Roux 1957, Le Roux PhD thesis 1957).

SÉANCE DU 13 JUIN 1957.

RADIOASTRONOMIE. — *Nouvelles observations du rayonnement du Ciel sur la longueur d'onde 33 cm.* Note de MM. JEAN-FRANÇOIS DENISSE, JAMES LEQUEUX et ÉMILE LE ROUX, présentée par M. André Danjon.

Rayonnement du Ciel. — En dehors des régions que l'on vient de décrire, la brillance du Ciel paraît uniforme. Son rayonnement est difficile à mesurer car on l'observe superposé aux émissions beaucoup plus intenses de l'environnement et au bruit propre du récepteur. Nos mesures ont toutefois permis de montrer que la température de brillance du Ciel est inférieure à 3° K et que ses variations d'un point à un autre sont inférieures à 0,5° K.

Reproduction of page 50 of   (Leroux's thesis).

En résumé, on a trois équations donnant T_c :

$$v_0 = 0 \qquad 13T = 138 - 0,485\ T_c \longrightarrow T_c = 2°K$$

(25)
$$v_0 = 5 \qquad 50 = 51,3 - 0,485\ T_c \longrightarrow T_c = 2,7°K$$

$$v_0 = -3 \qquad 215 = 218 - 0,77\ T_c \longrightarrow T_c = 3,9°K.$$

En fait, on devrait déduire, de plusieurs équations de ce genre, les coefficients $1/k$, f, f', f'' et T_c. Mais la bonne cohérence des valeurs obtenues pour T_c montre que les valeurs prises pour ces coefficients sont correctes avec une bonne approximation. Si on diminuait le coefficient $1/k$ on obtiendrait des valeurs négatives pour T_c, quelles que soient les valeurs prises pour f' et f'' qui interviennent de façon différente dans les 3 équations précédentes, le coefficient f' intervenant notamment de façon opposée dans les deux dernières équations. De même, une augmentation de $1/k$ de quelques pour cent donnerait des valeurs de T_c incohérentes. Enfin, un coefficient de réflexion du sol non nul donnerait $T_c < 0$.

Il est difficile de déterminer l'erreur sur cette valeur de T_c, basée sur la cohérence de différentes mesures. Nous pensons que l'erreur absolue doit être de l'ordre de 2° K, en prenant :

$$T_c = 3°K$$

Reproduction in F. Melchiorri,Y. Rephaeli lectures in Varenna 2004

More details about polarization

Stokes parameters

For a monochromatic plane wave:

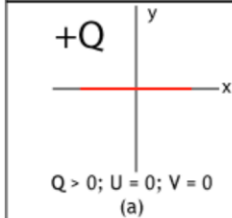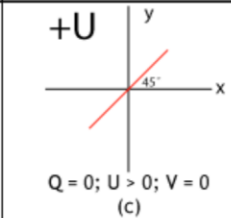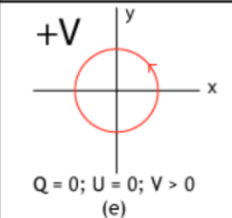$$E_x = a_x \cos\left[\omega_0 t - \theta_x(t)\right] \qquad E_y = a_y \cos\left[\omega_0 t - \theta_y(t)\right]$$
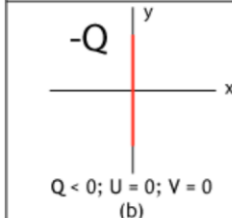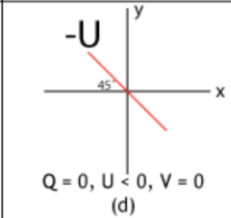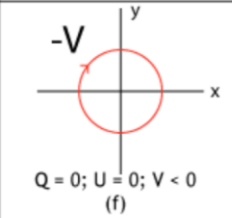
$\phi = \theta_x - \theta_y$
$\phi = 0 \Rightarrow$ linear polarization
$\phi = \pi/2,\ a_x = a_y \Rightarrow$ circular polarization

$$I \equiv \left\langle a_x^2 \right\rangle + \left\langle a_y^2 \right\rangle$$

$$Q \equiv \left\langle a_x^2 \right\rangle - \left\langle a_y^2 \right\rangle$$

$$U \equiv \left\langle 2 a_x a_y \cos(\theta_x - \theta_y) \right\rangle$$

$$V \equiv \left\langle 2 a_x a_y \sin(\theta_x - \theta_y) \right\rangle$$

100% Q	100% U	100% V
+Q	+U	+V
Q > 0; U = 0; V = 0 (a)	Q = 0; U > 0; V = 0 (c)	Q = 0; U = 0; V > 0 (e)
-Q	-U	-V
Q < 0; U = 0; V = 0 (b)	Q = 0, U < 0, V = 0 (d)	Q = 0; U = 0; V < 0 (f)

$$I^2 \geq Q^2 + U^2 + V^2$$

$$p \equiv \frac{\sqrt{Q^2 + U^2 + V^2}}{I}$$

- Equal holds for a monocromatic wave or, for superposition of many waves, entirely polarized radiation.
- P= degree of polarization
- In the following, we'll drop V (not produced in standard cosmology model.)

I Q U maps

- Healpix convention: Q and U defined in spherical coordinate system (e_θ, e_ϕ) where e_θ is tangent to the local meridian and directed from North to South, and e_ϕ is tangent to the local parallel, and directed from West to East.

Temperature (I)

Polarization (Q)
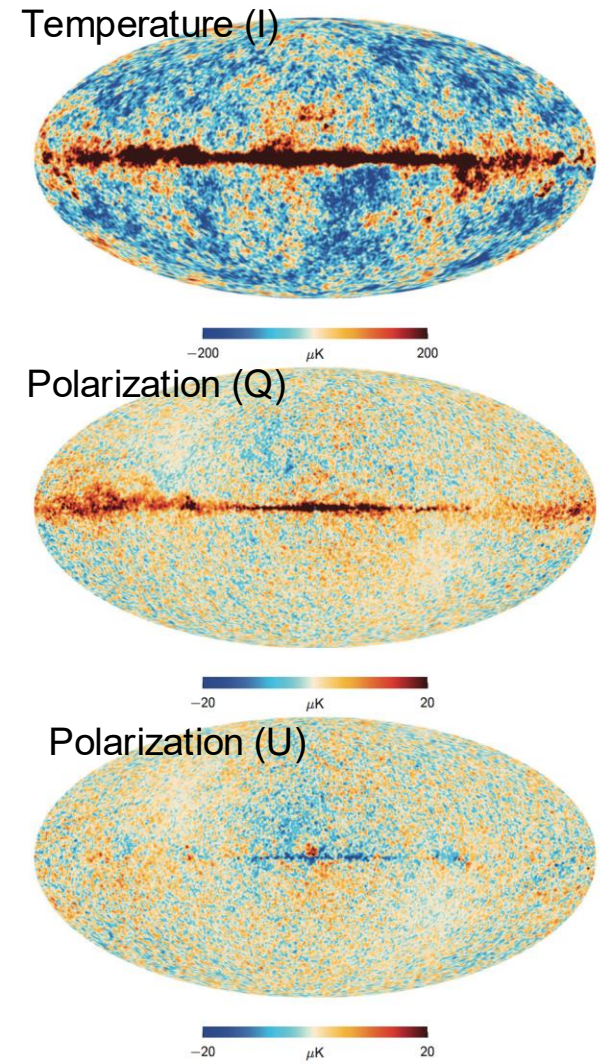
Polarization (U)

Fig. 12. LFI 70 GHz channel maps. From top to bottom: temperature, Q, and U polarization.
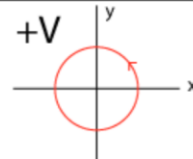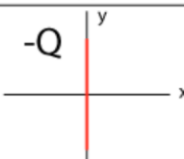
Stokes parameters
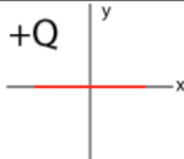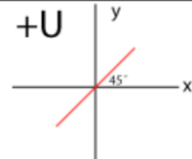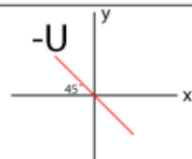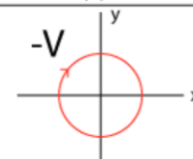
- Polarization is a headless vector, equal to itself after a 180deg rotation=>Q and U spin 2 fields.
- Problem: Q and U depend on reference system.

$$Q' = \cos(2\theta)Q + \sin(2\theta)U$$

$$U' = -\sin(2\theta)Q + \cos(2\theta)U$$

$$\boxed{Q' \pm iU' = e^{\mp 2i\theta}[Q \pm iU]}$$

100% Q	100% U	100% V
+Q	+U	+V
Q > 0; U = 0; V = 0 (a)	Q = 0; U > 0; V = 0 (c)	Q = 0; U = 0; V > 0 (e)
-Q	-U	-V
Q < 0; U = 0; V = 0 (b)	Q = 0, U < 0, V = 0 (d)	Q = 0; U = 0; V < 0 (f)

E and B modes

Q > 0   U = 0
E < 0

Q < 0   U = 0
E > 0

Q = 0   U < 0
B < 0

Q = 0   U > 0
B > 0
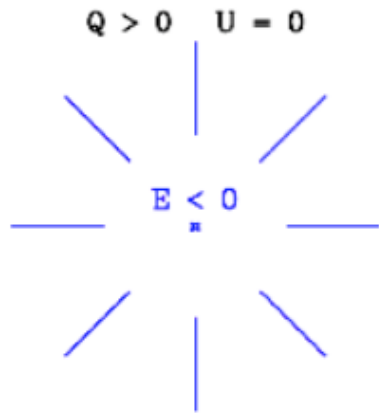
Qr and Ur around each point defined in radial coordinate system (e_r, e_t) where e_t is orthogonal to the radius and e_r is parallel
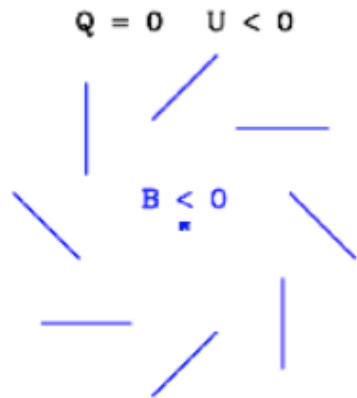
Q and U depend on the reference system=> not good to characterize the underlying physics!
A solution is to characterize polarization not by the characteristics in a point, but a non-local average 'pattern'around a point the sky.

From Q and U to E and B in a flat patch.

- Take the simplified case of a flat, small patch in the sky. We can define Q and U parameters in the radial coordinates around a given point θ (Zaldarriaga 2001) (e_r in the radial direction, e_θ in the orthogonal one).

- **E and B are then defined as the Q weighted averaged on the full sky**

$$E(\boldsymbol{\theta}) = \int d^2\tilde{\boldsymbol{\theta}}\omega(\tilde{\theta})Q_r(\boldsymbol{\theta}+\tilde{\boldsymbol{\theta}})$$

$$= \int d^2\tilde{\boldsymbol{\theta}}\omega(\tilde{\theta})[Q(\boldsymbol{\theta}+\tilde{\boldsymbol{\theta}})\cos{(2\tilde{\psi})} - U(\boldsymbol{\theta}+\tilde{\boldsymbol{\theta}})\sin{(2\tilde{\psi})}]$$

$$B(\boldsymbol{\theta}) = \int d^2\tilde{\boldsymbol{\theta}}\omega(\tilde{\theta})U_r(\boldsymbol{\theta}+\tilde{\boldsymbol{\theta}})$$

$$= \int d^2\tilde{\boldsymbol{\theta}}\omega(\tilde{\theta})[Q(\boldsymbol{\theta}+\tilde{\boldsymbol{\theta}})\sin{(2\tilde{\psi})} + U(\boldsymbol{\theta}+\tilde{\boldsymbol{\theta}})\cos{(2\tilde{\psi})}]$$

* All the points on this circle contributes with the same weight to the construction of E in θ, as they are all at the same distance.

* The value of Q and U depends on the angle ψ, but Q_r is constant on a circle, while U_r =0, so averaging on all the circles, E≠ 0, B=0

RADIAL COORDINATES

$Q= I_x-I_y = I_x \neq 0,$
$U = I_{45^\circ}-I_{-45^\circ} = 0$
$Q\_r < 0, U\_r=0$

$Q=0, U=0$
$Q\_r < 0, U\_r=0$

E-mode
Q_r < 0

In 2D Fourier space, the integrals become multiplications, so that in a flat patch of the sky:

$$Q(\boldsymbol{l}) = [E(\boldsymbol{l})\cos(2\phi_l) - B(\boldsymbol{l})\sin(2\phi_l)]$$
$$U(\boldsymbol{l}) = [E(\boldsymbol{l})\sin(2\phi_l) + B(\boldsymbol{l})\cos(2\phi_l)]$$

Zaldarriaga astro-ph/0106174
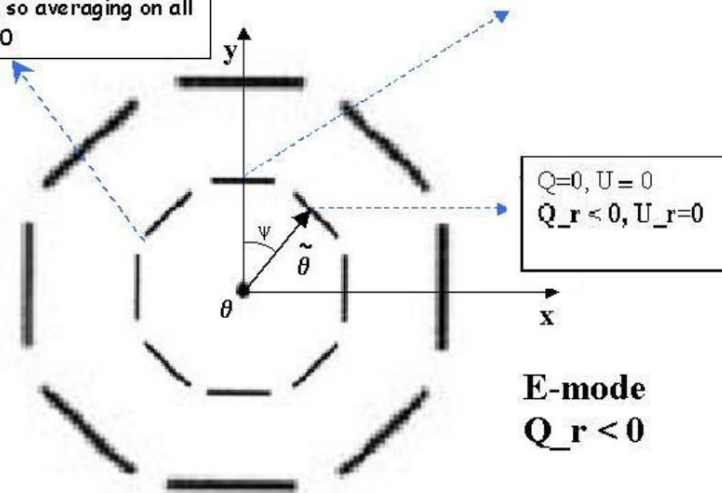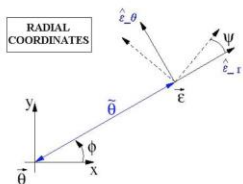
E and B on a sphere

- Extend this idea on a sphere (see Zaldarriaga & Seljak 1997, arXiv:astro-ph/9609170).

- 1)Similarly to the (scalar) T maps, we can decompose the Q and U maps (in healpix maps) on the eigenfunctions of the Laplace operator for spin fields, which are an orthonormal, complete basis.

$$(Q \pm iU)(\hat{n}) = \sum_{lm} a_{\pm 2,lm} \, _{\pm 2}Y_{lm}(\hat{n})$$

- 2)Obtain scalar quantities by using spin rising/lowering operators (that are rotationally invariant).

$$\eth^2(Q-iU)(\hat{n}) = \sum_{lm} \left[\frac{(l+2)!}{(l-2)!} \right]^{1/2} a_{-2,lm} Y_{lm}(\hat{n})$$

- 3) $a_{E,lm} = -(a_{2,lm} + a_{-2,lm})/2,$

  $a_{B,lm} = i(a_{2,lm} - a_{-2,lm})/2.$

- E and B are rotationally invariant.
- E and B are NON-LOCAL QUANTITIES!
- E remains unchanged under parity transformations (scalar), B changes the sign (pseudo-scalar!)
- In order to obtain (pseudo) scalar fields, need to multiply a_{Elm} by additional geometric factor!

$$\tilde{E}(\hat{n}) \equiv -\frac{1}{2}[\bar{\eth}|^2(Q+iU) + \eth^2(Q-iU)]$$

$$= \sum_{lm} \left[\frac{(l+2)!}{(l-2)!} \right]^{1/2} a_{E,lm} Y_{lm}(\hat{n}),$$

$$\tilde{B}(\hat{n}) \equiv \frac{i}{2}[\bar{\eth}^2(Q+iU) - \eth^2(Q-iU)]$$

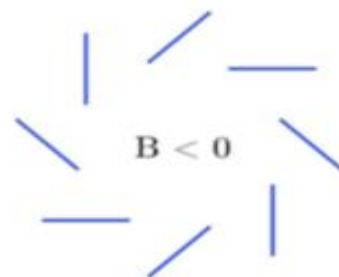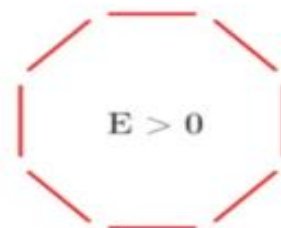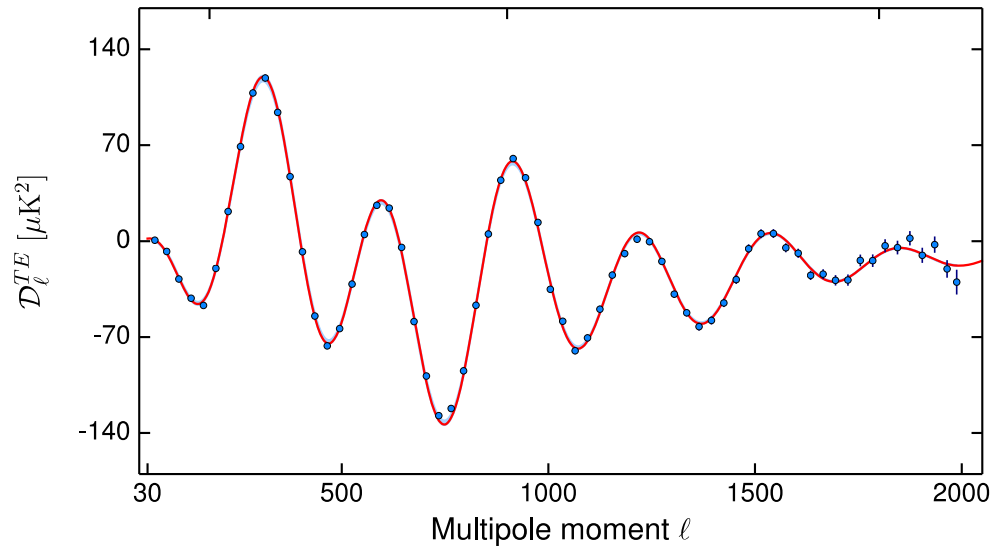$$= \sum_{lm} \left[\frac{(l+2)!}{(l-2)!} \right]^{1/2} a_{B,lm} Y_{lm}(\hat{n}).$$

$$= \quad\quad + \quad$$

E < 0   E > 0
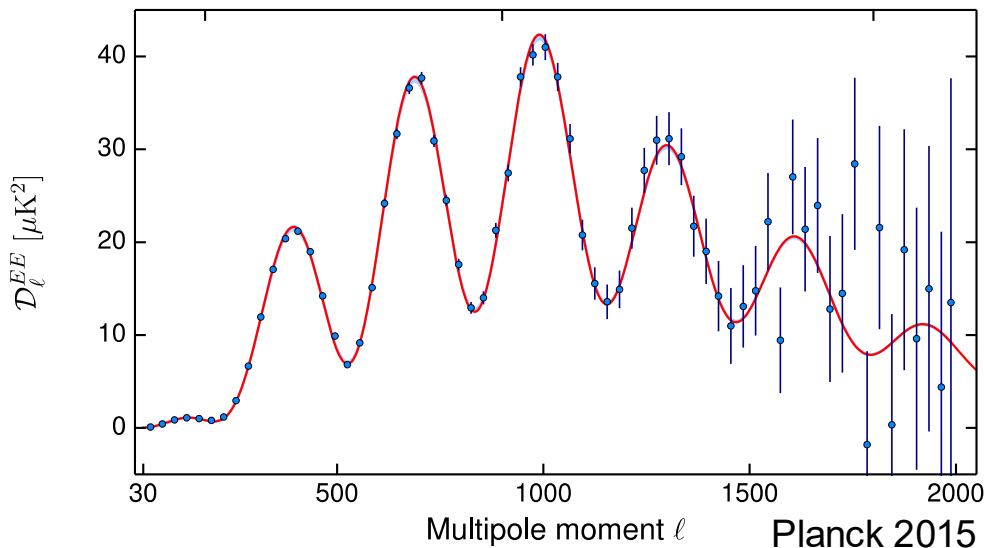
B < 0   B > 0
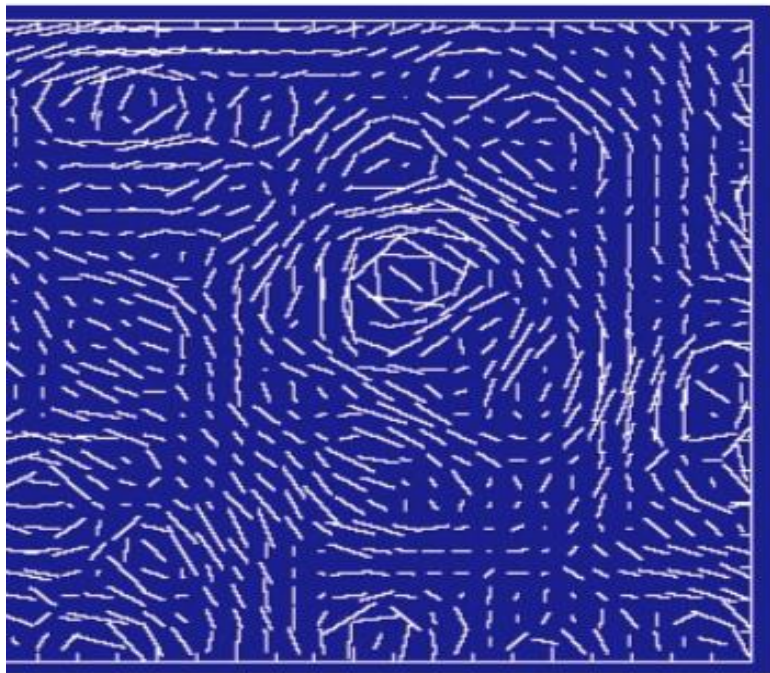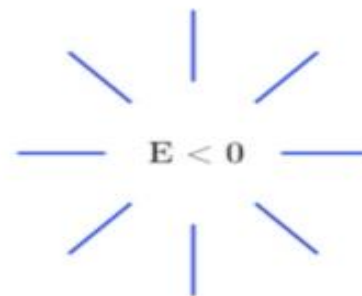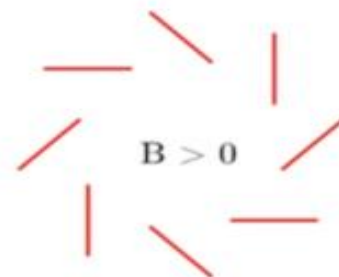
EE and TE power spectra

$$D_l = C_l\, l(l+1)/2\pi$$

$$C_{Tl} = \frac{1}{2l+1} \sum_m \langle a^*_{T,lm} a_{T,lm} \rangle$$

$$C_{El} = \frac{1}{2l+1} \sum_m \langle a^*_{E,lm} a_{E,lm} \rangle$$

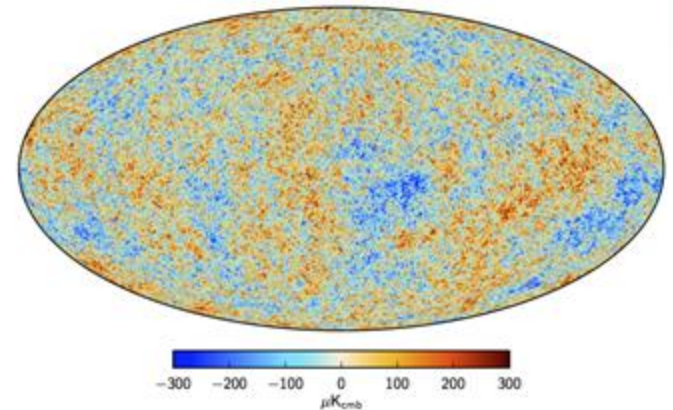$$C_{Bl} = \frac{1}{2l+1} \sum_m \langle a^*_{B,lm} a_{B,lm} \rangle$$

$$C_{Cl} = \frac{1}{2l+1} \sum_m \langle a^*_{T,lm} a_{E,lm} \rangle$$

Planck 2015

Miscellanea

The angular power spectrum

- The anisotropies are distributed as a random **gaussian** field.
- All the information is contained in the two point correlation function, or equivalently in the **angular power spectrum** in harmonic space.

Angular power spectrum

$D_l = C_l * l * (l+1) / 2\pi$

$$\Theta(\vec{x}, \hat{p}, \eta) = \sum_{l=1}^{\infty} \sum_{m=-l}^{l} a_{lm}(\vec{x}, \eta) Y_{lm}(\hat{p})$$

$$\langle a_{lm} a_{l'm'}^{*} \rangle = \delta_{ll'} \delta_{mm'} C_l$$

Multipole l
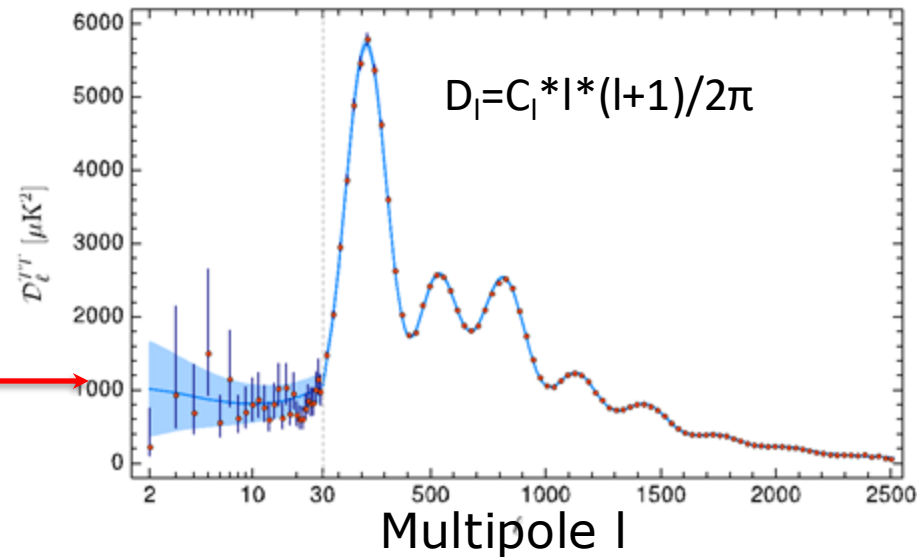
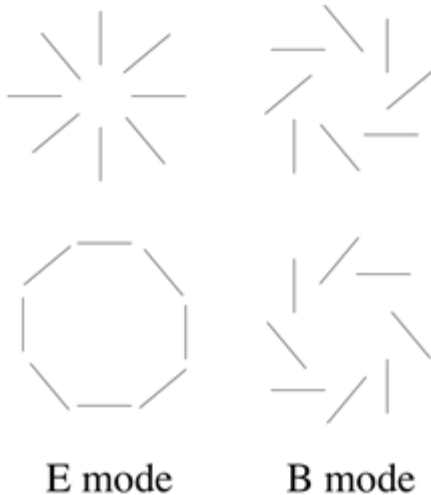Large scales   Small scales

CMB polarization

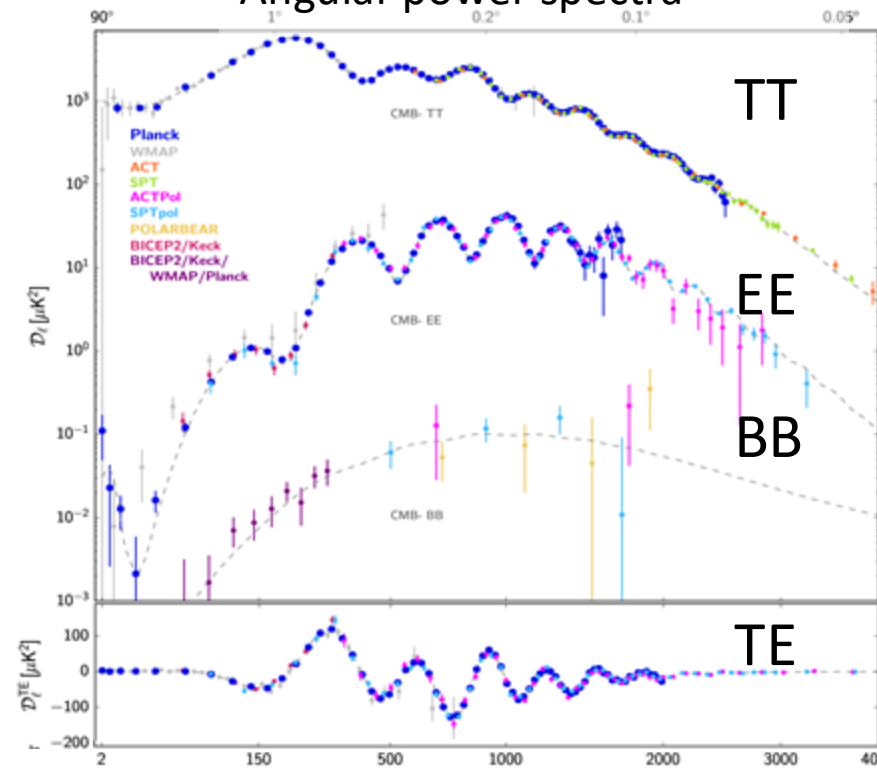Polarization generated Thomson scattering in the presence of a temperature quadrupole.
Different sources of quadrupole produce different patterns:

- Scalar (density perturbations): E-mode
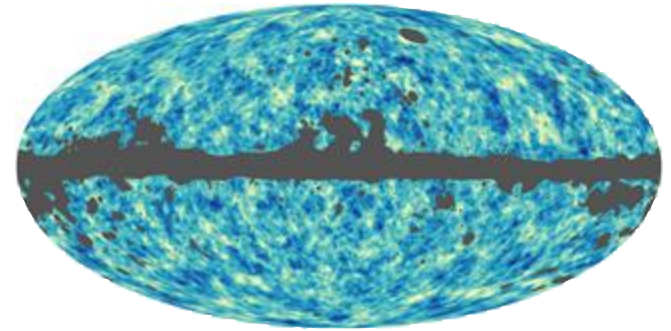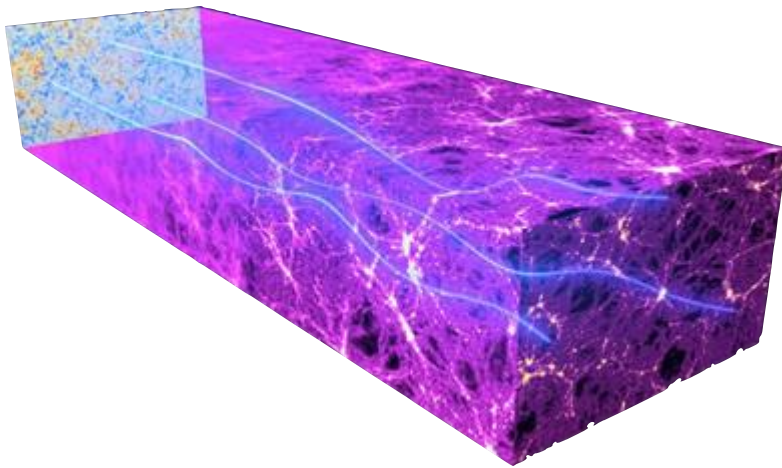- Tensor (e.g. gravitational waves): E-mode and B-mode

Polarization patterns

E mode   B mode

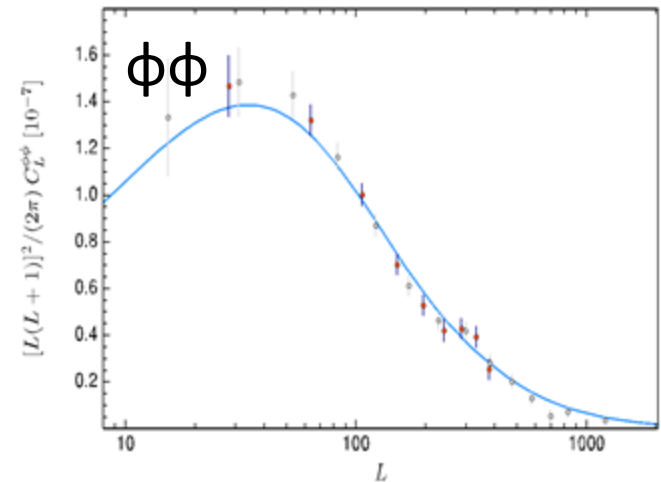Angular power spectra

TT

EE

BB

TE
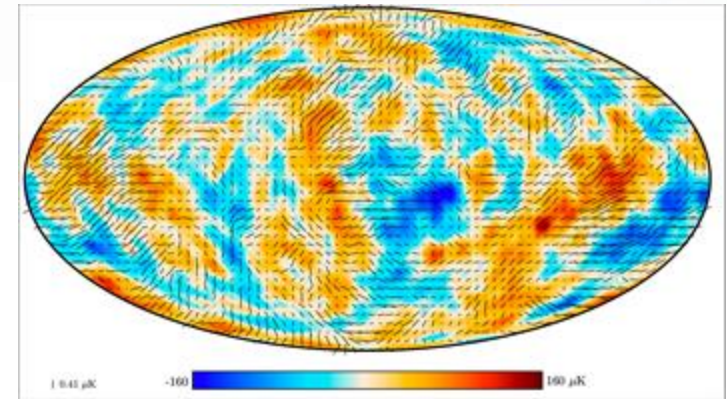
CMB lensing

- CMB lensing breaks isotropy of the CMB.
- Lensing potential map can be extracted from the non-gaussian 4-point correlation function.
- Lensing also impacts the primary power spectra, as well as distorts E-modes into B-modes
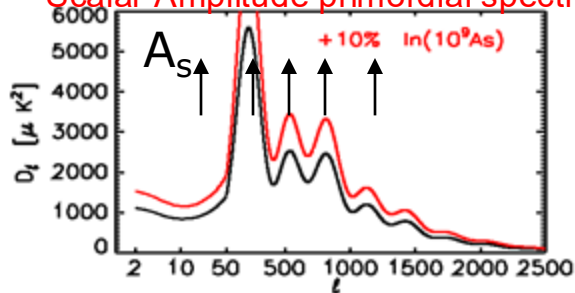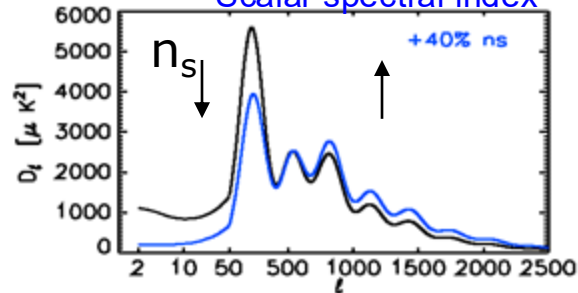

Lensing potential power spectrum

φφ

Planck 2018 VIII Lensing

The ΛCDM model

Standard model of cosmology: General relativity to describe gravity, standard model of particles for particle interactions, cosmological constant for dark energy and cold dark matter.
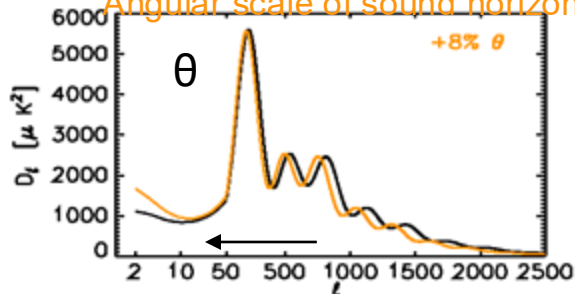

6 parameters:

- Initial conditions A_s, n_s
- Acoustic scale of sound horizon θ
- Reionization τ
- Dark Matter density $\Omega_c h^2$
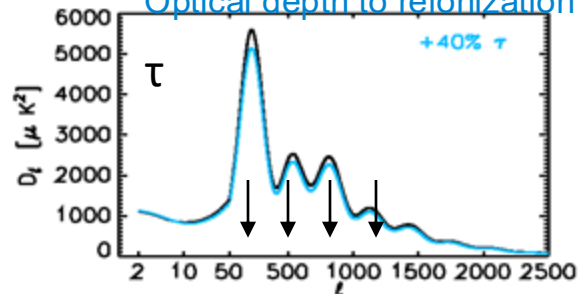- Baryon density $\Omega_b h^2$

Assumptions:
- Adiabatic initial conditions
- Neff=3.046
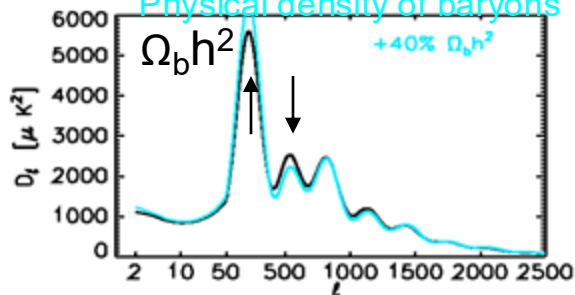- 1 massive neutrino 0.06eV.
- Tanh reionization (Δz=0.5)

The CMB is a laboratory to constrain cosmology and fundamental physics

CMB

Planck

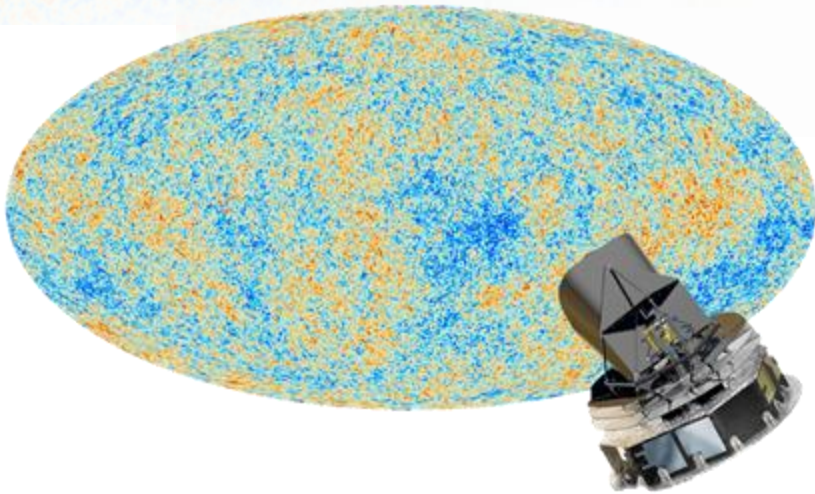**SPT-3G**

The Planck satellite

3rd generation full sky satellites (COBE, WMAP)
Launched in 2009, operated till 2013.
2 Instruments, 9 frequencies to **disentangle CMB from foregrounds**.
LFI:

- 22 radiometers at **30, 44, 70 Ghz.**

HFI:

- 50 bolometers (32 polarized) at **100, 143, 217, 353, 545, 857 Ghz.**
- **30-353 Ghz polarized.**

.   **1st release 2013: Nominal mission**,15.5 months, Temperature only (large scale polarization from WMAP).

.   **2nd release 2015: Full mission**, 29 months for HFI, 48 months for LFI, Temperature + Polarization, large scale pol. from LFI.
    Intermediate results 2016: low-l polarization from HFI

.   **3nd release 2018 (PR3): Full mission, improved polarization, low/high-l from HFI.**
    Better control of systematics specially in pol., still systematics limited.

Post PR3: new maps PR4 (LFI+HFI map-making, improved low-ell in polarization); new likelihoods and parameters from PR4; new maps Sroll2 (better low-ell polarization); several new estimation of opt. depth to reionization.
No substantially new result compared to PR3.

Planck 2018 power spectra

Planck collaboration 2018 VI.

ΛCDM is an excellent fit to the data. No evidence of preference for classical extensions of ΛCDM from Planck (and non-classical ones: dm annihilation, variation of fund. constants, primordial magnetic fields, variations in recombination, isocurvature, sterile neutrinos, dark energy, modified gravity)…..
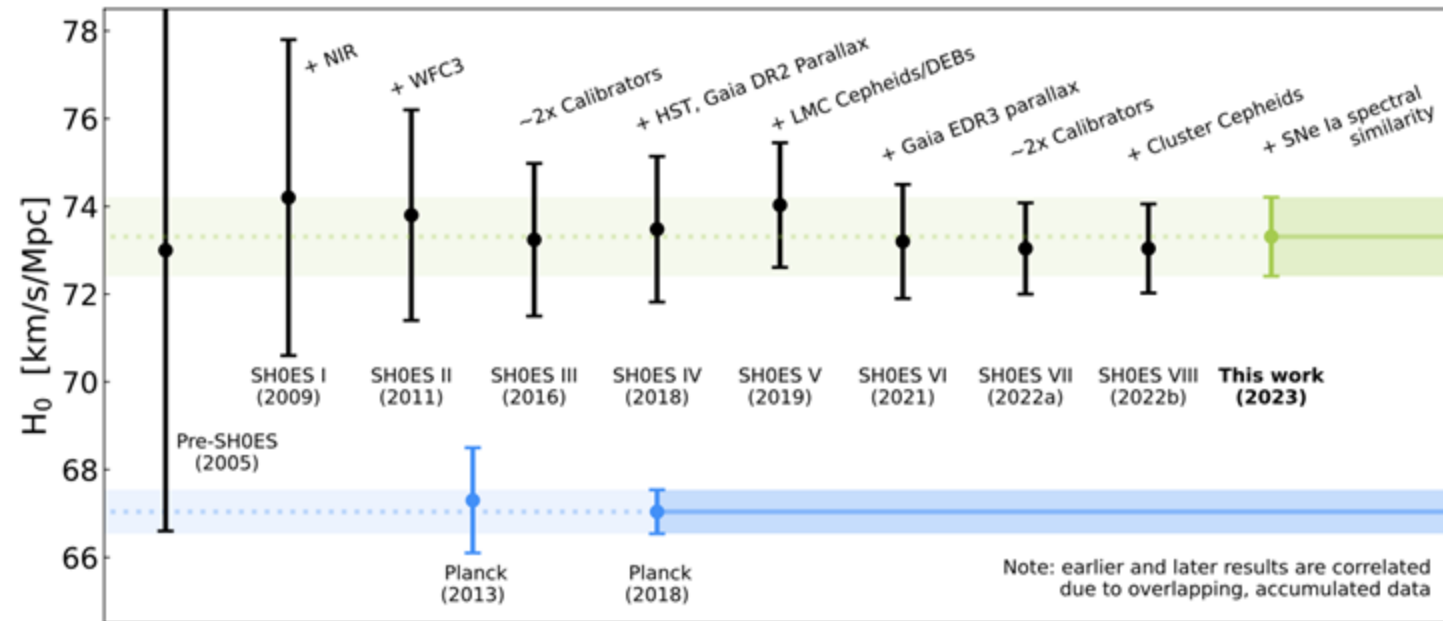
Baseline ΛCDM results 2018

(Temperature+polarization+CMB lensing)

	Mean	σ	[%]
$\Omega_b h^2$ Baryon density	0.02237	0.00015	0.7
$\Omega_c h^2$ DM density	0.1200	0.0012	1
100θ Acoustic scale	1.04092	0.00031	0.03
τ Reion. Optical depth	0.0544	0.0073	13
$\ln(A_s 10^{10})$ Power Spectrum amplitude	3.044	0.014	0.7
n_s Scalar spectral index	0.9649	0.0042	0.4
H_0 Hubble	67.36	0.54	0.8
Ω_m Matter density	0.3153	0.0073	2.3
σ_8 Matter perturbation amplitude	0.8111	0.0060	0.7

- Most of parameters determined at (sub-) percent level!

- Best determined parameter is the angular scale of sound horizon θ to 0.03%.

- τ low and tight, reionization at z~7.

- n_s is 8σ away from scale invariance (even in extended models, always >3σ)

- Best (indirect) **0.8%** determination of the Hubble constant to date.

Planck 2018 results. VI. Cosmological parameters (SG co-correponding author)

102

The Hubble tension

The Hubble tensions is the difference in the expansion rate of the universe today as measured from Supernovae IA calibrated with Cepheids and from the CMB and other early universe probes. Since the early universe measurements depend on a cosmological model, it could indicate the need of a change in the model, and thus **the discovery of new physics.**

Murakami+ 2023
Breuval+ 2024

5.7σ tension

Supernovae IA
+cepheid
SH0ES
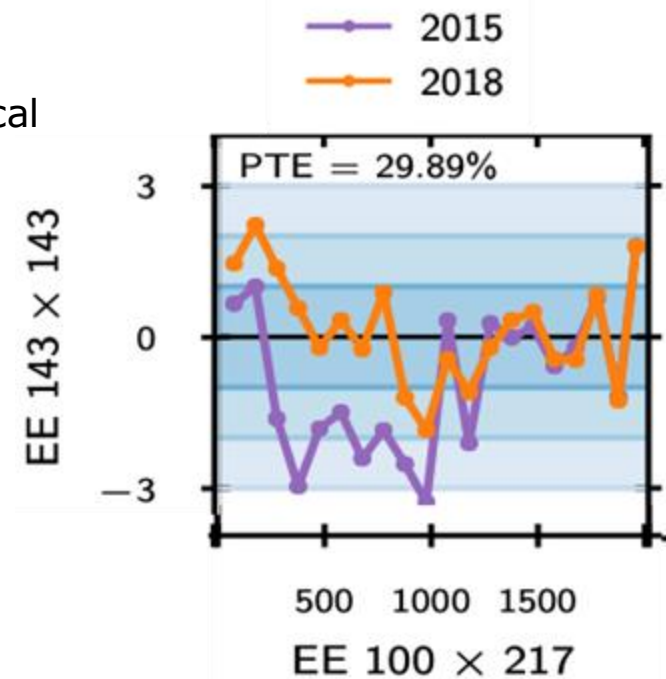H_0= **73.29±0.90** km/s/Mpc.

CMB (also BAO)
Planck 2018

H_0 =**67.36±0.54** km/s/Mpc.

The importance of robustness of results

- A **large impact** on the field (tens of thousands of citations)
- **Responsibility to provide the community robust results.**
- Many Tests:
  - **Redundancy** of the data is key in order to be able to do consistency tests at power spectrum or cosmological parameters level from **subsets of the data**, i.e.
    - from different frequency channels, which also corresponds to different detectors.
    - from different map cuts (half mission, versus detector sets)
    - from TT, TE or EE (model dependent).

  - Tested the consistency between a large number of **different analysis choices** on cosmological **parameters** (model dependent).
  - Compared different **analysis pipelines**, which was essential to improve the robustness of the final product.
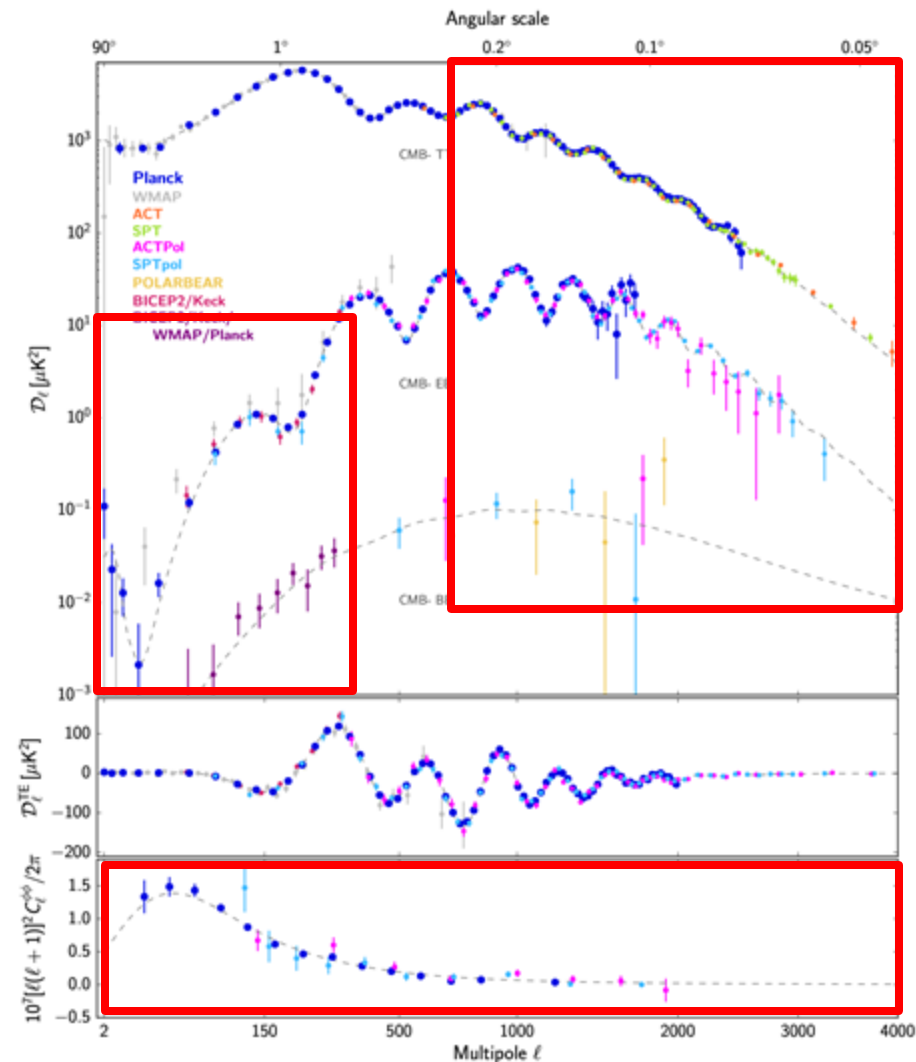 - **End-to-end simulations** also allowed us to validate the pipeline.

Difference between CMB-only, frequency power spectra in units of error bars in 2015 and 2018

In the second Planck 2015 release, test failed for polarization data. culprit was uncorrected systematics.
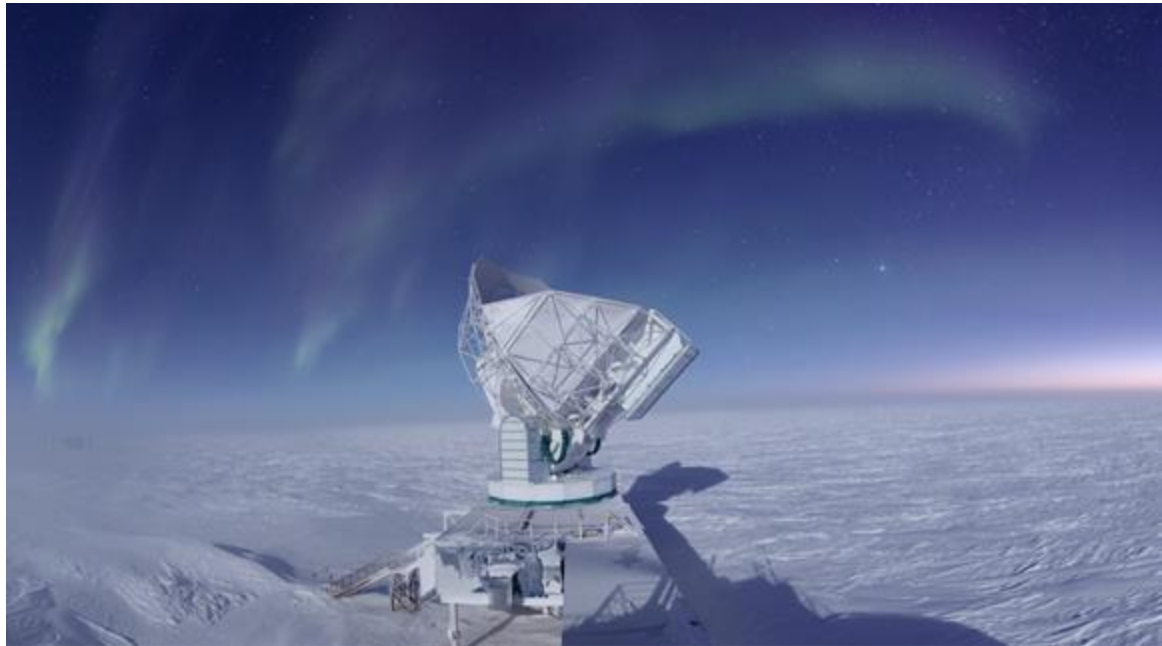
Planck 2018 results V.

From Planck to SPT-3G

- Planck results had a tremendous impact on cosmology. They confirmed the LCDM model. They were checked with many consistency tests.

- Planck opened new mysteries, such as the Hubble tension, that we will explore with upcoming and future experiments.

- There is still a very large amount of information in CMB to be uncovered. Upcoming experiments have two main goals:

  - at large multipoles in polarization, to detect primordial gravitational waves and measure reionization.

  - At small angular scales in polarization, to test cosmological models and the properties of the energy content of the universe.
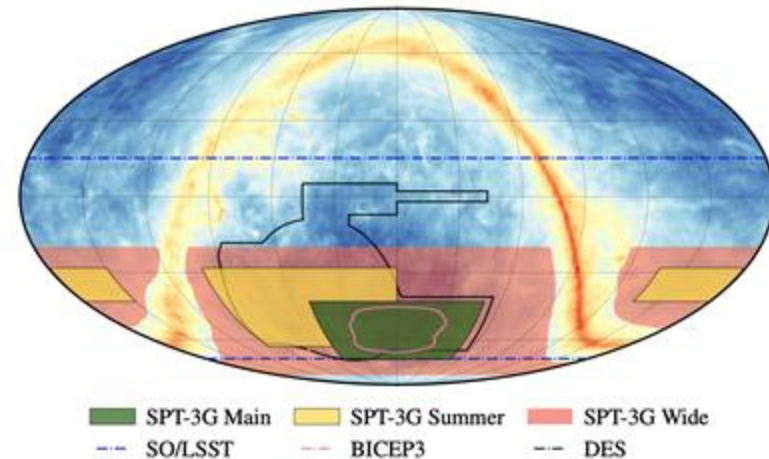
CMB

Planck

SPT-3G

The South Pole Telescope

- SPT is a 10m telescope at the South Pole. It is observing with its third generation camera, SPT-3G, with ~16,000 detectors at 95, 150, and 220 GHz at high resolution (~1 arcmin).

- It has observed **25%** of the sky:
  - **Main** Winter Field **1500 deg²** (5yrs done, 2yr TBD)
    Coadded noise **~17X** better than Planck.

  - **Summer** fields **2650 deg²** (4yrs done),
    coadded noise **4X** better than Planck.

  - **Wide** field **6000 deg²** (1yr)
    coadded noise **3X** better than Planck.

SPT-3G Main   SPT-3G Summer   SPT-3G Wide
SO/LSST   BICEP3   DES

- Many scientific goals:
  - **Cosmological constraints from CMB primary anisotropies and CMB lensing**
  - Delensing of the BICEP/Keck field to improve constraints on tensor to scalar ratio r.
  - High-ell TT foregrounds (including kSZ), Cross-correlations with other surveys, High-z galaxies, Clusters of galaxies, Transients etc…
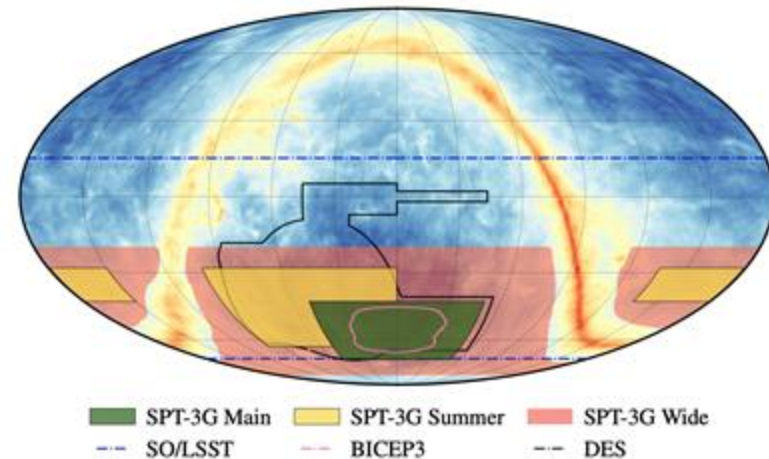
Prabhu…,**SG** et al. 2024

The South Pole Telescope

- SPT is a 10m telescope at the South Pole. It is observing with its third generation camera, SPT-3G, with ~16,000 detectors at 95, 150, and 220 GHz at high resolution (~1 arcmin).

- It has observed **25%** of the sky:
  - **Main** Winter Field **1500 deg²** (5yrs done, 2yr TBD)
    Coadded noise **~17X** better than Planck**.**

  - **Summer** fields **2650 deg²** (4yrs done),
    coadded noise **4X** better than Planck**.**

  - **Wide** field **6000 deg²** (1yr)
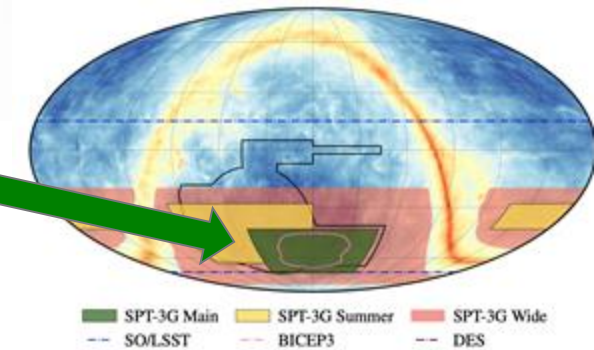   coadded noise **3X** better than Planck.

SPT-3G Main   SPT-3G Summer   SPT-3G Wide
SO/LSST   BICEP3   DES

Forecasts show we will measure parameters better than Planck by a factor of 2, and in combination with it by a factor of 3.

SPT-3G have the potential to take the lead on our understanding of the universe in the next years.

Ensuring the robustness of the results is even more critical.

*Planck 2018 had 74, 36, 53 µK-arcmin, coadded 27.6 µK-arcmin) over ~80% sky,
ACT DR6 has 15 µK-arcmin over 40% of sky

Prabhu…,**SG** et al. 2024

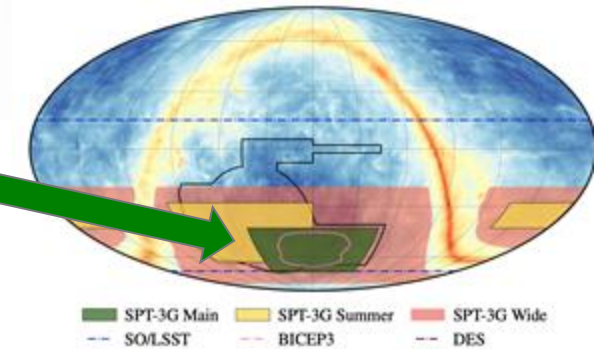# Published power spectrum SPT-3G results from Main field

Results based on the observations of the small but **deep Main field** observed during the Austral winter.

- **4 months of observations "SPT-3G 2018":** Used only half of the focal plane [published in 2021-2023]:
  - Analysis of **TEEE** (Dutcher,...SG+ 2021, Balkenhol,...SG+ 2021)
  - Analysis of **TTTEEE** (Balkenhol,...SG+ 2023)

- **2 years of observations "SPT-3G 2 year Main field":** Based on ~16 months of observations with the full focal plane.

  - Cosmology from CMB lensing and delensed EE power from polarization with **MUSE** (Ge., Millea,...SG+ 2024)

  - Constraints on Inflationary Gravitational Waves from large scale **BB** (Zebrowski,...SG+ 2025)

  - Constraints on duration of reionization from non-gaussianity of KSZ (Raghunathan+ 2024)

Published power spectrum SPT-3G results from Main field

Results based on the observations of the small but **deep Main field** observed during the Austral winter.

- **4 months of observations "SPT-3G 2018":** Used only half of the focal plane [published in 2021-2023]:
  - Analysis of **TEEE** (Dutcher,...SG+ 2021, Balkenhol,...SG+ 2021)
  - Analysis of **TTTEEE** (Balkenhol,...SG+ 2023)

- **2 years of observations "SPT-3G 2 year Main field":** Based on ~16 months of observations with the full focal plane.
  - Cosmology from CMB lensing and delensed EE power from polarization with **MUSE** (Ge., Millea,...SG+ 2024)
  - Constraints on Inflationary Gravitational Waves from large scale **BB** (Zebrowski,...SG+ 2025)
  - Constraints on duration of reionization from non-gaussianity of KSZ (Raghunathan+ 2024)

Early Data Release: SPT-3G TTTEEE 2018

- Data taken from **first 4 months** of data in **2018** from **half of the focal plane**, only from **winter main field.** First analysis only analysed **TEEE** (Dutcher,...SG+ 2021, Balkenhol,...SG et al. 2021).

- We added **TT** in a new analysis in Balkenhol,...SG+ 2023**.**
  - More **redundancy for tests**.
  - breaks degeneracies, specially for extensions of LCDM model e.g. primordial magnetic fields, EDE (Galli et al. 2022, Smith,... SG et al. 2022).

- The new **TTTEEE** analysis allowed us to introduce many **improvements** to increase the robustness of the results:
  - Developed **consistency** tests inspired on Planck
  - Implemented **blinding**
  - **Speed-up** MCMC chains with ML emulator of Boltzmann code (CosmoPower)
  - **Increased accuracy** of the power spectrum covariance matrix (based on simulations and in flat sky approximation, large off-diagonals terms tricky to model)
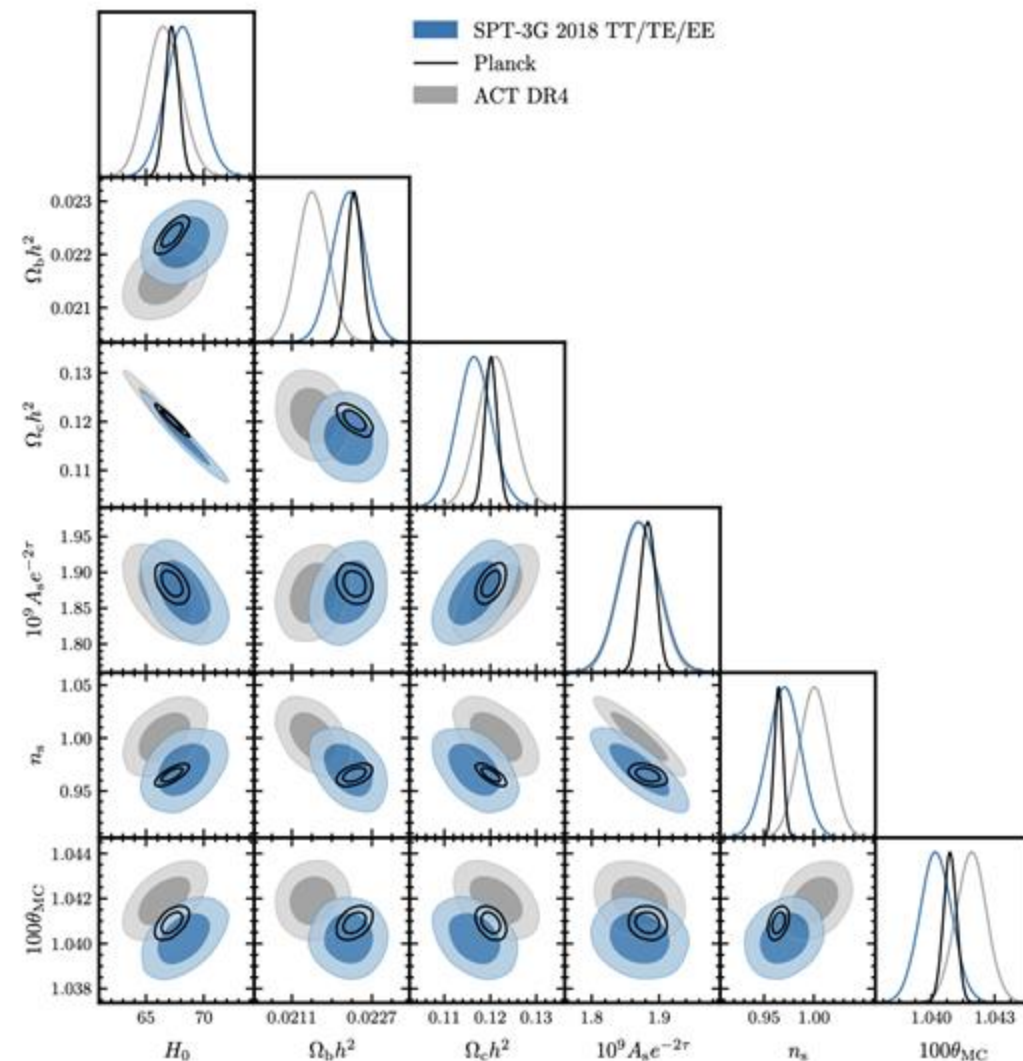
Lennart Balkenhol
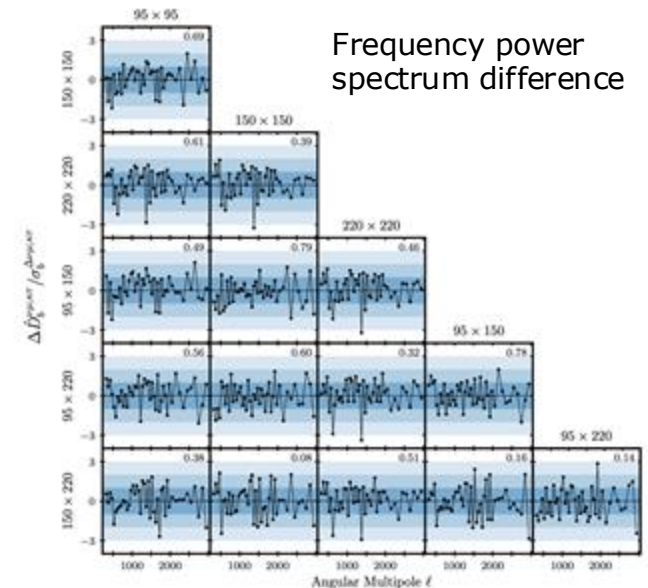
Frequency power spectrum difference

L. Balkenhol, D. Dutcher, A. Spurio Mancini, A. Doussot, K. Benabed, **SG** and the SPT collaboration arXiv:2212.05642

Results from SPT-3G TTTEEE 2018

- Errors from SPT3G were three times larger than Planck.
- ΛCDM is a good fit to the data, $\chi^2=763$ for 728 bandpowers (PTE=15%).
- Under ΛCDM, on the 5 parameters, Planck and SPT are consistent with PTE 76%.
- Results are consistent between ACT-DR4 and SPT3G-2018. Constraining power is comparable.

$H_0 = 68.3 \pm 1.5$ km s^{-1} Mpc^{-1}
$S_8 = 0.797 \pm 0.042$

No deviations from LCDM

L. Balkenhol, D. Dutcher, A. Spurio Mancini, A. Doussot, K. Benabed, **SG** and the SPT collaboration arXiv:2212.05642

Hubble tension models with SPT-3G 2018 TTTEEE

Ali Rida Khalife
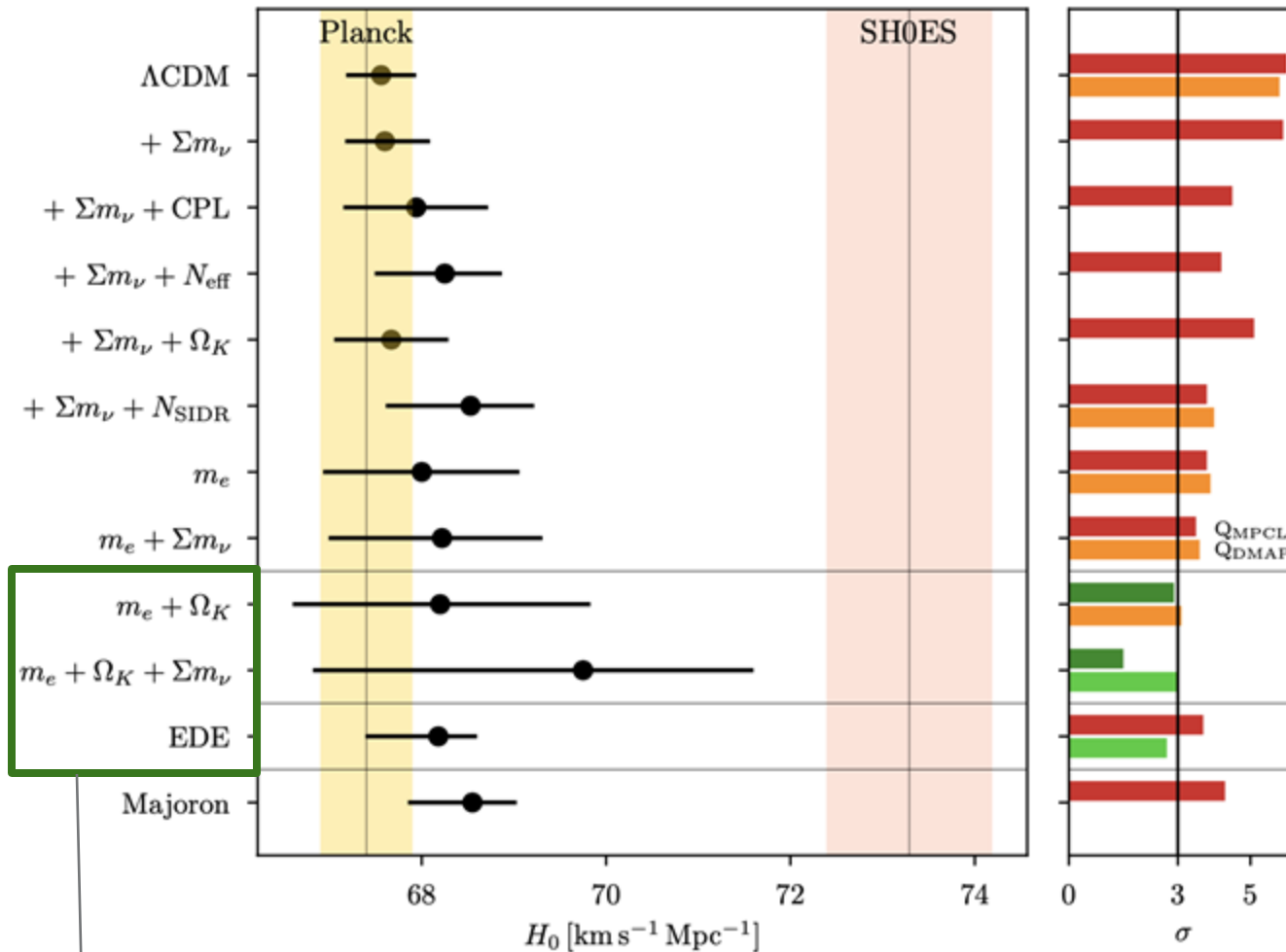
A few still viable models to solve the tension (others in the literature…)

Data:

Planck (TT,TE,EE+lowE+lensing), **SPT-3G 2018** (TT+TE+EE), **BAO** (6dFGS+DR7+DR12+DR16), and **SN Ia**

A. R. Khalife, M. Baryhami, **SG**, J. Lesgourgues, K. Benabed 2024

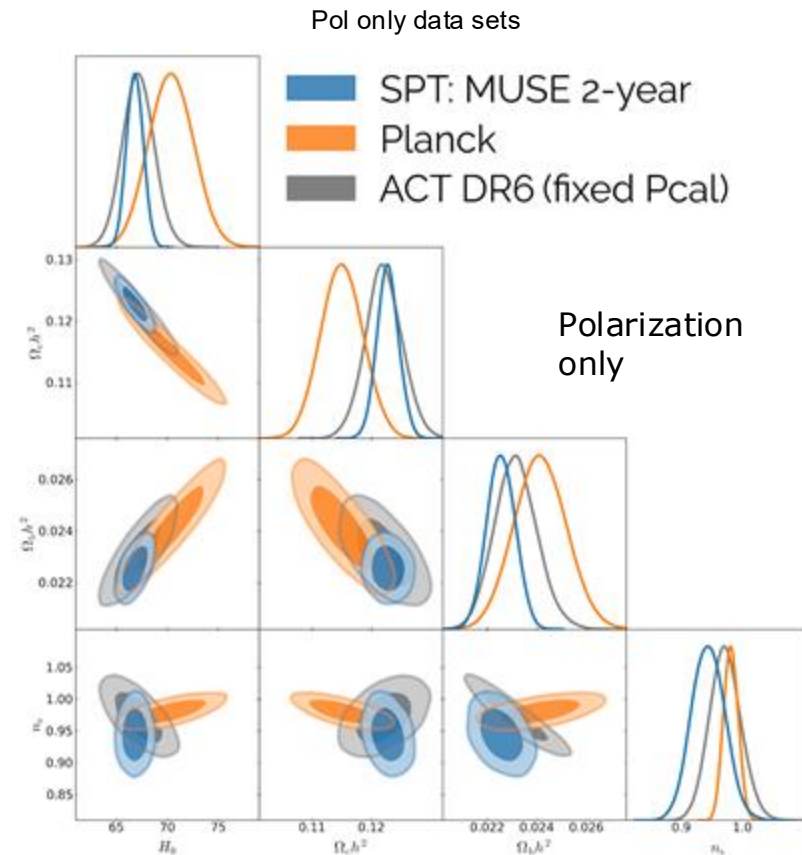# First analysis of polarization from Main 2 years: MUSE

Fei Ge   Marius Millea

- **MUSE**: Algorithm similar to simulation-based inference with semi-analytic compression statistic.

- Used only polarization data to estimate the CMB **unlensed EE power spectrum and lensing** reconstruction power spectrum.
- **Tightest bandpower** measurement of φφ **at L>350** and **EE at ℓ>2000**

- Tightest constraints on **LCDM parameters from CMB polarization-only inference EE**

Pol only data sets
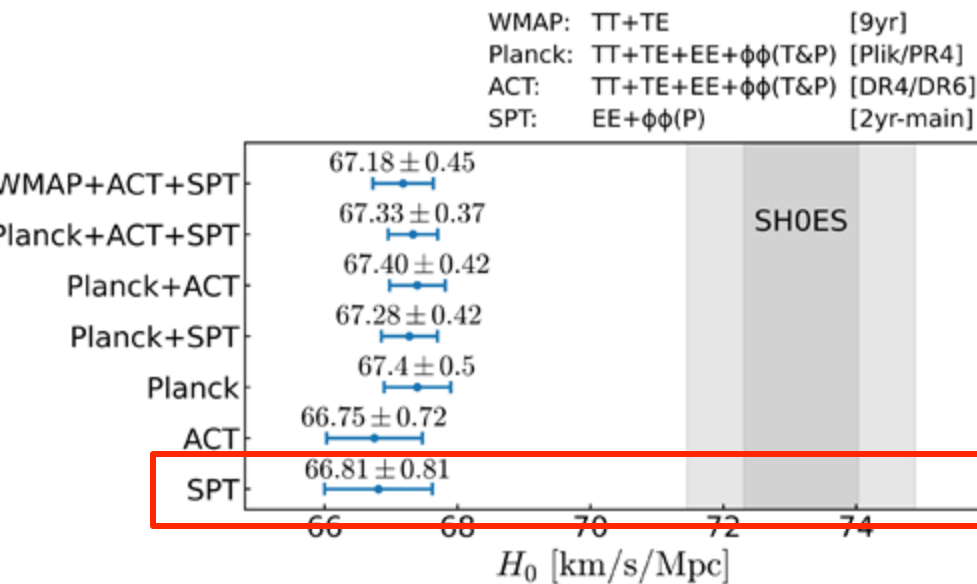

Polarization only

Likelihood public on our website

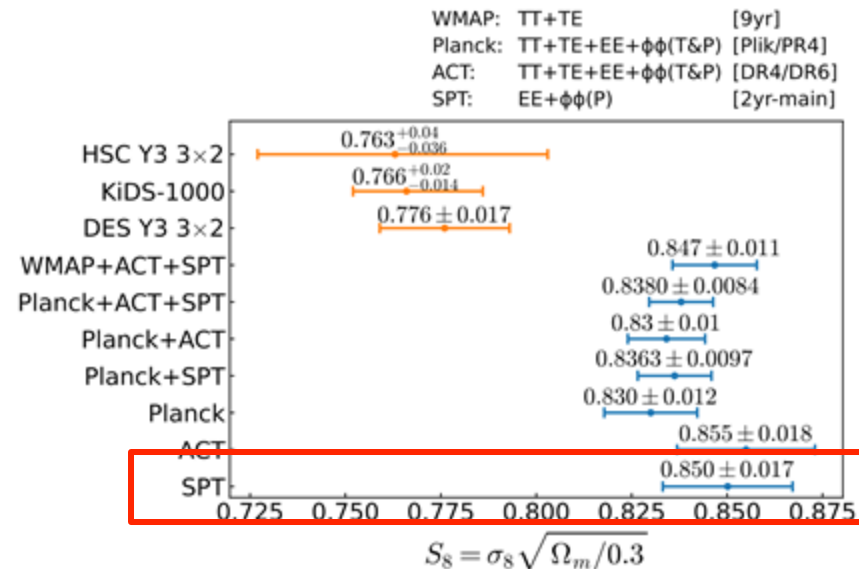https://pole.uchicago.edu/public/data/ge25/index.html
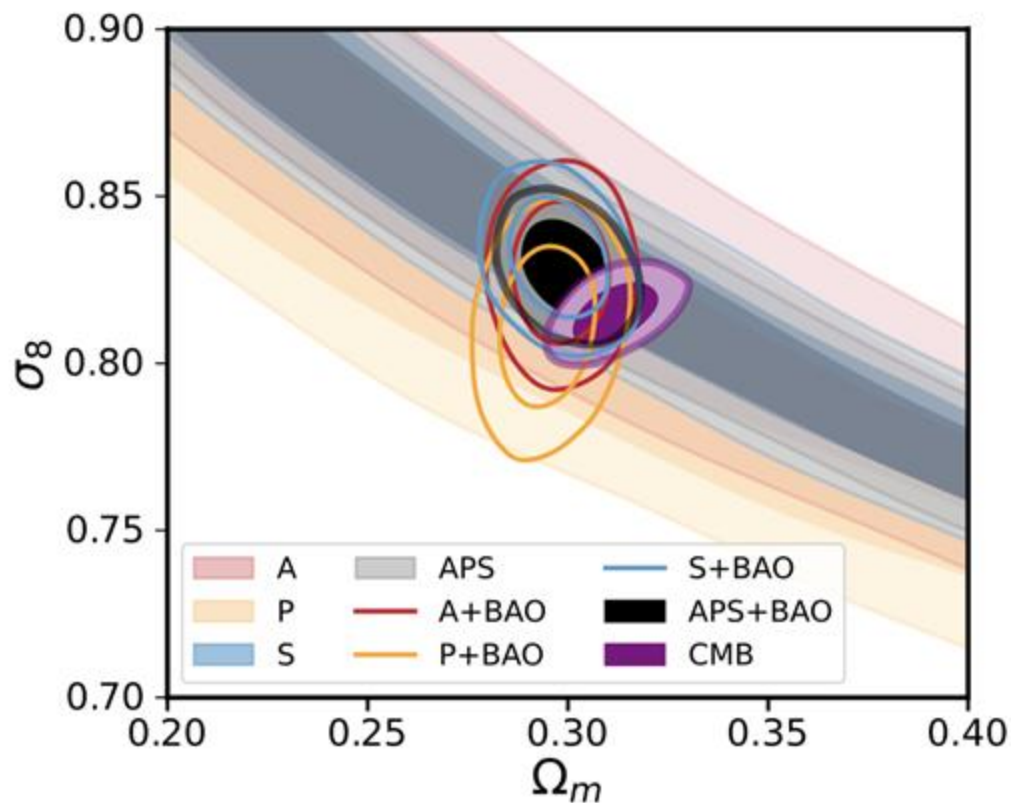
Ge, Millea...SG+ 2025

First analysis of polarization from Main 2 years: MUSE

Hubble tension with
SH0ES confirmed at 5.4σ
from SPT-3G alone.

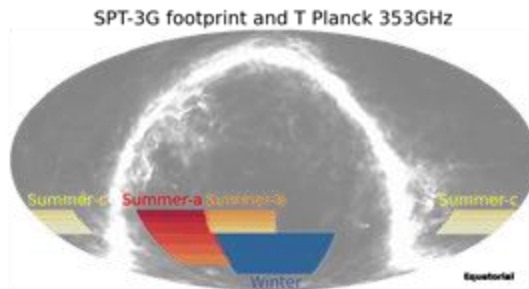S8 results in agreement
with other CMB
experiments.

Ge, Millea…SG+ 2025

ACT Planck SPT lensing combined

$$S_8^{\mathrm{CMBL}} = 0.825^{+0.015}_{-0.013} \; (68\% \; \mathrm{C.L.}, \quad \mathrm{APS}).$$

1.6% measurement from CMB lensing alone

Qu, Ge,…SG+ 2025

Coming next: Summer and Wide fields

Federica Guidi
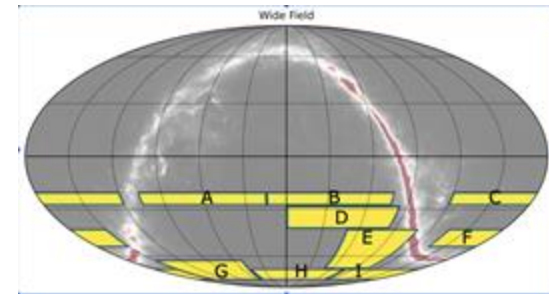

SPT-3G footprint and T Planck 353GHz

Aline Vitrier

Wide Field

- Challenges: Larger atmospheric fluctuations, galactic contamination, lower elevation.
- Mature analysis, to be in a few months (Guidi,...SG et al., in preparation).

- Challenge of analyzing 9 different subfields, each with different characteristics.
- Early stages of analysis, to be released within a couple of years (Vitrier,...SG et al., in preparation)

Conclusions and prospects

1. CMB is a leading probe of cosmology.

2. SPT-3G will improve over Planck results. We have the potential to constrain proposed solutions to the cosmological tensions.This power will come with the great responsibility of checking for consistency to ensure robustness.

3. Total dataset will be 7+ years of winter field, 4 of summer fields, 1 of wide fields.

4. SPT-3G will be replaced by SPT-3G+ in 2027.

5. The lessons we are learning will pave the way for the next generation of CMB experiments.
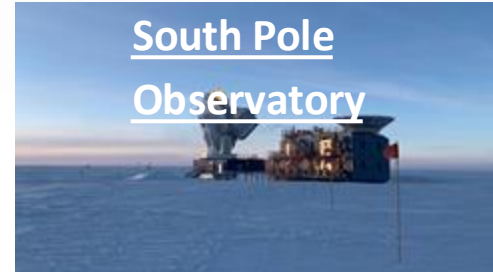
Signal-to-Noise of full SPT-3G survey
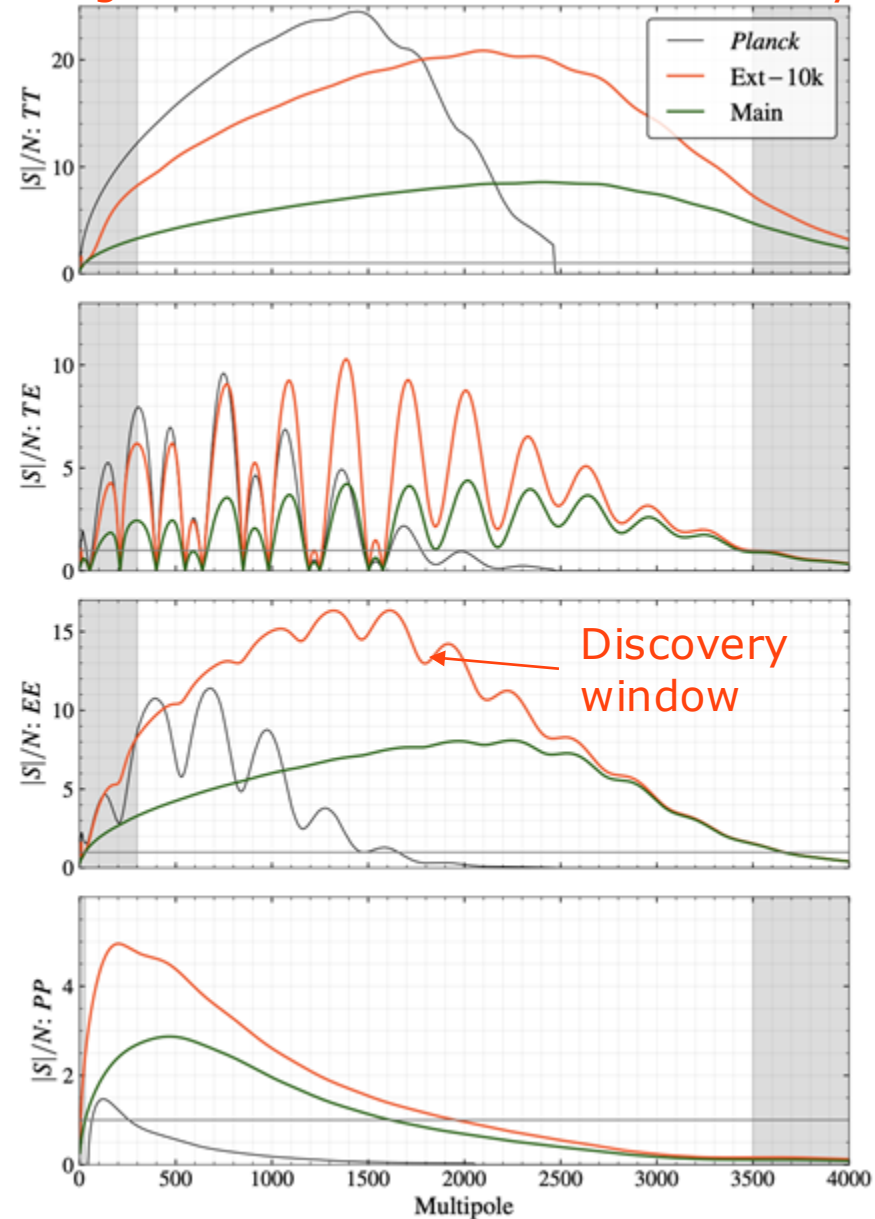
Discovery window

Conclusions and prospects

1. CMB is a leading probe of cosmology.

2. SPT-3G will improve over Planck results. We have the potential to constrain proposed solutions to the cosmological tensions.This power will come with the great responsibility of checking for consistency to ensure robustness.

3. Total dataset will be 7+ years of winter field, 4 of summer fields, 1 of wide fields.

4. SPT-3G will be replaced by SPT-3G+ in 2027.

5. The lessons we are learning will pave the way for the next generation of CMB experiments.

Current/upcoming

South Pole Observatory

SIMONS OBSERVATORY

Future

LiteBIRD

CMB -S4
Next Generation CMB Experiment